



MASTER OF SCIENCE THESIS

Wind Driven Reverse Osmosis Desalination for Small Scale Stand-Alone Applications

*Evaluation of system configurations and selection of an
optimal configuration for Somaliland by means of a
SIMULINK model*

C. Generaal B.Sc.
February 25, 2011

Wind Driven Reverse Osmosis Desalination for Small Scale Stand-Alone Applications

*Evaluation of system configurations and selection of an optimal
configuration for Somaliland by means of a SIMULINK model*

M.SC. THESIS

For obtaining the degree of Master of Science in Aerospace
Engineering at Delft University of Technology

C. Generaal B.Sc.

February 25, 2011



Delft University of Technology

Copyright © C. Generaal B.Sc.
All rights reserved.

DELFT UNIVERSITY OF TECHNOLOGY
DEPARTMENT OF
WIND ENERGY

The undersigned hereby certify that they have read and recommend to the Faculty of Aerospace Engineering for acceptance a thesis entitled **“Wind Driven Reverse Osmosis Desalination for Small Scale Stand-Alone Applications”** by **C. Generaal B.Sc.** in partial fulfillment of the requirements for the degree of **Master of Science**.

Dated: February 25, 2011

Professor:

prof.dr. G.J.W. van Bussel

Supervisors:

ir. H.F. Veldkamp

dr. ir. S.G.J. Heijman

"IF WE COULD EVER COMPETITIVELY, AT A CHEAP RATE, GET FRESH WATER FROM SEAWATER, THAT WOULD BE IN THE LONG TERM INTERESTS OF HUMANITY AND WOULD DWARF ANY OTHER SCIENTIFIC ACCOMPLISHMENT."

JOHN F. KENNEDY, APRIL, 1961

Abstract

The need for a sustainable water supply is high in many regions worldwide. The coastal city Berbera in Somaliland is one of those places where clean drinking water is not part of everyday life. With wind and saline water being freely available, wind driven reverse osmosis desalination can solve the problem. Existing solutions on wind driven reverse osmosis desalination are however limited. It is difficult to select the best configuration for a specific site. To deal with this issue the Wind2Water model is developed.

The Wind2Water SIMULINK model is a tool to select an optimal wind driven reverse osmosis system for a specific site. The model consists of four main blocks; the windturbine block, the transmission or coupling block, the pump block and the reverse osmosis array block. Two main configurations exist in the model; the mechanical coupling with gearbox and different gearbox ratios and the electrical coupling with battery. The Wind2Water model is organized in such a way that it is easy to implement additional components (such as a new wind turbine or pump).

The assumptions that were made for the creation of the mechanical Wind2Water model were validated by means of the experimental data from the prototype of Delft University of Technology built on Curaçao. The validation focussed on the permeate outflow around mean wind speed. With this focus the model matched the experimental results, proving that the assumptions were valid. The electrical Wind2Water model was validated by means of the prototype of Hatendoer Water. The efficiencies of the components in the electrical configuration were varied to find an electrical coupling that best matched the experimental results. This configuration was found and the characteristics of this configuration were used for the evaluation of other electrical configurations.

With the Wind2Water model brackish water configurations and sea water configurations were analyzed for regions with a mean wind speed of 5.9 m/s and 7 m/s. The evaluated configuration types were multi-bladed and three-bladed wind turbines with a mechanical coupling, and three bladed wind turbines with an electrical coupling. The effect of different pump sizes and, for the mechanical systems, transmission ratios were also taken into account. The water output for each configuration was estimated and from that the water cost could be defined. The total score of each configuration was based on the weighted score of the most important design criteria, being cost, maintenance, life and reliability.

For brackish water desalination the optimal configuration type (based on the four design criteria) is the mechanically coupled multi-bladed windmill. By looking only at the water cost the multi-bladed mechanical configuration is the best option as well. At higher mean wind speed three bladed mechanical configurations and the electrical configurations can however become cost competitive. The best configuration from a water output point of view depends on the mean wind speed. At high mean wind speeds the three bladed wind turbines, either mechanically or electrically coupled, are favorable. At low mean wind speeds a well chosen mechanical coupling with a multi-bladed wind turbine is preferable.

Also for sea water desalination the mechanical configuration with a multi-bladed windmill is the solution with the highest weighted score. In terms of water output the configurations with the mechanically coupled three bladed wind turbines are outperforming the others. Because of the higher system cost the water cost of these configurations is however similar to the water cost of the multi-bladed configurations. The three bladed mechanical configurations have a customized mechanical coupling. This results in lower scores on maintenance, life and reliability compared to the three bladed mechanical configurations with an off-the-shelf coupling.

For brackish water and for sea water desalination, the five configurations with the highest weighted score were selected. These configurations were analyzed with the monthly wind conditions of Berbera, Somaliland. For both brackish water and for sea water desalination the mechanically coupled multi-bladed configuration was found to be the optimal solution. The electrical configurations showed a higher average water output and a water cost score similar to the multi-bladed configuration for brackish water desalination and for sea water desalination this score was even higher than for the multi-bladed configuration. For application in a developing country the score on the ease of maintenance for the electrical system was however assumed to be lower than for the multi-bladed mechanical configuration, resulting in a slightly lower overall score for the electrical configuration.

The mean wind speed in Somaliland varies highly per month and even per day. Introducing a multi-bladed mechanical system that is able to switch between different transmission ratios during the year promises to be the best solution for both brackish water desalination as well as for sea water desalination in Somaliland. The variable transmission will allow for more water production in the low wind speed months, resulting in a higher average daily water output. With this higher water output the water cost will decrease and the weighted score of the multi-bladed mechanical configuration will increase.

Preface

In 2008, after showing my interest in developing work, Gerard van Bussel introduced me to Bas Heijman and the Drinking with the Wind project. The combination of a technical research and the application in a developing country immediately drew my attention.

The focus on Somaliland came from Daryeel, a foundation for the improvement of the well-being of the people in Somaliland. Daryeel had been looking for possibilities to desalinate water and the system tested by Delft University of Technology on Curaçao seemed a viable solution to them. Daryeel started talking with Bas Heijman and me, and we decided to work together to develop a commercially attractive system for Berbera, Somaliland.

For a commercially viable solution a focus on technology alone is not sufficient. A sound business plan is required as well. Together with Sjoerd Dijkstra, Aburhman Ahmed and, at the start, also Khaalid Hassan, we developed the Winddrinker Businessplan. With this and the knowledge we gained from this thesis work we believe we can establish profitable water selling businesses first in Somaliland and after that in many regions worldwide.

The Winddrinker business plan kept me motivated for my thesis work even at times SIMULINK failed on me (or I failed on SIMULINK). For that I would like to thank Sjoerd and Abdi. I hope we will have a successful future with the Winddrinker together. Credits also go to Floris Wiegerinck, the illustrator of the drawing on the cover of this thesis. Furthermore thanks go to my supervisors Bas Heijman and Dick Veldkamp and the professors Hans van Dijk and Gerard van Bussel for their support and advice. Finally, I would like to grab this opportunity to thank the main sponsors of this master thesis, my parents. Cobie and Siebe, thanks for all support and for providing such a loving home.

Table of Contents

Abstract	vi
Preface	ix
Nomenclature	xxi
1 Introduction	1
1-1 What?	1
1-2 Why?	2
1-2-1 The need for a stand alone sustainable water supply	2
1-2-2 Existing solutions	3
1-3 How?	3
1-3-1 Research objective	3
1-3-2 Report structure	4
I Selection of the System Components	7
2 Selection of the System Components	9
2-1 System overview	9
2-2 Wind turbine component	9
2-2-1 Selection of promising wind turbines	10
2-2-2 Selection of wind turbines for SIMULINK model	11
2-2-3 Preparation of wind turbine component for SIMULINK model	12
2-3 Pump component	15
2-3-1 Selection of promising pumps	16
2-3-2 Selection of pumps for SIMULINK model	17
2-3-3 Preparation of the pump component for the SIMULINK model	17
Danfoss pump calculations	17
Orbit pump calculations	18

Pearson pump	18
2-4 Reverse osmosis array component	20
2-4-1 Selection of the reverse osmosis array for the SIMULINK model	20
2-4-2 Preparation of reverse osmosis component for SIMULINK model	21
2-5 Coupling component	22
2-5-1 Preparation of the coupling component for SIMULINK model	23
II SIMULINK model and validation	25
3 Description of the Wind2Water SIMULINK model	27
3-1 Overview of the Wind2Water model	28
3-1-1 Mechanically coupled system	28
3-1-2 Electrically coupled system	29
3-2 Wind turbine	30
3-3 Coupling	31
3-3-1 Fixed mechanical transmission	31
3-3-2 Electrical transmission	31
3-4 Pump	33
3-5 RO Array	33
3-6 Water tank	33
4 Validation of the Wind2Water model	37
4-1 Comparison with data from Curaçao	37
4-2 Validation by means of Hatenoer configuration	43
4-3 Conclusion of Wind2Water model validation	47
III Selection for configuration Somaliland	49
5 Promising configurations	51
5-1 Design criteria and weighting factors	51
5-2 System configurations used for evaluation	52
5-3 Brackish water system	54
5-3-1 Mechanical configuration	54
5-3-2 Electrical configuration	60
5-3-3 Configuration selection for $U_{mean} = 5.9$ m/s and $U_{mean} = 7$ m/s	62
5-3-4 Conclusions for brackish water desalination	66
5-4 Sea water system	67
5-4-1 Mechanical configurations	67
5-4-2 Electrical configurations	71
5-4-3 Configuration selection for $U_{mean} = 5.9$ m/s and $U_{mean} = 7$ m/s	73
5-4-4 Conclusion for sea water desalination	76

6	Configuration for Somaliland	79
6-1	Wind input for Somaliland configuration	79
6-2	Brackish water system	80
6-2-1	Conclusion for brackish water desalination in Somaliland	81
6-3	Sea water system	82
6-3-1	Conclusion for sea water desalination in Somaliland	82
7	Conclusions and recommendations	85
7-1	Conclusions	85
	Objective 1: Design a tool to evaluate and optimize wind driven reverse osmosis desalination configurations for specific sites	85
	Objective 2: Apply the tool to find the best configuration for Berbera, Somaliland	85
7-2	Recommendations	86
	Bibliography	89
IV	Appendices	91
A	Research and development on small scale wind turbines and desalination	93
B	Preliminary research into a wind driven RO system	97
C	Wind turbine selection	103
C-1	Wind approximation with the Weibull distribution	103
C-2	Basic calculations to define needed capacity	104
C-3	Wind turbine specifications	105
C-4	Obtaining $C_q - \lambda$ and λ_{design} for each wind turbine	109
C-4-1	Select the airfoil	109
C-4-2	Find $C_{l,design}$ and α_{design}	110
C-4-3	Define the blade shape	111
C-4-4	Apply the blade element momentum method to get $C_q - \lambda$ and λ_{design}	112
	Momentum theory	112
	Blade element theory	113
	The BEM code	114
C-4-5	The $C_q - \lambda$ curve and λ_{design}	115
C-5	Load cases for wind turbine applications	115
D	Additional pump information	123
D-1	Orbit pump equations	123
D-1-1	Orbit pump GW0504	123
D-1-2	Orbit pump GW0704	124
D-1-3	Orbit pump GW1304	126
D-1-4	Data sheets manufacturer	127
D-2	Energy recovery systems and pump combinations commonly used for RO applications .	132
D-2-1	Pump combinations commonly used for RO applications	133
	Spectra Clark pump	133
	Danfoss SWPE	134
	X-pump	135

E Additional reverse osmosis information	137
E-1 Membrane cleaning	137
E-1-1 Spiral wound membranes	137
F Wind2Water model verification by means of EXCEL calculations	139
G Pearson pump model compared to experimental data	145
H Batteries: system configuration and cost	149
I Results Curaçao model	151

List of Figures

1-1	Thesis Outline	4
2-1	Components of the wind driven reverse osmosis system	10
2-2	Fortis Alize wind turbine performance curves	13
2-3	Turbex wind turbine performance curves	14
2-4	Overview of pump types	15
2-5	Danfoss Sea Water Pressure Exchanger	17
2-6	Performance curves of the Orbit GW0904 pump	19
2-7	Principle of osmosis and reverse osmosis	20
2-8	Overview of wind driven reverse osmosis desalination system configurations	23
3-1	Mechanical Wind2Water model	28
3-2	Overview of the mechanical Wind2Water model	28
3-3	Electrical Wind2Water model	30
3-4	Overview of electrical Wind2Water model	30
3-5	Overview of the battery model	32
3-6	Structure of Simulink model of array of RO elements	34
3-7	Overview of the water tank in the SIMULINK model	35
4-1	Results of mechanical Wind2Water model at the base configuration	39
4-2	Influence of changing the feed salt concentration	40
4-3	Influence of changing the system inertia	41
4-4	Comparison of permeate flow with the Curacao experiment	42
4-5	Wind profile of Hatenoer test	44
4-6	Power delivered and required electrical Wind2Water model without battery	45

4-7	Permeate flow of model compared with the Hatenboer test data	46
4-8	Zoom of the permeate flow of model compared with the Hatenboer test data	47
4-9	Power required and delivered for electrical Wind2Water model with battery	48
5-1	Torque over time for Turbex windmill with GW0504 Orbit pump	54
5-2	Pump speed and water output for Turbex-GW0504 system	55
5-3	Movement over the C_q - λ -curve to find the operating point	56
5-4	Angular velocity of Turbex-GW0504 system	57
5-5	Performance Turbex -GW0904 system	58
5-6	Torque for $V = 6$ m/s of the Alize-GW0504 system	59
5-7	Daily water output of the Fortis Alize-Orbit electrical system	60
5-8	Water output of the Fortis Alize-Orbit electrical system at 500 and 700 rpm	61
5-9	Wind input for evaluation of system configurations	62
5-10	Water output of the Turbex-APP1.0/APM0.8 mechanical system	68
5-11	Pump speed of the Turbex-APP1.0/APM0.8 mechanical system	68
5-12	Water output of the Turbex-APP1.5/APM1.2 and APP2.5/1.8	69
5-13	Water output of the mechanically coupled Fortis Alize-Danfoss systems	70
5-14	Water output of the mechanically coupled Bergey Excel-Danfoss systems	71
5-15	Water output for electrically driven sea water desalination at 700 rpm	72
5-16	Water output for electrically driven sea water desalination at 2900 rpm	72
6-1	Windspeed model for Berbera, Somaliland	80
6-2	Daily water output of different system configurations for brackish water desalination	80
6-3	Water output for sea water desalination in Somaliland	82
A-1	Wind powered desalination configurations and the corresponding power output curves	94
B-1	Overview of the 'Wind to water' matlab model	98
B-2	Wind turbine and pump torque and power curves	100
C-1	Definition of the blade variables	110
C-2	Airfoil geometry for analysis of a horizontal axis wind turbine	111
C-3	Geometry for rotor analysis	113
C-4	Fortis Montana wind turbine performance curves	116
C-5	Bergey Excel wind turbine performance curves	117
C-6	M5015 wind turbine performance curves	118
C-7	Performance curves for different wind turbine types	120
C-8	Wind turbine power as a function of angular velocity for different wind speeds	121
C-9	The torque of the load as a function of its rotational speed for different load cases	121

C-10	Load type $n = 2$ including static friction influences	121
D-1	Performance curves of the Orbit GW0504 pump	124
D-2	Performance curves of the Orbit GW0704 pump	125
D-3	Performance curves of the Orbit GW1304 pump	126
D-4	Technical data on the Danfoss APP/APM pumps	127
D-5	Power requirement of the Danfoss APP/APM pumps	127
D-6	Technical data on the Danfoss APP pumps	128
D-7	Power requirement of the Danfoss APP pumps	128
D-8	Flow rate and power characteristics of the Franklin GW0504 Orbit pump	129
D-9	Flow rate and power characteristics of the Franklin GW0704 Orbit pump	130
D-10	Flow rate and power characteristics of the Franklin GW0904 Orbit pump	131
D-11	Schematics of a rotary pressure exchanger	132
D-12	Spectra Clark pump	133
D-13	Schematic overview of the Clark pump principle	133
D-14	Two Clark pump-RO configurations	134
D-15	X-pump	135
E-1	Spiral-wound configuration [van Dijk, 2008]	138
F-1	Torque generated under constant wind speed	140
F-2	Ω for constant wind speed input	141
F-3	Torque generated under step wise increasing wind speed input	141
F-4	Ω for step wise increasing wind speed input	142
F-5	Torque generated under gradually increasing wind speed input	142
F-6	Ω for gradually increasing wind speed input	143
G-1	Schematic overview of Pearson pump model	146
G-2	Power from Pearson pump experiment compared to model	146
G-3	Required pressure from Pearson pump experiment compared with model	147
G-4	Permeate flow from Pearson pump experiment compared with model	147
H-1	Overview of two ways of including the battery in the model	149
H-2	Relative water cost for influence of battery on Hatlenboer system performance	150
H-3	Relative water cost by shorter lifetime of battery	150
I-1	Data of experiment done on Curaçao [Rabinovitch, 2008]	151
I-2	Permeate flow over time of the model compared with the Curaçao experiment	152
I-3	Permeate flow over wind speed of the model and the Curaçao experiment	153
I-4	Pump velocity over time of the model compared with the Curaçao experiment	154
I-5	Pump velocity over wind speed of the model compared with the Curaçao experiment	155

List of Tables

1-1	Wind powered RO studies	3
2-1	Summary of wind turbine characteristics	11
2-2	Wind turbines selected for implementation in SIMULINK model	12
2-3	Power factors for the Danfoss pumps	18
2-4	In- and outputs of RO array model	21
2-5	Variables of the reverse osmosis array	21
2-6	Variables of the coupling system that need to be defined before running the SIMULINK model	24
3-1	Parts available in the model	27
3-2	Wind turbines available in the SIMULINK model	31
3-3	Pump types available in the SIMULINK model	33
4-1	Variables of the mechanical Wind2Water model	38
4-2	Varied configuration parameters of the mechanical Wind2Water model	38
4-3	Influence of model parameters on water output	44
4-4	Water output of selected electrical configurations	47
5-1	Weighting factor definition	52
5-2	Selected system combinations for brackish water desalination and sea water desalination	53
5-3	Approximated cost of selected system parts	53
5-4	Water output for the three bladed wind turbines with the Orbit pumps	59
5-5	Comparison of the water cost in a region with a mean wind speed of 5.9 m/s	64
5-6	Score of selected configurations on each design critirerion	65
5-7	Comparison of the water cost at a site with a mean wind speed of 7 m/s	66

5-8	Score of selected configurations for brackish water desalination at 7 m/s	67
5-9	Score of selected configurations for sea water desalination at 5.9 m/s	73
5-10	Water cost for sea water desalination at 5.9 m/s	74
5-11	Water cost for sea water desalination at 7 m/s	75
5-12	Score of selected configurations for sea water desalination at 7 m/s	76
6-1	Mean monthly wind speeds in Berbera	79
6-2	Comparison of the water cost for brackish water desalination in Somaliland	81
6-3	Weighted score for selected configurations for brackish water desalination in Somaliland	81
6-4	Comparison of the water cost for sea water desalination in Somaliland	83
6-5	Weighted score for selected configurations for sea water desalination in Somaliland	83
A-1	Wind powered RO studies	95
B-1	Energy losses of the mechanical coupling of the Curaçao prototype	99
B-2	Minimum required transmission ratio for Danfoss APP1.5 pump	99
B-3	Wind speed at which the APP1.5 pump starts running	99
B-4	Water output for for different rotor radius and number of blades	101
B-5	Influence of wind profile on water output	101
C-1	Energy production in kWh	104
C-2	Energy production in kWh for 10kW wind turbine and $U_{rated} = 12$ m/s	105
C-3	Airfoil characteristics for the wind turbines in the SIMULINK model	110
C-4	Selected blade shape for each wind turbine used in the SIMULINK model	112
D-1	Energy recovery devices	132
E-1	Positive and negative points of spiral wound modules	138
F-1	Input for the verification with EXCEL	139

Nomenclature

Abbreviations

C_c	Salt concentration in concentrate water [ppm]	
P	Power in W	
TDS	Total dissolved solids	[ppm]
U	Wind speed in m/s	
q	flow rate in cubic meters per hour	
W	water output in cubic meters	

Greek Symbols

$\alpha_{l,design}$	Design angle of attack	[-]
δ_{pump}	Difference between delivered and required torque	[Nm]
$\eta_{bat}, \eta_{battery}$	Efficiency of the battery	[-]
η_{conv}	Efficiency of the converter	[-]
$\eta_{coupling}$	Efficiency of the coupling	[-]
$\eta_{generator}, \eta_{gen}$	Efficiency of the generator	[-]
$\eta_{inverter}$	Efficiency of the inverter	[-]
η_{mech}	Mechanical efficiency of coupling	[-]
η_{motor}, η_{mot}	Efficiency of the motor	[-]
η_{pump}	Efficiency of the pump	[-]
λ	Tip speed ratio	[-]
λ_{design}	Design tip speed ratio	[-]
λ_{memb}	friction factor of membrane	[-]

μ	Viscosity of the fluid	$[kg/sm]$
ω, Ω	Angular velocity	$[rad/s]$
π_f	Osmotic pressure	$[bar]$
ρ_{sw}	Density of sea water	$[kg/m^3]$

Latin Symbols

B	Number of blades	$[-]$
C	Salt concentration	$[mg/L]$
C_{bat}	Capacity of the battery	$[Wh]$
C_c	Salt concentration of the concentrate water	$[mg/L]$
C_f	Salt concentration of the feed water	$[mg/L]$
$C_{l,design}$	Design lift coefficient	$[-]$
C_p	Power coefficient	$[-]$
C_p	Salt concentration of the permeate water	$[mg/L]$
C_q	Torque coefficient	$[-]$
D_h	Membrane diameter	$[m]$
DOD	Depth of discharge	$[-]$
i	Transmission ratio	$[-]$
J	Inertia	$[kg/m^2]$
J_{gear}	Inertia of the gearbox	$[kg/m^2]$
J_{pump}, J_p	Inertia of the pump	$[kg/m^2]$
J_{rot}	Inertia of the wind turbine rotor	$[kg/m^2]$
k	Weibull shape factor	$[-]$
l	length of membrane	$[m]$
m	Mass	$[kg]$
M_b	Mass of a rotor blade	$[kg]$
n, N	Rotational velocity	$[rpm]$
n_{fixed}	Fixed rotational velocity of the electrical pump	$[rpm]$
n_{rot}	Rotational velocity of the rotor	$[rpm]$
P	Power	$[W]$
P_f	Pressure of the feed water	$[bar]$
P_{gen}	Power from the generator	$[W]$
P_{load}	Power required by the load	$[W]$
P_{nd}	Net driving pressure	$[bar]$
P_{pump}	Power required by the pump	$[W]$

P_p	Pressure of the permeate water	[bar]
P_{rat}	Power at rated wind speed	[W]
P_{WT}	Power from the wind turbine	[W]
P_r	Pressure	[bar]
P_{hydr}	Hydraulic pressure of a membrane	[bar]
q_{cons}	Water flow for consumption	[m ³ /h]
q_c, Q_c	Concentrate water flow	[m ³ /h]
q_f	Feed water flow	[m ³ /h]
Q_{pump}	required pump torque	[Nm]
q_p	Permeate water flow	[m ³ /h]
Q_{rot}	torque delivered by the wind turbine	[Nm]
R	Wind turbine rotor radius	[m]
T	Temperature	[°C]
t	Time	[s]
U	Wind speed	[m/s]
U_{cut-in}	Cut in wind speed of wind turbine	[m/s]
U_{mean}	Mean wind speed	[m/s]
U_{rat}	Wind speed at rated power	[m/s]
U_{start}	Wind speed at which the pump starts	[m/s]
$U_{Weibull}$	Wind speed from Weibull equation	[m/s]
V	Liquid velocity	[m/s]
W_{total}	Water output after total simulation	[m ³]

Subscripts

day	Daily average	[-]
-------	---------------	-----

Other

BEM	Blade Element Momentum	
CF	Calculation factor; a factor defined by Danfoss	[-]
PF	Power factor; defines power relation for Danfoss pumps	[-]

Chapter 1

Introduction

This chapter will give a short insight in **what** the topic of the research is, **why** it is interesting focus on this and **how** the research is formulated and organized in this report. The first section provides the background in the most important concepts discussed in this thesis work (section 1-1). After that the need for sustainable drinking water sources and for a method to find optimal configurations for wind driven reverse osmosis desalination is explained (1-2). Finally, the research objective is given together with the thesis outline (section 1-3).

1-1 What?

In this section an introduction to the thesis topic is given. This is done by giving a short explanation of the different aspects of the thesis title and subtitle:

**Wind Driven Reverse Osmosis Desalination for Small Scale Stand-Alone
Applications**

Evaluation of system configurations and selection of an optimal configuration for Somaliland by means of a SIMULINK model

Wind driven The system will be powered by means of wind energy. Two types of wind turbines are considered, the multi-bladed windmills and the three bladed wind turbines. Multi- bladed windmills are commonly used for water pumping purposes and are characterized by high torque and low speed. Three bladed wind turbines are commonly used for electricity generation and characterized by low torque and high speed.

Reverse osmosis desalination Salt water is pressurized by means of a pump until the pressure in the saline water is higher than the osmotic pressure (and some additional pressure to account for losses). The saline water is fed through membranes and pushed through the membranes leaving the salt particles on the one side of the membrane and the fresh water on the other side.

Small scale stand-alone application Stand-alone refers to an off-grid solution. With small scale we mean that the system is designed to provide a village or a small city of fresh water.

The capacity of a small scale system is in the range of 0 - 60 m³/day. A configuration with a capacity of 20 m³/day would already be a big achievement. With 20 m³/day and a daily drinking water need of 4 liters 4000 people can be served.

System configurations The system consists of four main components; the wind turbine, the coupling, the pump and the reverse osmosis array. Of each component several variants are implemented in the SIMULINK model, resulting in many possible system configurations.

Optimal configuration The optimal configuration is the system configuration that has the highest weighted score based on the four design criteria; cost, maintenance, life and reliability. The cost is a function of the total system cost and the average daily water output that can be estimated with the SIMULINK model.

Somaliland Somaliland is an independent part of Somalia which is located in the Horn of Africa. At the end of 2011 the Winddrinker team will install the first prototype for brackish water desalination in Berbera, Somaliland. The Winddrinker is a startup with the mission to create profitable local water selling businesses that use the stand-alone wind driven reverse osmosis desalination technology.

SIMULINK model SIMULINK is a programming environment for model based design for dynamic systems. It is a good tool for the modeling of the dynamic response of the desalination system to the variability of the wind. With SIMULINK it was possible to create a model with a clear graphical structure that allowed for easy implementation of new types of components, the Wind2Water model.

1-2 Why?

The need for a sustainable water supply is high in many regions worldwide (section 1-2-1) and existing solutions are limited (section 1-2-2). No tool for the selection of an optimal configuration for a specific site is currently available.

1-2-1 The need for a stand alone sustainable water supply

At the moment almost 900 million people worldwide do not have access to clean drinking water sources. Most of them live in rural areas, resulting in a need for off grid, stand-alone solutions.

The drinking water problem is acknowledged by the global society and with the Millennium Development Goals (MDG) the United Nations (UN) has set targets to solve the problem. The goal is to half the proportion of people without access to safe drinking water and basic sanitation from 2005 to 2015. It is a huge challenge to achieve this goal and technological developments and innovations in the field of fresh water production are crucial for success [MDG, 2006].

Another issue that is high on the agenda of the UN is the reduction of carbon dioxide emissions. Using renewable energy as a power source will be in line with the targets set by the UN with the MDGs. An advantage of using renewable energy is also that it makes the system independent of the variable fossil fuel prices. Currently available subsidies and other incentives make it even more attractive to use renewable energy.

1-2-2 Existing solutions

No commercial wind driven reverse osmosis desalination systems for small scale stand alone applications exist at the time of writing. Several institutes all over the world are researching the topic and an overview of the most important researches is given in table A-1. In appendix A a discussion of studies can be found. The main conclusion is that wind driven reverse osmosis desalination is technically and economically feasible provided that the system design and site selection are done correctly.

Table 1-1: Wind powered RO studies

Author	U_{mean} [m/s]	TDS [ppm]	E/M*	Output [m ³ /day]	Cost [\$/m ³]	Comments
Heijman [Heijman et al, 2010]	7	sea	M	5-10	na	Multi-bladed 5m diameter windmill
Habali [Habali et al, 1994]	4.7	1500-4000	E	22 - 33	0.99-1.71	Aeroman 15 kW windturbine
Miranda [Miranda, 2002]	8.3	40000	E	8.5	-	2.2 kW wind turbine, no batteries
Robinson [Robinson et al, 1992]	3	2000-6000	M	0.2	20	Multi-bladed 4 m diameter windmill
Essam [Essam et al, 2004]	5.7	40000	E	8.5	7.2	10kW wind turbine and 35 % PV system
Liu [Liu et al, 2002]	5	3000	M	3.7	na	Multi-bladed 4.3 m diameter windmill
Moreno [Moreno et al, 2004]	7 - 9	35000	E	0.4	na	1.5kW wind generator

The current researches tend to zoom in on one specific design configuration and evaluate the performance by means of experiments done on a prototype and in some cases on a theoretical model (for example the study of Essam). A method of evaluating the performance of different configurations for one specific site and thereby selecting an optimal configuration for that site is currently not available.

1-3 How?

In this section the focus of the thesis work will be set by means of the research objective (subsection 1-3-1). This will be followed by a description of how the report is structured (subsection 1-3-2).

1-3-1 Research objective

In 2008 Delft University of Technology (DUT) installed a mechanically coupled wind driven reverse osmosis system for sea water desalination on Curaçao [Heijman et al, 2010]. One of the main partners of this project was Hatenboer Water. Back in the Netherlands Hatenboer Water decided to continue the project with an electrically coupled system. DUT was however still interested in the direct mechanical coupling and how the performance of such a system compares to an electrical system. Comparing different configurations for wind driven reverse osmosis desalination and finding the optimal configuration for a specific site, in this case the site in Somaliland, became the focus of this thesis. The complete research objective is defined as follows:

1. Design a tool to evaluate and optimize wind driven reverse osmosis desalination configurations for specific sites
 - Create a tool that allows for easy implementation of new types of components
 - How reliable is the tool?

2. Apply the tool to find the best configuration for Berbera, Somaliland
 - What is the best configuration for brackish water desalination?
 - What is the best configuration for sea water desalination?
 - How does a mechanical coupling perform compared to a electrical coupling for both brackish water and sea water desalination?

1-3-2 Report structure

The outline of this report is given in figure 1-1. The body of the report is divided into three parts. The report ends with conclusions and recommendations.

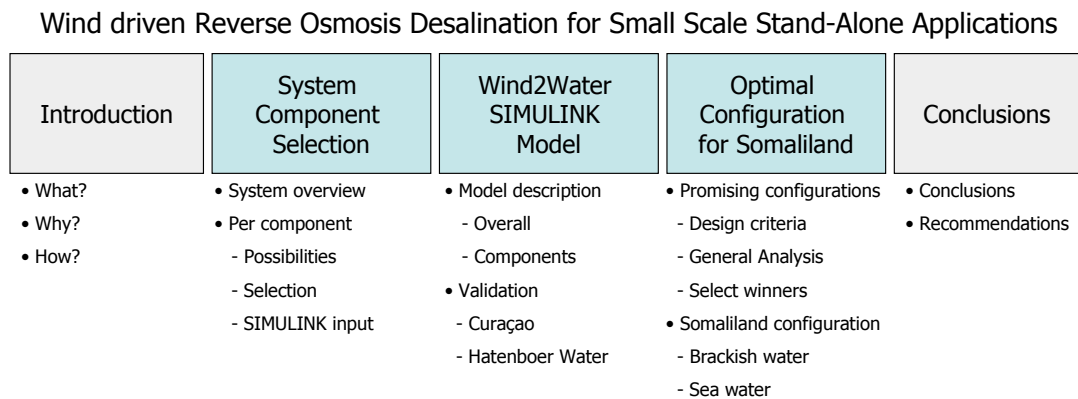


Figure 1-1: Thesis Outline

Part I gives the background on the system components that are implemented in the SIMULINK model. Per component it is shortly discussed what the possibilities are, what the reasoning behind the selected types is and what we need to know or calculate to get the correct input for the SIMULINK model. So for the pumps for example, first an overview of available pump types is given. After that the choice for the Orbit and Danfoss pumps is explained. These pumps need to be made available in SIMULINK and for that some calculations are necessary. A short description of what has to be done before the pumps can be used in the SIMULINK model is therefore also given.

Part II describes the Wind2Water SIMULINK model. The overall system and the influence of the different components upon each other is described. This is done both for the mechanical and the electrical system. Then the inputs, outputs and some other relevant information about the component models is given. Finally the total system is evaluated with experimental data. The mechanical system is validated with the data obtained from the experiments done by DUT on Curaçao and the electrical system is validated by means of data from the 'Drinking With The Wind' system of Hatenboer Water.

In Part III a selection of brackish water configurations and sea water configurations is made. These configurations are analyzed over constant wind input between 3 and 9 m/s. Based on those results the most promising configurations are selected and evaluated for sites with a mean velocity of 5.9

m/s and/or 7 m/s. For these configurations also the weighted score on the four design criteria (cost, maintenance, life and reliability) is obtained and based on this the 5 best configurations are selected for brackish water and for sea water desalination. These configurations are then evaluated with the monthly conditions of Berbera, Somaliland and from that the optimal solution for brackish water desalination and for sea water desalination in Berbera is selected.

Part I

Selection of the System Components

Chapter 2

Selection of the System Components

This chapter explains the selection of the different components for implementation in the SIMULINK model. The SIMULINK model is built such that in the future other component types (larger wind turbines, better pumps, etc.) can be easily added. It was chosen to focus on off-the-shelf components. Off-the-shelf components are generally cheaper than custom made ones and are also tested and used before, reducing the amount of operational problems.

For this research five wind turbines and three main pump types were selected and included in the model (see section 2-2 and 2-3 respectively). Also details on the selection of the reverse osmosis array and the coupling type are given (section 2-4 and 2-5). For each system component the overall possibilities are discussed, followed by the argumentation for the selected items. Furthermore it is explained how the selected items were included in the SIMULINK model. Extra calculations that were done in order to make the item available in the model are given here.

2-1 System overview

Figure 2-1 gives an overview of the system components used in a wind driven reverse osmosis system. Basically it consists of four components: the wind turbine, the coupling, the pump and the reverse osmosis array. The pump is driven by the energy provided by the wind turbine. This is done either electrically or mechanically depending on the coupling type. With the operational pump the saline water is pressurized and pushed through the membranes in the reverse osmosis system. The salt remains at the 'front' side of the membrane and clean water results at the other side. More details on the system components can be found in the following sections.

2-2 Wind turbine component

Many wind turbine manufacturers exist for all sorts of wind turbines. For small scale applications the multi-bladed windmills, small (electrical) wind turbines and vertical axis machines are of interest. Because of their low efficiency vertical axis machines were disregarded.

Multi-bladed windmills These windmills have a high start up torque and are commonly used for direct mechanical coupling, such as for water pumping purposes. Most mechanical couplings



Figure 2-1: Components of the wind driven reverse osmosis system

result in a translational movement of the vertical axis. For the coupling to the pump a rotational movement is however preferred. A disadvantage of the multi-bladed windmills is their low angular velocity. For the connection to a desalination unit a high angular velocity is favorable.

Small three (or two) bladed wind turbines The three bladed wind turbines are commonly designed for electricity generation. With good cooperation with the manufacturer it might be possible to couple them directly to the desalination unit. An advantage of these wind turbines is their high angular velocity. They are also characterized by their low start up torque which is a disadvantage for the direct mechanical coupling.

2-2-1 Selection of promising wind turbines

A selection of the available wind turbines on the market had to be made. This was done based on the following criteria:

- **Capacity** By means of preliminary calculations the size of the wind turbine was estimated (see appendix C-2). It was found that the wind turbines had to be in the range of 10-20 kW rated power (depending on the mean wind speed at the site). The calculations were based on the power requirement of the Spectra Pearson pump.
- **Experience** A manufacturer with experience in rural and isolated areas is an advantage. Even better is it when they have experience in developing countries, especially in Africa.
- **Cost** Only wind turbines with an investment cost below €40.000 were considered. In developing countries investment costs that are too high can be a problem for future adaptation of the system.
- **Location of manufacturer** To realize a good sustainable partnership it is preferable that the manufacturer is located in or close to the Netherlands. Therefore special attention was paid to Dutch/Belgium manufacturers. **Ease of installation** Preferably the wind turbine can be installed without the use of a crane.

In table 2-1 an overview of the selected wind turbines with their characteristics are given. More details on the wind turbines can be found in appendix C-3.

Table 2-1: Summary of wind turbine characteristics; more details in appendix C-3

	Multi bladed wind turbines				Small high λ wind turbines			
	Turbex	Kijito	M-1015	Southern Cross	Eco	TML	Alize	Bergey
Investment cost	€20k	€13k	€10k	€5.3k	€20k	-	€37k	€30k
Diameter	7.8 m	7.9 m	10 m	7.5 m	8 m	9.5 m	7 m	7 m
Output/ Power	48 m ³ /day	20 m ³ /day	11 m ³ /day	30 m ³ /day	20 kW	15 kW	10 kW	10 kW
Mechanical coupling	++	+	+	+	-	-	-	-
Experience	++	++	+	+	-	-	+/-	++

The multi-bladed Southern Cross and Kijito windmills were selected because of their long experience in development countries in Africa. Turbex is also an experienced player in the African market and is especially interesting because of the included transmission to a vertical rotary axis. The M1015 is the larger variant of the windmill used on Curaçao and was therefore also considered.

The small high tip speed ratio machines that were selected are the 10 kW Eco wind turbine, the TML 15 kW machine, the Fortis Alize 10 kW wind turbine and the Bergey Excel 10 kW wind turbine. The Eco comes from a US manufacturer. The price range seems good and the company has around 15 years of experience. They are however not particularly known for applications in developing countries. The TML wind turbine is situated in Belgium and they claim to have experience in rural areas. Unfortunately no details on price and power curve were received. Because there is not much know about their experience in the African market either this wind turbine was not selected for further research. The Fortis Alize wind turbine comes from a Dutch manufacturer called Fortis Wind Energy. Fortis also provided the wind turbine for the electrical wind driven reverse osmosis system developed by Hatenboer. Their experience with the concept and with the Winddrinkers partner, Hatenboer, is an advantage of this wind turbine over others. Finally the Bergey Excel wind turbine was selected. The Bergey Excel is a windturbine from the US commonly used in rural environments and the manufacturer has experience with combining the wind turbine to a water pump.

2-2-2 Selection of wind turbines for SIMULINK model

The SIMULINK model contains five wind turbines and are given in table 2-2. Three wind turbines were selected based on analysis of the promising wind turbines from the previous section and the two others were included because they were needed for the validation of the SIMULINK model.

The multibladed windmill that is selected is the Turbex windmill because of the promising water output and the transmission to a rotational vertical axis. This is favorable because the pumps used for the reverse osmosis desalination are driven by a rotational axis as well. The chosen high tip speed ratio machines are the Fortis Alize and the Bergey Excel machine. These wind turbines outperform the other two on experience with water pumping applications, have a reasonable price and the partnership between Fortis Wind Energy and Hatenboer Water is also an advantage.

Two M5015 windmill and the Fortis Montana were included for the validation of the model by means of experimental data. The M5015 windmill was implemented for the validation of the data obtained from the experiments done on Curacao [Rabinovitch, 2008]. The Fortis Montana was added for the validation of the test done by Hatendoer on their electrically coupled wind driven reverse osmosis system [J.A. de Ruijter, 2010].

Table 2-2: Wind turbines selected for implementation in SIMULINK model

	Multi-bladed windmill	Small high λ wind turbines
For validation	M5015	Fortis Montana
For evaluation	Turbex	Fortis Alize Bergey Excel

2-2-3 Preparation of wind turbine component for SIMULINK model

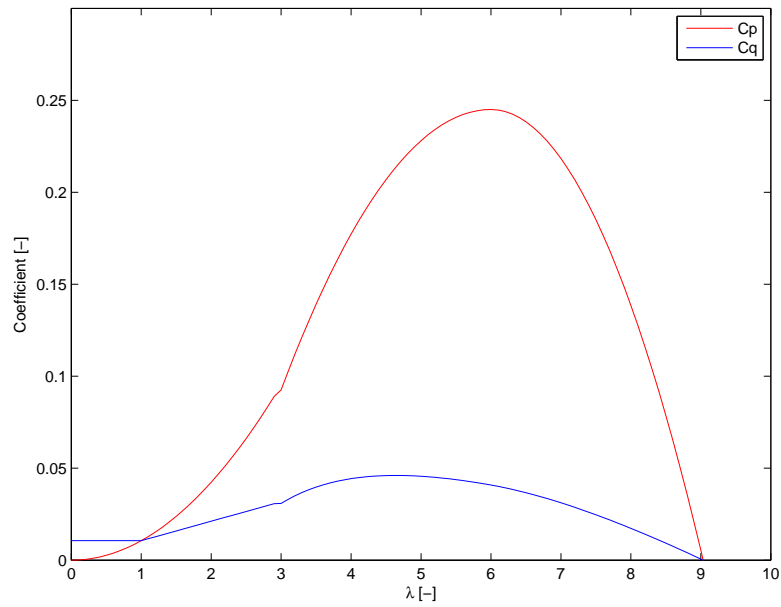
The SIMULINK model simulates the performance of the wind turbine by means of the Ω -U curve and the C_q - λ curve. Usually wind turbines operate at their design tip speed ratio (λ_{design}), the ratio at which the power coefficient is maximum. The C_q - λ curve is the torque coefficient over the tip speed ratio and the Ω -U curve the wind turbine angular velocity over the wind speed. The angular velocity is defined by means of equation 2-1. In order to use the SIMULINK model correctly the design tip speed ratio and the C_q - λ curve for each wind turbine have to be known.

$$\Omega = \frac{\lambda U}{R} \quad (2-1)$$

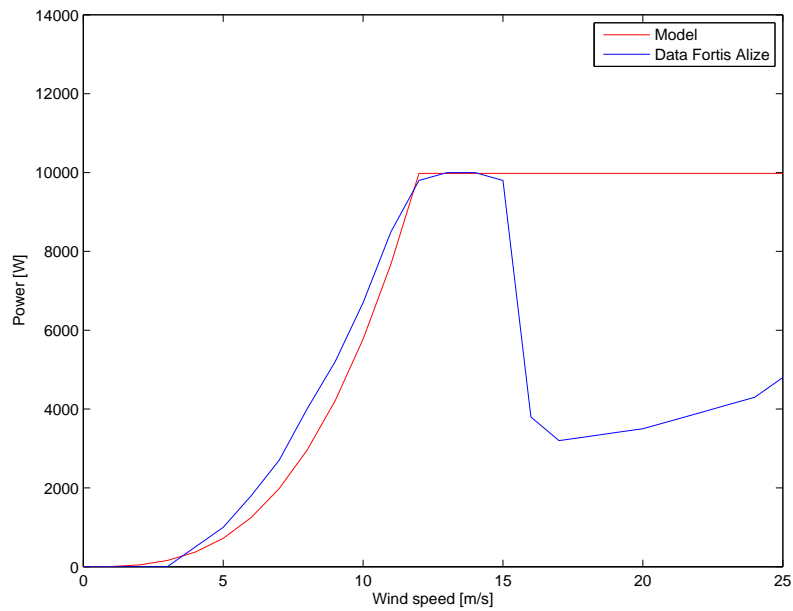
For each wind turbine the λ_{design} and the C_q - λ can be obtained by means of the blade element momentum (BEM) method (see section C-4-4). Before BEM can be applied the blade shape needs to be defined. This is done by linearizing the optimal blade shape (see section C-4-3). The optimal blade shape is a function of the design lift coefficient ($C_{l,design}$) and the design angle of attack (α_{design}) which is found from the aerodynamic properties of the selected airfoil (see section C-4-2). For the multi-bladed windmills the airfoils that were used for the analysis were curved plates with a tube at 0.25 chord. The Fortis Alize wind turbine uses the NACA 4415 airfoil and the Bergey Excel the SH3052 airfoil.

The BEM method results in a power and torque coefficient that describe the performance of the wind turbine at the selected tip speed ratio. The code is used iteratively for a range of tip speed ratios from $\lambda = 0$ to at least the tip speed at which the coefficients are zero. From this the C_p - λ , C_q - λ are obtained for each wind turbine. Figure 2-2(a) shows the curves for the Fortis Alize wind turbine. The curves for other three-bladed high tip speed machines, the Bergey Excel and the Fortis Montana are given in appendix C-4-5.

The BEM code delivered some unexpected results for the multi-bladed wind turbines. It was therefore decided to use the coefficients found with BEM at the design tip speed ratio and use that to approximate the shape of the curves. Figure 2-3(a) gives the C_q - λ curve and the C_p - λ curve for the Turbex windmill. The shape is also similar to what is expected based on literature. By looking at figure C-7 in which the ranges of the power and torque coefficient for different wind turbine types are given, we can conclude that the Turbex curve is within the expected range. It was decided to keep the torque coefficient at $\lambda < 1$ at the same value as the torque coefficient at $\lambda = 1$. This is a somewhat conservative approximation, which was preferred above the risk of assuming a torque too high at small tip speed ratios. With the current approximation the torque at $\lambda < 1$ is already significantly higher than the torque at similar tip speed ratios for three bladed

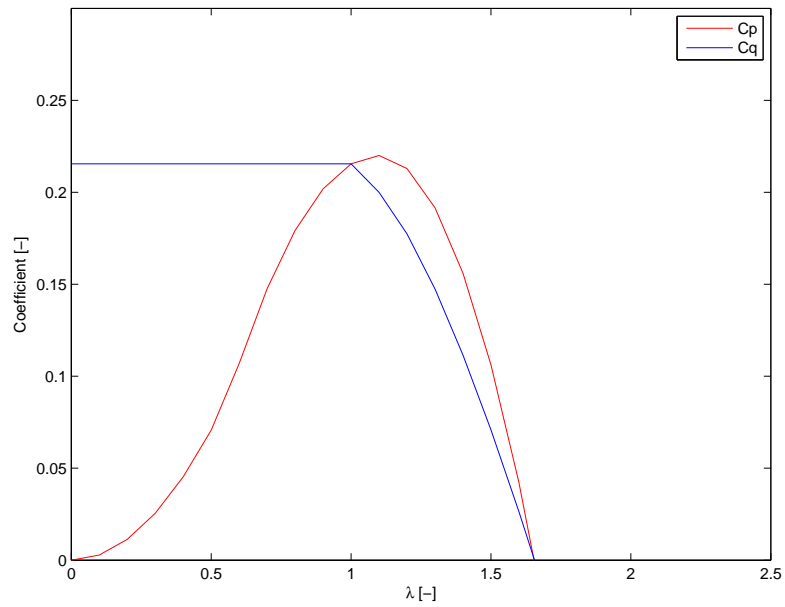


(a) Torque and power coefficient over tip speed ratio

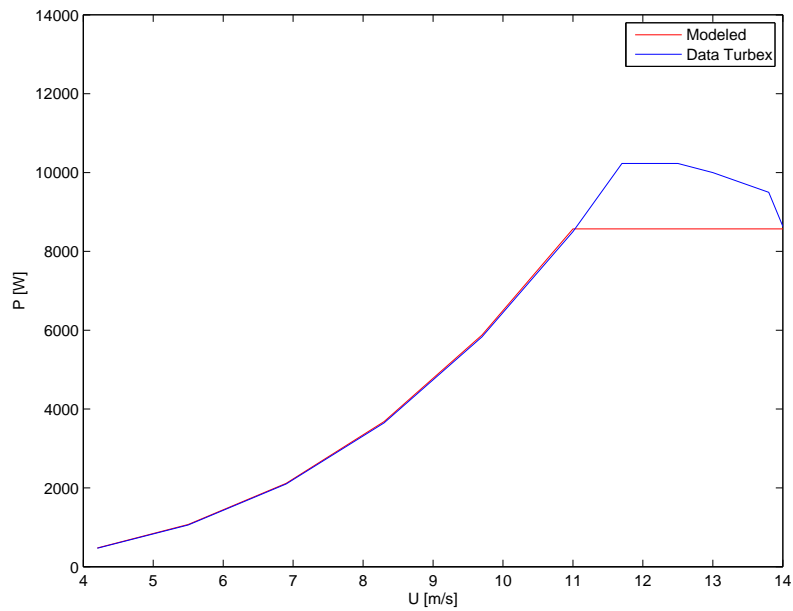


(b) Power curve from model compared to data from manufacturer

Figure 2-2: Fortis Alize wind turbine performance curves



(a) Torque and power coefficient over tip speed ratio



(b) Power curve from model compared to data from manufacturer

Figure 2-3: Turbex wind turbine performance curves

wind turbines. The power curve at design tip speed ratio (i.e. $\lambda = 1$) is in accordance with the data provided by the manufacturer as can be seen in figure 2-3(b).

2-3 Pump component

Figure 2-4 shows that pumps can be categorized into four main groups, namely rotodynamic pumps, special rotodynamic pumps, positive displacement pumps and other pump types, such as ejectors and disc pumps. For reverse osmosis applications the rotodynamic pumps and the positive displacement pumps are of interest.

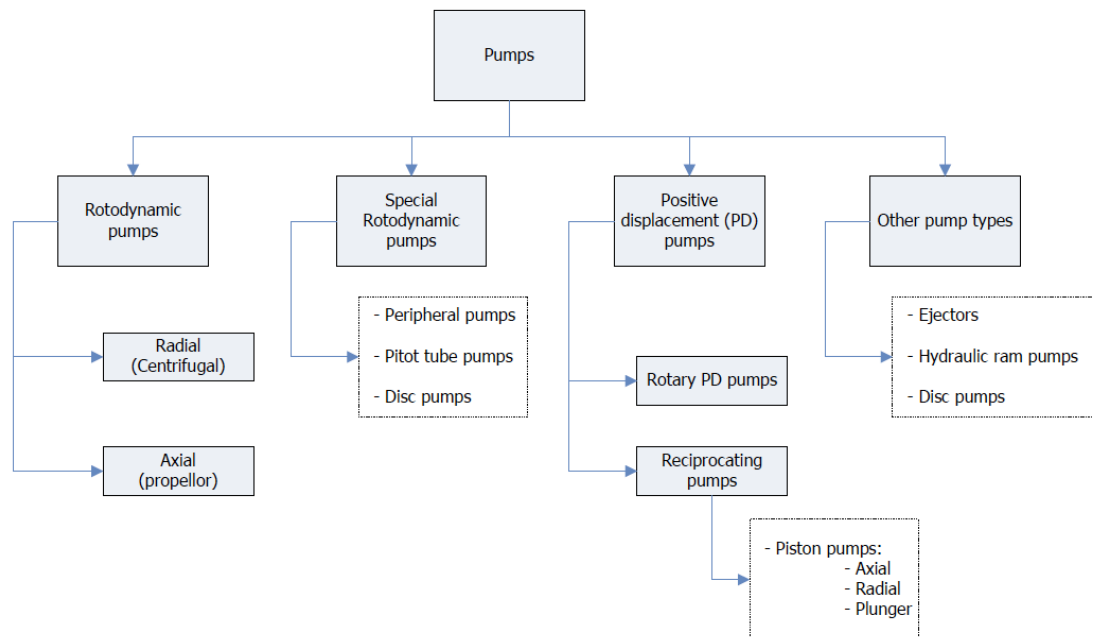


Figure 2-4: Overview of pump types

Rotodynamic pumps Two types of rotodynamic pumps exist, namely radial or axial pumps. In practice radial pumps are often called "centrifugal" and axial pumps "propellor" pumps. The radial flow pumps operate at higher pressures and lower flow rates than axial flow pumps. To achieve optimum efficiency with a centrifugal pump the rotor speed must be matched to the flow/pressure operating point, which is not easy in a system where both the flow and pressure must vary according to the available power.

Positive displacement pumps Positive displacement pumps deliver constant volume of liquid for each cycle at varying discharge pressure or head. The oldest positive displacement pump is the piston pump, which falls into the reciprocating pumps category. A plunger pump is a variant of the piston pump and is often used in small scale reverse osmosis systems with an efficiency typically over 85% for seawater applications. At reduced pressures plunger pumps are much less efficient [Thomson et al, 2002].

Positive displacement pumps generally provide more pressure than rotodynamic pumps. The required feed pressure for the reverse osmosis system varies with the flow rate. Since the flow rate depends on the variable wind speed, the selected pump should be able to deal well with the variability in pressure. Positive displacement pumps fulfill this requirement. For rotodynamic

pumps these pressure changes have however a large effect on the efficiency. The feed pressure changes are especially true for brackish water desalination, the effect is less for sea water applications. Sea water desalination however requires more pressure that generally can not be provided by rotodynamic pumps.

The load case of a centrifugal pump is much more in line with the performance of a wind turbine than the load case of a displacement pump (see appendix C-5). Using a centrifugal pump for medium pressure applications (i.e. brackish water) sounds therefore interesting. Based on the variability of the required feed pressure it was however decided to opt for displacement pumps for both brackish water and sea water desalination.

2-3-1 Selection of promising pumps

The pump selection for sea water desalination is different than for brackish water desalination. For brackish water desalination medium pressure pumps can be used which require much less energy than high pressure pumps. For sea water desalination we need however more pressure than obtained from these medium pressure pumps.

Fortunately the introduction of energy recovery devices reduced the energy requirement and therefore the cost of sea water desalination significantly. With energy recovery the pressure of the brine is reused to get the feed water to the necessary pressure. This can substantially reduce the energy demand of the reverse osmosis system. The amount of reduction depends on the efficiencies of the energy recovery devices and pumps. More details on energy recovery are provided in appendix D-2.

The pumps were selected based on the following criteria:

- **Capacity** The goal is to create a system that can produce around 25 m³/day fresh water. The pump should have the capacity to do realize that (provided that there is sufficient power available).
- **Energy recovery for sea water desalination** With energy recovery the energy requirement is reduced significantly. Pumps that are combined with such a system and manufacturers that have experience with energy recovery are an advantage.
- **Experience** Pump manufacturers that have experience with pressurizing water for reverse osmosis applications are favorable.
- **Saline water** The pumps should be able to deal with the saline water.

The combination of energy recovery devices with high pressure pumps is done by Spectra Watermakers and Danfoss. Ocean Specific is also working on a high pressure pump with energy recovery, called the Xpump. The Xpump promises to be an efficient pump combination for sea water desalination but is at the moment of writing still in development and not available on market yet [Ocean Pacific Technologies,]. Spectra's Clark energy recovery system can also be used in combination with a medium pressure pump to produce high pressure feed water. The size of the Clark pump system is however too small for the water output we strive for (more details in appendix D-2). Spectra Watermakers also developed an integrated high pressure pump and energy recovery device, the Pearson pump. The Spectra Pearson pump was tested in combination with reverse osmosis arrays and a variable power input by Delft University of Technology in 2010.

2-3-2 Selection of pumps for SIMULINK model

Three main pump types were added to the system. The Danfoss pump was implemented for sea water desalination and the Orbit pump for brackish water desalination. The Spectra Pearson pump was also added in order to compare the results of the model with the test results (see appendix G). Despite the good match of the model with the experiment, the Pearson pump was not used for further evaluation in the SIMULINK model because of the uncertainties of the behavior at start up (see appendix G).



Figure 2-5: Danfoss Sea Water Pressure Exchanger (SWPE)

The Danfoss pump is a high pressure piston pump that is directly combined with an energy recovery unit. Danfoss has a lot of experience with desalination and saline water applications. The Danfoss APP1.5/APM1.2 and the APP1.0/APM0.8 pumps were part of the Curaçao and Hatenoer prototype respectively. These two pumps were thus added for the validation of the model (see chapter 4) and also used for evaluation of other configurations in chapter 5 and 6. Also the larger APP2.5/APM1.8 pump was implemented. With these three types the

range of sizes of the Danfoss sea water pressure exchanger (SWPE) is covered.

For the brackish water system Franklin Electrics Orbit GW positive displacement pumps were implemented. The Orbit pump is a medium pressure pump with good salt protection. The pump is based on the helical rotor technology and suitable to drive directly by means of a rotary windmill. The GW0504, GW0704, GW0904 and GW1304 were the types added to the model.

Other pump types can be easily included in SIMULINK model. So when for example the Xpump is launched and successful it can be easily implemented and evaluated within the desired wind driven desalination system.

2-3-3 Preparation of the pump component for the SIMULINK model

The inputs of the pump block for the mechanical configuration are the pump angular velocity and the feed pressure. The outputs for this configuration are the feed flow and the required pump torque. For the electrical configuration the only variable input is the power delivered. The pump shaft speed is fixed. The output is the power required and the feed flow.

Danfoss pump calculations

The Danfoss SWPE energy recovery unit consists of an APP pump and an APM motor, both connected to the same shaft. At start up there can be no energy recovery, so the system will operate as a single APP motor. The flow/rpm ratio of the Danfoss APP pump is constant, and is used to calculate the output flow with the known shaft speed. The power delivered by the wind turbine needs to be higher than the power required by the APP pump, which is calculated by means of equation 2-2. In this equation P_{pump} is the required pump power, q_f is the feed flow in m^3/h and P_f is the feed pressure in bar. CF is the calculation factor and is obtained directly from the datasheet of which the important parts are included in appendix D.

$$P_{pump} = \frac{16.7q_f P_f}{CF} \quad (2-2)$$

Once the system is running the system uses the energy recovery unit. From the SWPE datasheet the flow/rpm ratio could be extracted (see appendix D). Furthermore a relationship between flow, pressure and power required was extracted and implemented as the 'power factor' in the model [Danfoss, 2007]. The power factor (PF) is calculated by means of equation 2-3 in which η_{motor} is the efficiency of the pump electrical motor. The power factors for different pump speeds and feed pressures are calculated. They are very similar and averaging this will result in one power factor for a certain pump type. In table 2-3 the power factors for the different pump types are given. With the energy recovery unit the power needed at a certain shaft speed decreases significantly.

$$PF = \frac{P_{pump}\eta_{motor}}{q_f P_f} \quad (2-3)$$

Table 2-3: Power factors (PF): factor that relates flow, pressure and power required for the Danfoss pumps (see equation 2-2)

Danfoss model	PF
APP1.0/APM0.8	20.1
APP1.5/APM1.2	18.8
APP2.5/APM1.8	49.8

Orbit pump calculations

Based on the data sheets provided by Franklin Electric relations were derived to approximate the flow rate and power required at the pump as a function of pump angular velocity and feed pressure. The datasheets are provided in appendix D-1-4. Equation 2-4 and 2-5 approximate the GW0904 pump and are plotted in figure 2-6 for a range of pump speeds. The derived curves are in line with the data provided by Franklin Electric (see appendix D-1-4). The start-up torque of the GW0904 is 30 Nm.

$$q_f = 7.6 \cdot (1 - 0.0075 \cdot (\frac{Pr}{30})^{1.65}) + 1.65(\frac{n - 900}{200}) \quad (2-4)$$

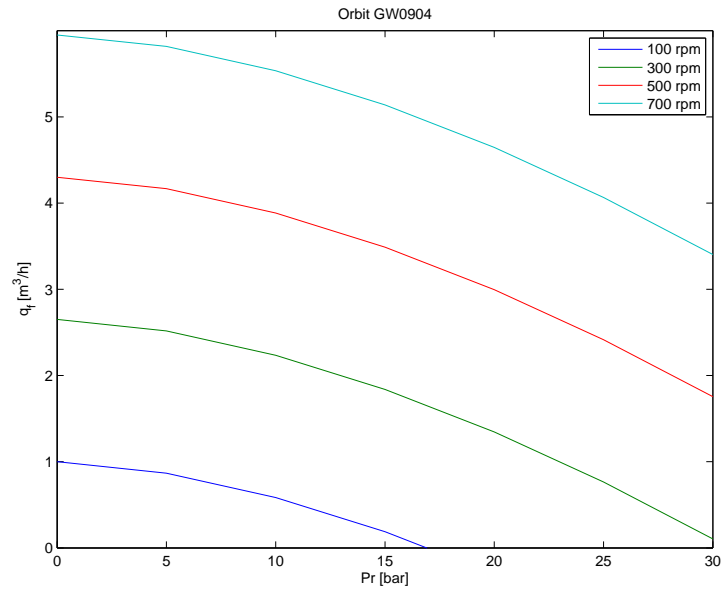
$$P = 1.2 + (\frac{(7.5 - 1.2) \cdot 30}{300} + 0.16\frac{n - 900}{200})\frac{Pr}{30} + 0.2(\frac{n - 900}{200}) \quad (2-5)$$

The GW0504, GW0704 and GW1304 equations were obtained similarly and are given in appendix D-1 together with the figures that illustrate the pump performance (i.e. the feed flow and power over pressure curves for varying pump shaft speed). The start-up torque of the GW0504 is 22 Nm and that of the GW0704 and the GW1304 is 30 Nm.

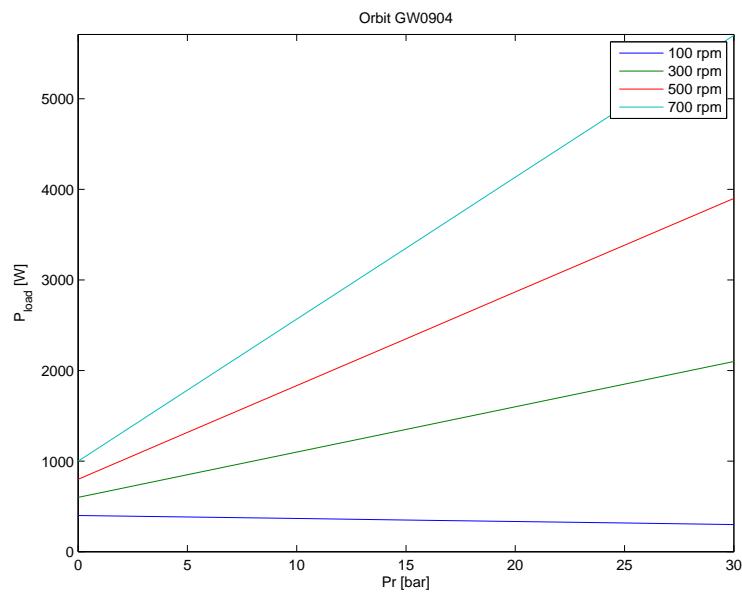
Pearson pump

The Pearson pump of Spectra Watermakers is a positive displacement reciprocating high pressure pump with fixed recovery ratio. The operating pressure of the Pearson Pump varies with pump speed, feed water salinity and feed water temperature. The pump implemented in the SIMULINK model has 20% recovery. Optimum pump speed is between 900-1000 rpm and the operating range of the Pearson pump is between 750-1200 rpm. According to the specifications the energy consumption is 11 Wh per gallon (= 2.9 kWh) for sea water applications and even lower for brackish

water applications [Spectra Watermakers, 2009]. More information on the Pearson Pump model can be found in section G.



(a) Flow rate (q_f) over pressure (Pr) for different pump angular velocities (n)



(b) Power (P_{load}) over pressure (Pr) for different pump angular velocities (n)

Figure 2-6: Performance curves of the Orbit GW0904 pump

2-4 Reverse osmosis array component

The membranes used for reversed osmosis are semi-permeable. They are very permeable for water, but their permeability for dissolved matter is low. A pressure difference across the membrane will force the feed water through the membrane resulting in a permeate (the fresh water) and concentrate (the saline water) flow. The driving force between the reverse osmosis is the applied pressure minus the osmotic pressure. The energy consumption is thus directly related to the salt concentration, since a higher salt concentration has a higher osmotic pressure [van Dijk, 2008]. The principle of reverse osmosis is illustrated in figure 2-7.

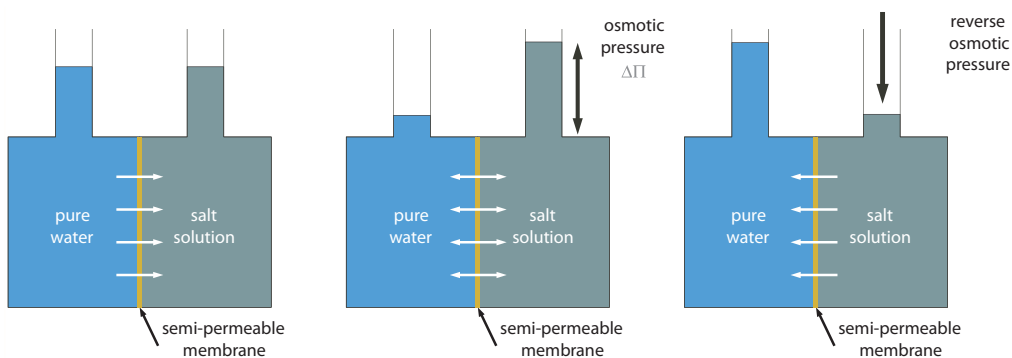


Figure 2-7: Principle of osmosis and reverse osmosis [van Dijk, 2008]

A problem arising with reverse osmosis is the fouling of the membrane. The two fouling processes are biofouling, when retained particulate matter functions as nutrient for biomass, and scaling, which is the formation of salt precipitates. Membrane fouling can not totally be avoided. Effective pre-treatment of feed water will result in a reduction. Existing fouling layers have to be removed by membrane cleaning (more details in appendix E-1) before they damage the membranes permanently. Another problem is concentration polarization (see appendix E). Increasing the velocity along the membrane might be a way to limit concentration polarization. Furthermore the effect can be minimized by using small recovery ratios. In the SIMULINK model the effect of fouling and concentration polarization is not included.

2-4-1 Selection of the reverse osmosis array for the SIMULINK model

Differences between types of membranes are not included in the model. The membranes characteristics can however easily be varied by changing the variables that specify the membranes before running the SIMULINK model (see section 2-4-2). The membranes that are implemented at the moment are of the commonly used spiral wound configuration. These type of membranes have a high specific surface, which is beneficial for the permeate production (see appendix E-1-1).

The variation that can be made in the SIMULINK model is the number of membranes in the array. Arrays with two, three or four membranes are available. With higher flux more membranes can be put in series resulting in more water output. At lower flux the number of membranes should however not be too large as that might result in fouling. The configurations used in the chapters 5 and 6 all used the array with four membranes.

2-4-2 Preparation of reverse osmosis component for SIMULINK model

The flow and concentration of the permeate of an individual membrane element are a function of the flow, temperature, concentration and pressure of the feed. The structure of the SIMULINK model of het RO array is shown in figure 3-6 in chapter 3-5. The inputs and outputs are defined as stated in table 2-4.

The temperature, the pressure of the permeate, the salt concentration of the feed water and the variables that define the membrane characteristics (see table 2-5) are defined before running the SIMULINK model. With these preset values combined with the feed flow delivered by the pump the required feed pressure can be calculated. The feed pressure is one of the inputs for the pump block. The required feed pressure should be high enough to push the water through the membranes resulting in a permeate flow at the given permeate pressure.

Inputs		Outputs	
q_f	Feed flow	Q_c	Concentrate flow
C_f	Feed concentration	C_c	Concentrate concentration
		P_f	Pressure of the feed
		q_p	Permeate flow
		C_p	Permeate concentration

Table 2-4: In- and outputs of RO array model

The model first calculates the small pressure drop in the feed/concentrate channel with equation 2-6, with the variables as defined in table 2-5 [van Dijk, 2008]. These variables were defined in the MATLAB code and not changed in the SIMULINK model. The friction factor λ_{memb} for spiral wound membranes is given by equation 2-7, with the Reynolds number calculated by means of equation 2-8.

$$P_{hydr} = \frac{\lambda_{memb} \rho_{sw} V^2}{2D_h l} \quad (2-6)$$

λ_{memb}	friction factor of membrane
ρ_{sw}	Density of sea water [kg/m ³]
V	liquid velocity [m/s]
D_h	membrane diameter [m]
l	length of membrane [m]
μ	viscosity of the fluid [kg/ s·m]

Table 2-5: Variables of the reverse osmosis array that need to be defined before running the SIMULINK model

$$\lambda_{memb} = 6.23 Re^{-0.3} \quad (2-7)$$

$$Re = \frac{V \cdot D_h}{\mu} \quad (2-8)$$

The osmotic pressure (π_f) is calculated using equation 2-9 [Thomson, 2003], the feed pressure is found by simply adding the small pressure drop of the feed/concentrate channel (P_{hydr}) to the concentrate pressure (P_c). P_c is the same as the feed pressure of the next membrane. For that reason only for the final membrane the concentrate pressure is unknown.

$$\pi_f = \frac{0.002654C(T + 273.15)}{1000 - C/1000} \quad (2-9)$$

In order to calculate the feed pressure of the final membrane (so without the input of the concentrate pressure available), it was assumed that the feed pressure had to be large enough to overcome pressure losses. This means that the net driving pressure was assumed to be zero. The net driving pressure is given by equation 2-10. It can be seen that with P_{hydr} , π_f and P_p known and P_{nd} set to zero the feed pressure can be obtained.

$$P_{nd} = P_f - \frac{\Delta P_{hydr}}{2} - \pi_f - P_p \quad (2-10)$$

With the water mass balance and a know recovery for a membrane element the concentrate water and permeate water flow can be obtained (equation 2-11). The feed water flow is the input of the reverse osmosis array and comes from the pump. The recovery, γ of the membranes is assumed to be 10%. This means that 10% of the feed water is produced as permeate (q_p).

$$q_f = q_c + q_p \quad (2-11)$$

The rejection of a membrane indicates the amount of material rejected by a membrane and provides a relation between the feed and concentrate concentration (equation 2-12). The rejection is assumed to be 99%.

$$R = 1 - \frac{C_p}{C_f} \quad (2-12)$$

The only remaining unknown is the concentrate concentration (C_c). Applying the mass balance equation, i.e. equation 2-13, resolves this problem.

$$q_f C_f = q_c C_c + q_p C_p \quad (2-13)$$

The total permeate flow and total permeate concentration are a function of the outputs of the individual membranes. The total permeate flow can be found by simply adding the permeate flows of the individual membranes and the permeate concentration is found by using equation 2-14).

$$1 = \frac{q_{p,total} C_{p,total}}{q_{p,memb1} C_{p,memb1} + q_{p,memb2} C_{p,memb2}} \quad (2-14)$$

2-5 Coupling component

Different methods of coupling between wind turbine and pump are possible. Figure 2-8 illustrates some possible system configurations. Hydraulic couplings are not considered due to the focus on simple and available off-the-shelf configurations.

Configuration A is the mechanical coupling with a gearbox. The gearbox consists of a transmission system with a certain transmission ratio, i , and has an efficiency depending on the type of transmission. The transmission ratio and the efficiency can be easily varied in the SIMULINK model. The mechanical coupling is a direct coupling and the pump exerts a moment on the wind turbine as well. How this works is explained in section 3-1.

Configuration B is the direct electrical coupling and can be interesting when the wind turbine generates enough torque to run the pump for long periods of time. That is the case when the wind speed is sufficiently high. Evaluation of this configuration is not part of this research. The wind speed in Somaliland is in certain months relatively low in the mornings. Operating an

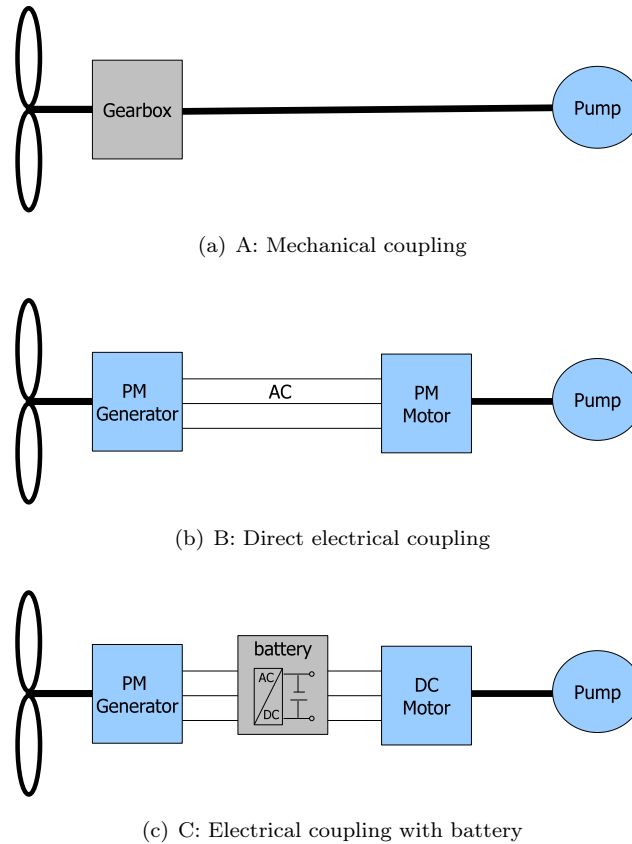


Figure 2-8: Overview of wind driven reverse osmosis desalination system configurations

electrical system without any batteries in this region is therefore expected to result in very low water output. For future research it is however interesting to evaluate this configuration, especially in combination with a larger wind turbine and/or a different location. Changing those conditions might result in the electrical configuration being able to provide sufficient power to drive the pump directly (at least most of the time).

Configuration C is the electrical coupling with battery. The battery capacity is the input for the SIMULINK model, as well as the generator-, converter-, battery- and motor-efficiency. An electrical coupling with a battery experiences many losses. Batteries are not cheap either. Storing the energy in high wind speed periods might however compensate for the low wind speed periods. Furthermore the wind turbine can operate at its design speed because it is operating separately from the pump (for details read section 3-1). If the advantages of the electrical coupling with battery outweigh the disadvantages is part of this research. In section 4-2 the prototype with electrical coupling of Hatenoer Water is compared with the model results. From this evaluation reasonable values for the efficiencies were found (see also table 2-6). These efficiencies were then used to evaluate new promising configurations of which the results are given in chapter 5.

2-5-1 Preparation of the coupling component for SIMULINK model

The equations describing the different coupling types are kept as simple as possible. They are performed in the SIMULINK model and will therefore be explained in the chapter that discusses the model (i.e. chapter 3).

Some variables need to be defined before starting the Wind2Water simulation. These variables are listed in table 2-6.

Table 2-6: Variables of the coupling system that need to be defined before running the SIMULINK model

Symbol	Description	Standard value
i	transmission ratio	<i>varied</i>
η_{mech}	Efficiency of mechanical coupling	88 %
η_{gen}	Efficiency of generator	90%
η_{conv}	Efficiency of the converter	90%
C_{bat}	Battery capacity	400 [Ah] · 48 [V]
η_{bat}	Efficiency of the battery (same for charging and discharging)	80%
DOD	Depth of discharge	0.75%
η_{mot}	Efficiency of the motor	90%
n_{pump}	Pump shaft speed for electrical coupling	<i>varied</i> [rpm]

Part II

SIMULINK model and validation

Chapter 3

Description of the Wind2Water SIMULINK model

The performance of the Wind2Water system can be calculated in different ways. One way could be to do the calculations in EXCEL. This will probably suffice, but when we want to chose between different components and add all these different calculations in EXCEL, it is hard to keep a proper overview. The same is true for performing all calculations in MATLAB. With SIMULINK it is easier to keep a good overview. Also SIMULINK works better to make a dynamic simulation. This allows for better modeling of the start-up torque. Furthermore the influence of the difference in required and delivered torque can be included relatively simple.

The Wind2Water model consists of four main blocks; the windturbine block, the transmission block, the pump block and the RO block. The water tank is added to simulate the water storage capability, but is of less importance for the evaluation of the system at this point. Table 3-1 states which parts are present in the model. Two main transmission configurations exist in the model. The mechanical coupling with gearbox and different gearbox ratios and the electrical coupling with a battery. The Wind2Water model is organized in such a way that it is easy to implement additional component types in the future (such as a new wind turbine or pump).

Table 3-1: Parts available in the model

Wind turbine	Transmission	Pump	RO
Turbex	Mechanical coupling	Danfoss APP1.0/APM0.8	2 membranes
M5015	Electrical coupling	Danfoss APP1.5/APM1.2	3 membranes
Fortis Montana		Danfoss APP2.5/APM1.8	4 membranes
Fortis Alize		Orbit GW0504	
Bergey Excel		Orbit GW0704	
(BEM code)		Orbit GW0904	
		Orbit GW1304	
		Spectra Pearson LB1800	

3-1 Overview of the Wind2Water model

The Wind2Water model is different for an electrical coupling than for a mechanical coupling. Section 3-1-1 explains how the mechanical model works and section 3-1-2 how the electrical system works.

3-1-1 Mechanically coupled system

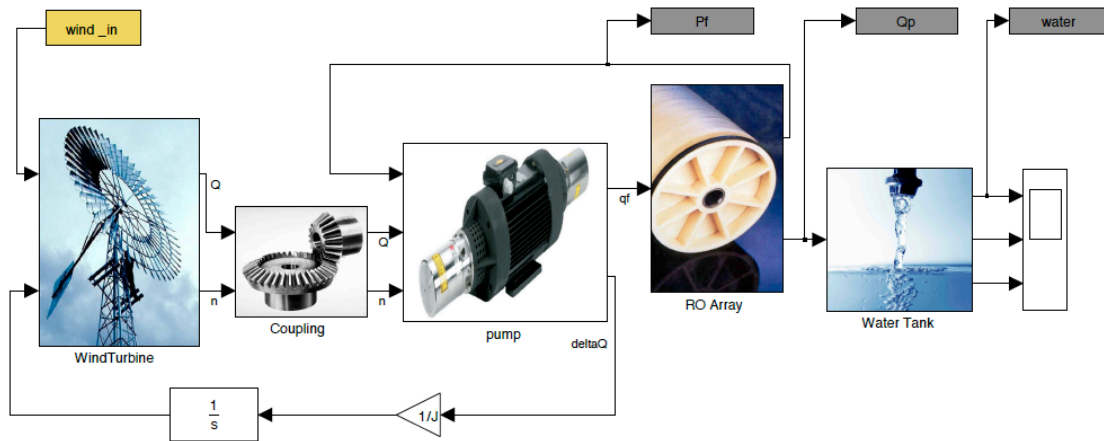


Figure 3-1: SIMULINK model of the mechanically coupled wind driven reverse osmosis system

The overall mechanically coupled system is shown in figure 3-1 and a schematic representation is given in figure 3-2. The wind drives the turbine which generates a certain amount of torque. This torque has to meet the torque requirements of the pump. If the torque delivered by the windmill is too low, the angular velocity of the windmill will decrease, such that the torque increases. If the torque of the windmill is higher than the torque required by the pump, the windmill will run faster which will to decrease the torque. The difference in torque delivered by the windmill and required

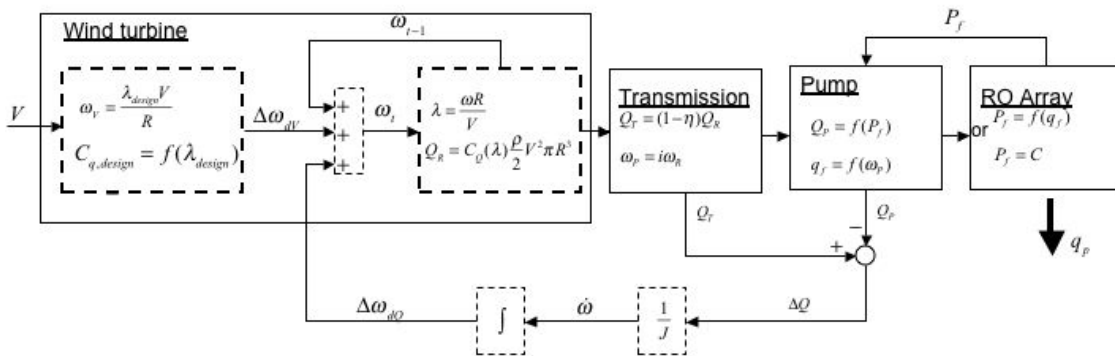


Figure 3-2: Overview of the wind driven reverse osmosis system with mechanical coupling

by the pump causes an acceleration (or deceleration) of the windmill. This acceleration is equal to dQ/J , where J is the inertia of the entire system and is defined as $J = J_{rot} + J_{gear} + i^2 J_{pump}$ in $kg \cdot m^2$. The entire system for a non variable transmission can be described by the differential equation 3-1. Inertia is the product of the rotating weight with the square of its radius of gyration,

see equation 3-2.

$$(J_{rot} + J_{gear} + i^2 J_{pump})\dot{\omega} = Q_{rot}(\omega, U) + Q_{gear}(\omega) + iQ_{pump}(\omega) \quad (3-1)$$

$$J_{rot} = \int m(r)r^2 dr \quad (3-2)$$

$$J_{pump} = 0.03768\left(\frac{P}{N}\right)^{0.9556} \quad (3-3)$$

The moment of inertia of the pump is usually obtained from the manufacturer. Literature gives some empirical equations, which can be used to obtain a rough idea of the inertia when data from a manufacturer is not directly available. Thorley presented an equation for centrifugal pumps, equation 3-3, where P, the pump mechanical power in kW and N, the pump angular velocity in 1000 rev/min (i.e. 1000 rpm) [Larsen, 2006]. The pump inertia of our system can be approximated by assuming a power of 6.6 kW and an angular velocity 1200 rpm, which is representative for the values of the prototype on Curaçao. Applying these values results in a pump inertia of $0.19 \text{ kg}\cdot\text{m}^2$. Looking at different existing gearboxes and transmission configurations shows that the inertia of a gearbox for our system will not exceed $0.01 \text{ kg}\cdot\text{m}^2$ (website Apex Dynamics). A multi-bladed rotor can be seen as a massive disk of which the inertia is $J = 1/2mR^2$. Now assume a rotor consisting of 8 blades of each 5 kg and a radius of 3 meter. The inertia of this rotor is approximately $180 \text{ kg}\cdot\text{m}^2$. This is a conservative calculation for the rotor inertia because the rotors used will most likely be larger and heavier, but it shows that inertia of the rotor (J_{rot}) is dominant. For further calculations the inertia of the pump and gear can therefore be neglected.

With the integral of the acceleration due to the difference in torque and the difference in angular velocity due to a varying wind speed the new angular velocity of the wind turbine can be calculated (see equation 3-4).

$$\begin{aligned} \omega_{new} &= \omega_{new_{t-1}} + d\omega_{dQ} + d\omega_{dU} \\ &= \omega_{new_{t-1}} + \int_{t-1}^t \frac{dQ}{J} dt + d\omega_{dU} \end{aligned} \quad (3-4)$$

With the new angular velocity the torque of the windmill will converge to the required pump torque. The pump torque is a function of the membrane feed pressure which is in its turn a function of the salt concentration of the water. When the torque requirement is met, the system will start to deliver water as a function of the pump angular velocity.

3-1-2 Electrically coupled system

The system with an electrical coupling works different. The windturbine and the pump operate independently in that case. In figure 3-3 the electrical coupling as programmed in SIMULINK is shown and in figure 3-4 its schematic representation. The model of the electrical coupling is basic, because this is sufficient to get a feeling of the performance of the system. It includes losses for the generator, which also incorporates the rectifier loss, losses for the pump motor, losses for the inverter and if a battery is included, the battery losses at charging and discharging are also applied.

The 'No Battery' configuration simply checks if the delivered power is larger than the required power. The configuration with battery is a function of the capacity of the battery bank (C_{bat}), the power delivered by the generator (P_{gen}), the power required by the pump including the inverter

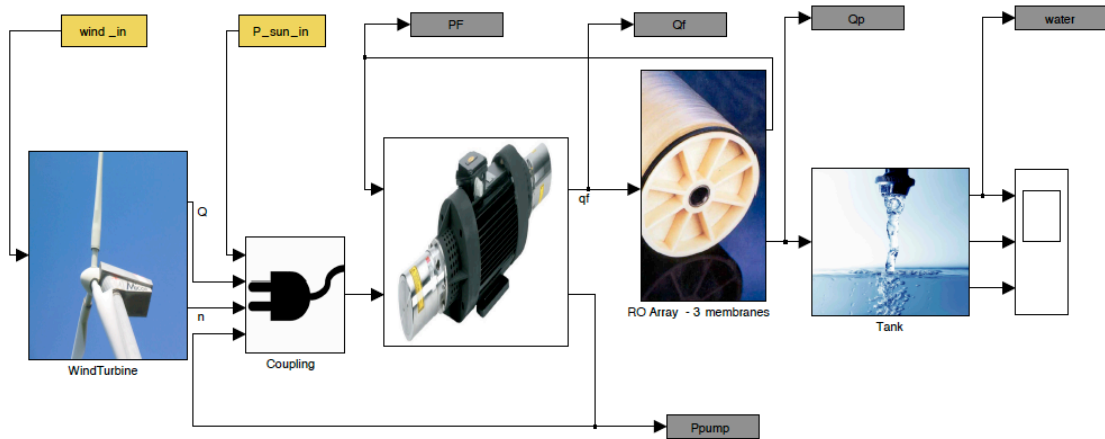


Figure 3-3: SIMULINK model of the electrically coupled wind driven reverse osmosis system

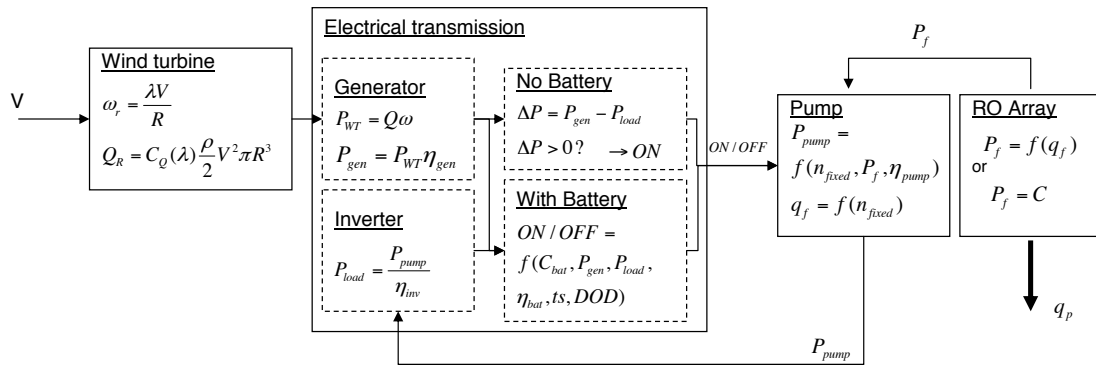


Figure 3-4: Overview of the wind driven reverse osmosis system with electrical coupling

loss (P_{load}), the battery efficiency (η_{bat}) and the depth of discharge (DOD), which is the amount that the battery can be discharged without decrease of performance. The time step, ts , is used to change from power to capacity/energy and vice versa. A detailed description of the battery model is given in section 3-3-2. If there is enough power available the coupling block will provide the 'ON' signal to the pump block and clean water will be produced in line with the operating speed of the pump.

3-2 Wind turbine

The wind turbine module uses the wind to generate power, P , and angular velocity, ω . The torque delivered by the wind turbine is calculated by means of equation 3-5.

$$Q = \frac{P}{\omega} \quad (3-5)$$

The input of the wind turbine module is the wind speed [m/s] and the outputs are torque in Nm and angular velocity in rpm. Table 3-2 gives an overview of the wind turbines that are available in the SIMULINK model.

Table 3-2: Wind turbines available in the SIMULINK model

Multi-bladed windmills	Three-bladed windmills
<i>low speed; high start up torque</i>	<i>high speed; low start up torque</i>
M5015 Turbex	Fortis Montana Fortix Ailze Bergey Excel

In chapter 2-2 and C-4 it is described how the C_q - λ curve and the design tip speed were defined for each wind turbine. The design tip speed is used to calculate the Ω - U curve by means of equation 3-6.

$$\Omega = \frac{\lambda U}{R} \quad (3-6)$$

These curves are used in Simulink to select the wind turbine angular velocity at a certain wind speed and the correct torque coefficient at the given tip speed ratio. The tip speed ratio changes due to the influence of the pump load until the system converged to the operating point.

3-3 Coupling

The coupling between the wind turbine and the pump can be done electrically or mechanically. A mechanical coupling can have a fixed or a variable transmission. At the moment only a fixed mechanical transmission is incorporated in the model.

3-3-1 Fixed mechanical transmission

The angular velocity of the rotor (n_{rot}) has to be increased in order to comply with the pump shaft speed requirements, see equation 3-7. Gears can be used to realize all sorts of transmission ratios. These gears together with the bearings and other components in the transmission induce losses on the system, which are combined under the term η_{mech} . With this the torque that arrives at the pump (Q_{pump}) can be calculated (equation 3-8).

$$n_{pump} = n_{rot}i \quad (3-7)$$

$$Q_{pump} = Q_{rot}(1 - \eta_{mech})i \quad (3-8)$$

At the moment the losses as defined in the report on the Curaçao prototype are implemented (i.e. 12%) [Rabinovitch, 2008]. For detailed designs this can easily be changed to data provided by manufacturers. The losses are assumed to be independent of shaft speed.

3-3-2 Electrical transmission

An overview of the electrical transmission is given in section 3-1. With an electrical coupling the windturbine is connected to a generator that converts the mechanical energy to electrical energy, usually AC current.

The generator can be directly coupled to a motor with a converter in between. Converters consist of a rectifier and an inverter. The rectifier changes the AC current to DC and the inverter changes the DC current back to AC. This conversion comes with losses, but by doing this the electrical energy can be converted to the desired Ampere and Voltage. A converter is also capable of smoothening the electrical energy, which is helpful within a circuit applied to a wind turbine. The last effect is however not included in the SIMULINK model.

Another option is to connect the windturbine to a battery bank. This implies extra losses, but the generated power can be stored until the system 'saved' enough energy to drive the pump at the pre-installed pump speed (n_{fixed}).

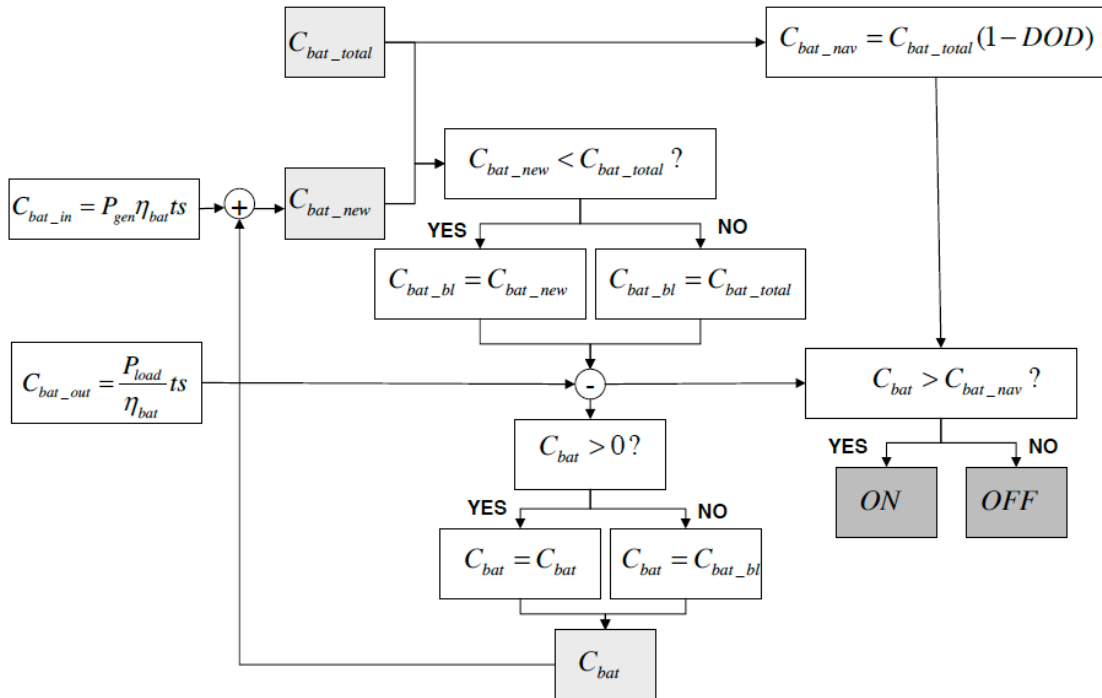


Figure 3-5: Overview of the battery model

Figure 3-5 gives an overview of the battery model. The windturbine generator delivers a certain power for a certain moment in time. This power production is then assumed to apply for a certain amount of time until the next point in time provides the next power estimate. This amount of time is called the time step, ts . Multiplying the generator power with the battery charging efficiency and the time step results in the energy added to the battery ($C_{bat_{in}}$) in Wh. Adding this to the energy already present in the battery gives you the new battery energy ($C_{bat_{new}}$). This is however limited by the maximum capacity of the battery. The energy needed to drive the pump is then extracted from the battery bank. The battery bank can not be discharged more than prescribed with the depth of discharge percentage, so the battery should still be full enough after extraction of the energy to drive the pump otherwise the system will shut OFF. Also when the battery does not have enough capacity to deal with the pump load, the pump stops and the battery starts charging. The battery capacity is obtained by multiplying the current of the battery bank with the voltage.

3-4 Pump

Three main pump and energy recovery systems are involved in the model, namely the Danfoss high pressure pumps, the Spectra Pearson pump and the Orbit medium pressure pumps. Table 3-3 gives the pump types available in the SIMULINK model.

Table 3-3: Pump types available in the SIMULINK model

Manufacturer	Orbit	Danfoss	Spectra Watermakers
Application	Brackish water	Sea water	Sea water
Pump type available in SIMULINK	GW0504 GW0704 GW 0904 GW1304	APP1.0/APM0.8 APP1.5/APM1.2 APP2.5/APM1.8	Pearson LB1800

The relations that describe the performance of the pumps are derived from the data sheets of the manufacturer as explained in chapter 2-3-3. The inputs of each pump block in the model are the pump shaft angular velocity and the pressure of the feed water. For the electrically coupled system the output is the power required by the pump load (P_{load}) and the feed water flow rate. These variables follow directly from the derived equations given in chapter 2-3-3. For the mechanically coupled systems the output is the difference in torque between the delivered torque from the wind turbine and the required pump torque (δQ) and the feed water flow rate. The required pump torque is calculated from the pump power output and the shaft angular velocity by means of equation 3-5.

3-5 RO Array

The SIMULINK model contains three RO arrays. Available are an array with two membranes, an array with three membranes and an array with four membranes. More membranes in an array results in higher recovery and therefore more permeate output. If the flow rate is however too small the risk of fouling is higher with more membranes. Fouling reduces the performance of the membranes and should be avoided as much as possible.

This section will explain how the RO array is modeled in SIMULINK. The flow and concentration of the permeate of an individual membrane element is a function of the flow, temperature, concentration and pressure of the feed. The structure of the SIMULINK model of the RO array is shown in figure 3-6, and the inputs and outputs are defined as stated in table 2-4 in chapter 2-4. The permeate pressure, P_p and the temperature are also inputs for the RO element model, but they are global variables and not passed from one block to the other.

3-6 Water tank

The SIMULINK model does contain a water tank of which the principle is illustrated in figure 3-7. The water tank is filled with the permeate flow from the reverse osmosis system. The water is consumed at a flow rate, q_{cons} . The model checks if there is enough water in the tank for consumption. It also checks if there is too much water produced. This results in water overflow.

The evaluation of the system configurations is however done by means of the total permeate water output regardless of the size of the tank. The total water output was calculated with equation

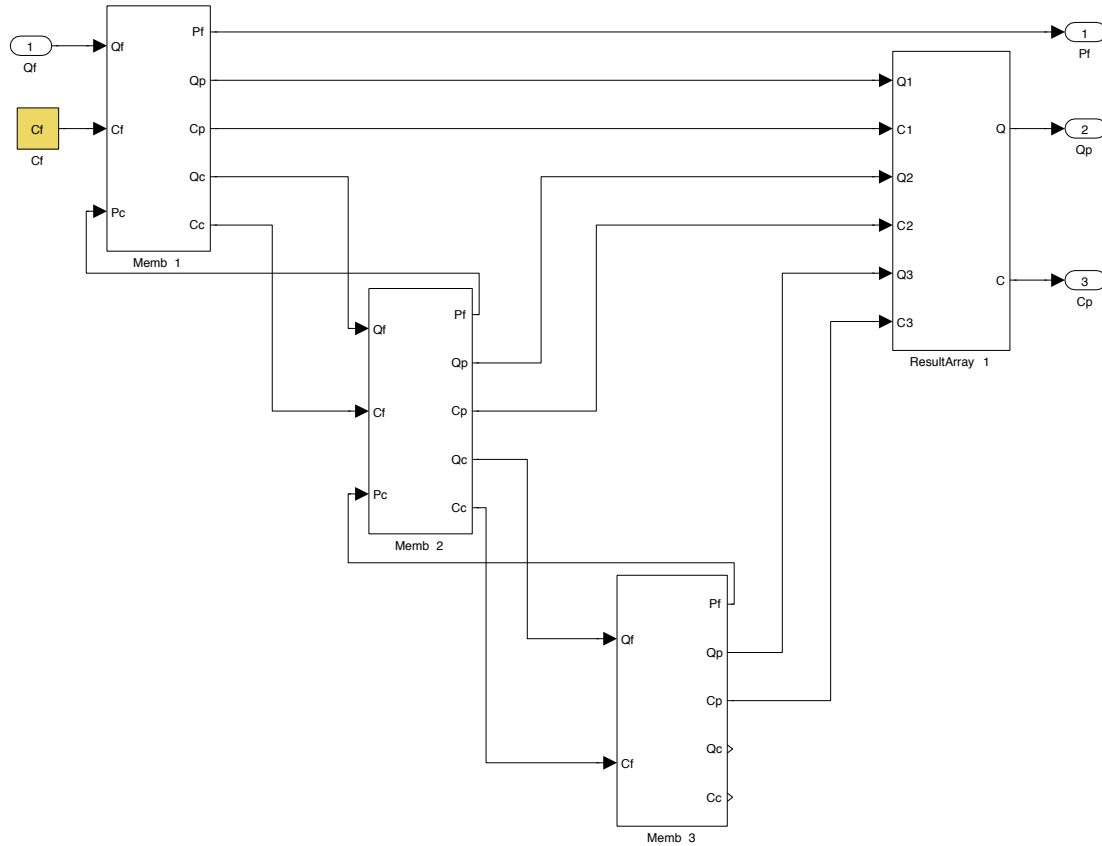


Figure 3-6: Structure of Simulink model of array of RO elements

3-9 in which q_p is the permeate flow rate in m^3/h and ts is the amount of hours between two consecutive moments in time (usually set at 1, meaning that every step represents an hour). The total water output (W_{total} in m^3) is then divided by the total simulation time in hours and multiplied by 24 hours to get the daily water output (equation 3-10).

$$W_{total} = \int_0^t q_p t s dt \quad (3-9)$$

$$q_{p,day} = \frac{W_{total}}{t} \cdot 24 \quad (3-10)$$

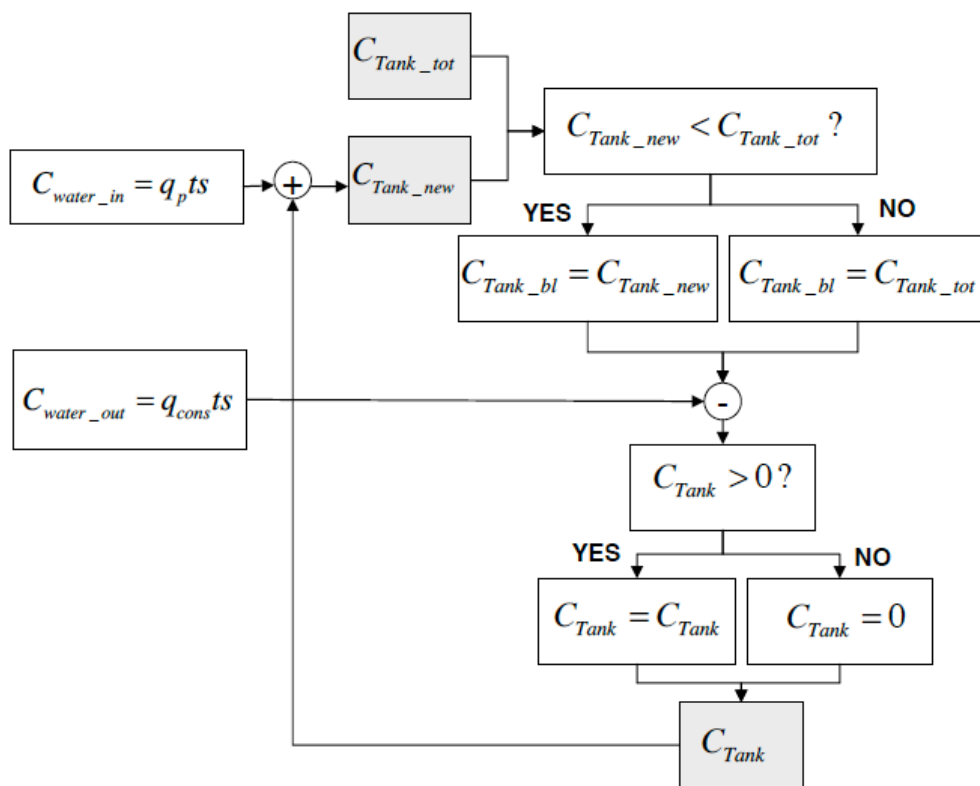


Figure 3-7: Overview of the water tank in the SIMULINK model

Validation of the Wind2Water model

In this chapter the Wind2Water model will be validated by means of the experiments done on Curaçao by Delft University of Technology on a mechanical configuration (see section 4-1) and by means of the experiments of Hatenoer water on an electrical configuration (see section 4-2).

Before the validation was done, the model was verified by means of calculations in EXCEL. The results are given in appendix F. It showed that the main operation of the Wind2Water model is correct. The torque and angular velocity of the pump and windmill are converging to its operating point. In the case of non constant wind input the model slightly differed from the hand calculations. This was probably caused by a small time-lag. Overall it could however be concluded that the model is operating sufficiently well.

4-1 Comparison with data from Curaçao

On Curaçao the first prototype was built and tested. The prototype consisted of a M5015, a multi-bladed windmill with a diameter of 5 meters, a mechanical transmission with transmission ratio 1:40, a Danfoss APP1.5/APM1.2 high pressure pump and 2 SWC1-4040 (4 inch) Hydanautics membranes. The experimental data can be found in figure I-1 in appendix I.

The characteristics of the windmill and the pump where incorporated in the SIMULINK model and the results were compared with the results from the experiments done on Curaçao. The data set from the Curaçao experiment is small, so care should be taken when drawing strict conclusions based on this. It does however provide a good initial understanding of the performance of such a mechanically coupled windmill reverse osmosis system.

To make the SIMULINK model work, assumptions had to be made to define certain parameters. Table 4-2 gives an overview of these parameters and the initial assumed values, the base values. Figure 4-1 shows the performance of the model with the parameters at the base values. From this base configuration the parameters were changed one by one to observe the influence on the model output. The mass of the blade M_b was not changed, since changing the mass will have a similar effect as changing the pump inertia (J_p). Increasing the blade mass or the pump inertia both increase the overall system inertia. It is therefore sufficient to evaluate only one of these parameters.

Table 4-1: Values of the variables in base configuration of the mechanical Wind2Water model (configuration I)

Variable	Value	Description
C_f	40000 mg/L	Salt concentration in feed water
M_b	5 kg	Mass per blade
$\eta_{coupling}$	0.12	Losses in the coupling
J_p	0 kg/m^2	Inertia of the pump
δ_{pump}	-0.9 Nm	Torque threshold margin

Table 4-2: Configuration parameters of the mechanical Wind2Water model that are varied to evaluate the influence of each parameter on the system output

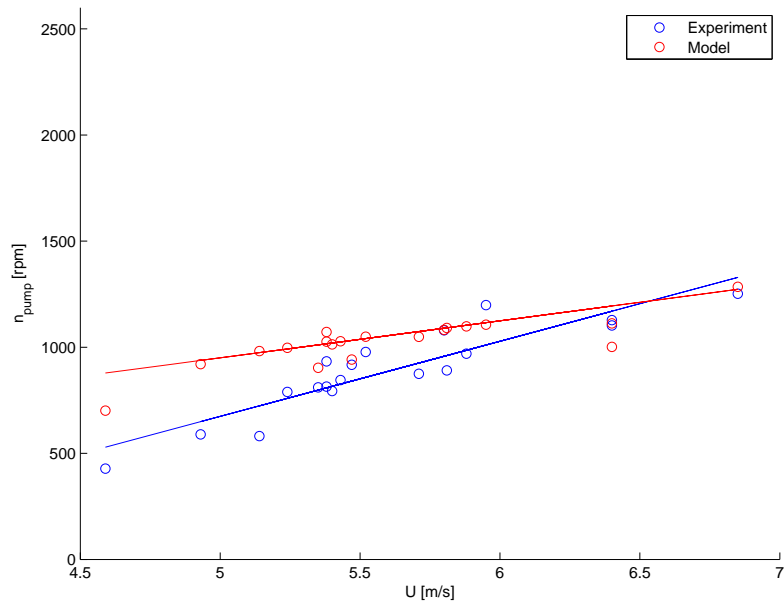
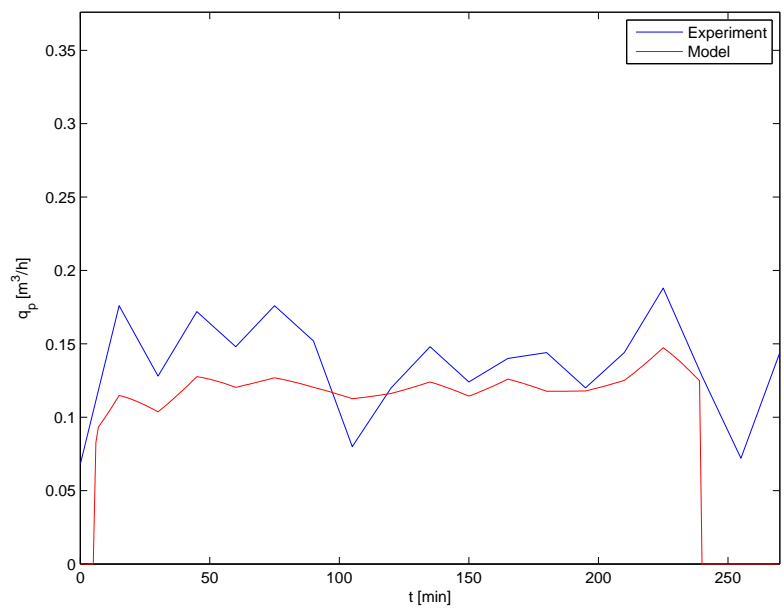
Variable	Unit	I	II	III	IV	V
C_f	mg/L	40000	35000	40000	40000	40000
M_b	kg	5	5	5	5	5
$\eta_{coupling}$	-	0.12	0.12	0.32	0.12	0.12
J_p	kg/m^2	0	0	0	10	0
δ_{pump}	Nm	-0.9	-0.9	-0.9	-0.9	3

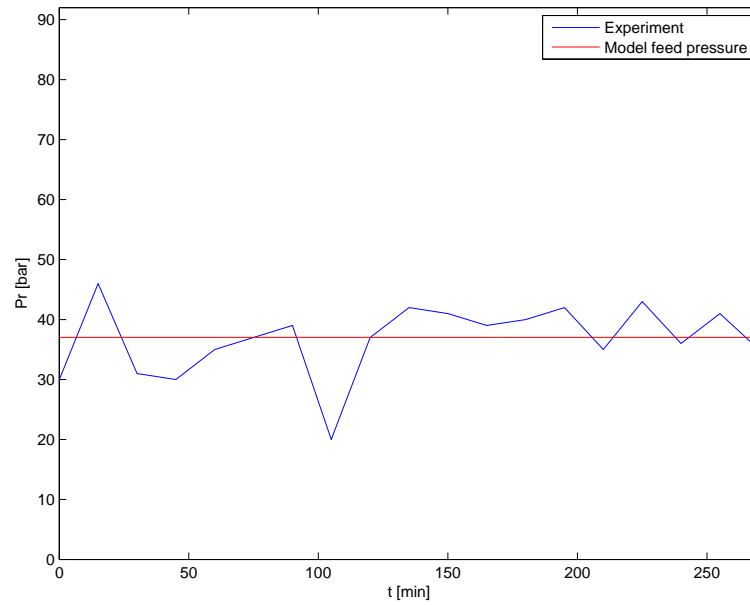
The salt concentration in the feed water, C_f , determines the required feed pressure that has to be delivered by the pump. The model assumes a constant feed pressure and has to be within a reasonable range of the variable feed pressure of the experimental data. Figure 4-2 shows that a salt concentration of 40.000 mg/L results in a good feed pressure match, assuming a smaller salt concentration results in a feed pressure that might be too small. The figures in appendix I also show that reducing the feed water salt concentration to 35000 mg/L results in slightly worse results compared to the experimental data, for the angular velocity as well as the permeate flow.

The threshold for the pump torque margin, δ_{pump} , is implemented to define a range around the operating point where the pump runs as well. Increasing this parameter reduces the occurrence of start up issues in the model. The effect of changing this parameter to 3 Nm is very small. The permeate flow over time does have slightly better results for the larger torque margin. It is however preferred to keep this torque margin as close to zero as possible. The initial value of 0.9 Nm is therefore chosen for the final configuration.

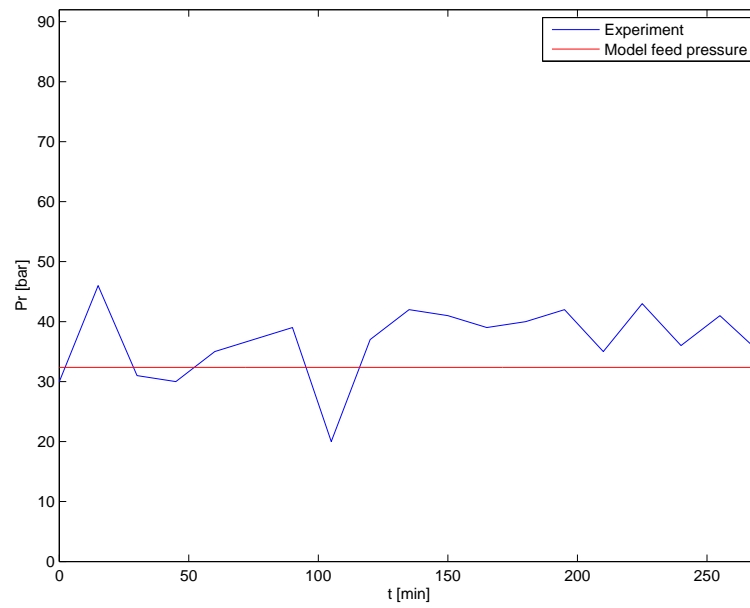
An increased system inertia results in a slower response on torque differences. Setting the pump inertia to 10 kg/m^2 is an extreme case of increasing the system inertia as can be seen in figure 4-3. The high torque indicates that the model does not have time to respond to the torque differences. The system angular velocity therefore increases not as fast, resulting in a larger error.

Finally the losses in the mechanical coupling, $\eta_{coupling}$ can be changed. The mechanical loss in the base configuration was taken from the report on the experiment in Curaçao [Rabinovitch, 2008], this was however an assumption and not a measurement. Increasing the loss, decreases the angular velocity of the pump, making it a better match around the mean wind speed. In the same time it also decreases the permeate outflow, resulting in a larger error on the permeate outflow around mean wind speed.

(a) Pump angular velocity (n) over wind speed (U)(b) Permeate outflow (q_f) over time (t)**Figure 4-1:** Result of the model with the parameters of the mechanical Wind2Water model at base value (see table 4-2)

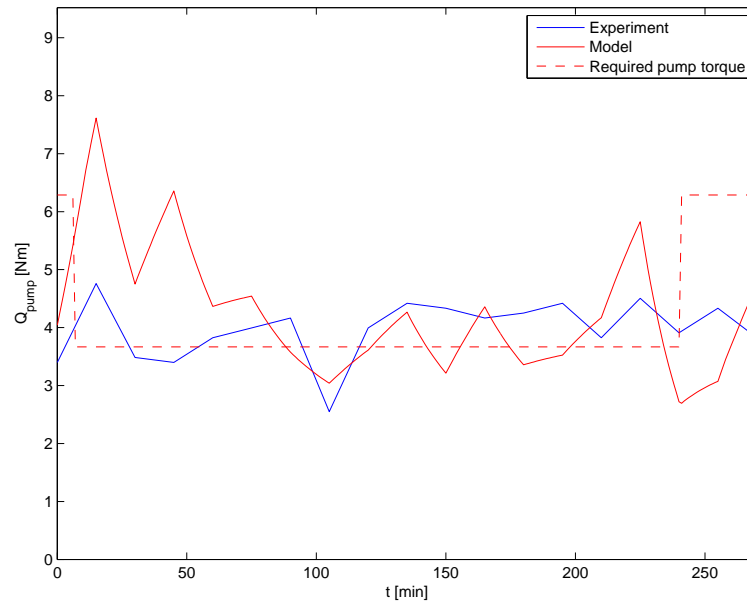
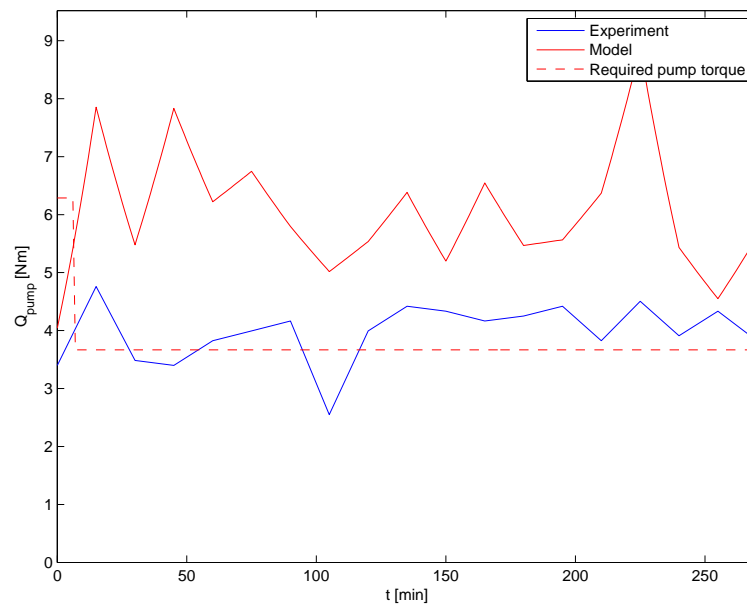


(a) Salt concentration feed water, $C_f = 40000$ mg/L



(b) Salt concentration feed water $C_f = 35000$ mg/L

Figure 4-2: Influence of changing the feed salt concentration on pressure over time

(a) Inertia of system according to base configuration ($J_p = 0 \text{ kg/m}^2$)(b) Increased system inertia ($J_p = 10 \text{ kg/m}^2$)**Figure 4-3:** Influence of changing the system inertia on the delivered pump torque over time

The permeate outflow is a direct function of the rotational angular velocity of the pump and the pressure of the feed water. From figure 4-2 it followed that the difference in feed water pressure is small during the experiment. Furthermore the figures in appendix I show that the influence of these small variations in pressure are negligible. For sea water desalination the permeate outflow

can therefore be regarded as a direct function of the rotational angular velocity only. If the model provides a good match for the permeate outflow it is expected to match similarly well with the pump rotational angular velocity. This is however not the case and changing one of the variables does not make a difference, since it can not change the fixed pump angular velocity and permeate flow relation.

It should be noted that the pump has a minimum operational speed of 700 rpm according to the manufacturer. The experimental data give values starting from 500 rpm. An explanation for the difference in the pump angular velocity and permeate flow relation might thus be accounted to a consistent measurement error. Another explanation can be that the data on the data-sheet on which the model is based is incorrect. This is however unlikely, since that implies that they are promoting a higher angular velocity requirement (i.e. more power) for the same permeate flow.

For the selection of the optimal configuration the focus was on two points:

1. **Permeate flow match:** As said before the relation between permeate flow and pump angular velocity can not be improved and the difference is most likely caused by a measurement error. The permeate flow is the most important parameter for the evaluation of the system and a good match of this parameter was aimed for.
2. **Match around mean wind speed (5.6 m/s):** Because the experimental data set was limited it was decided to focus on a good match around mean wind speed where the most data points are located

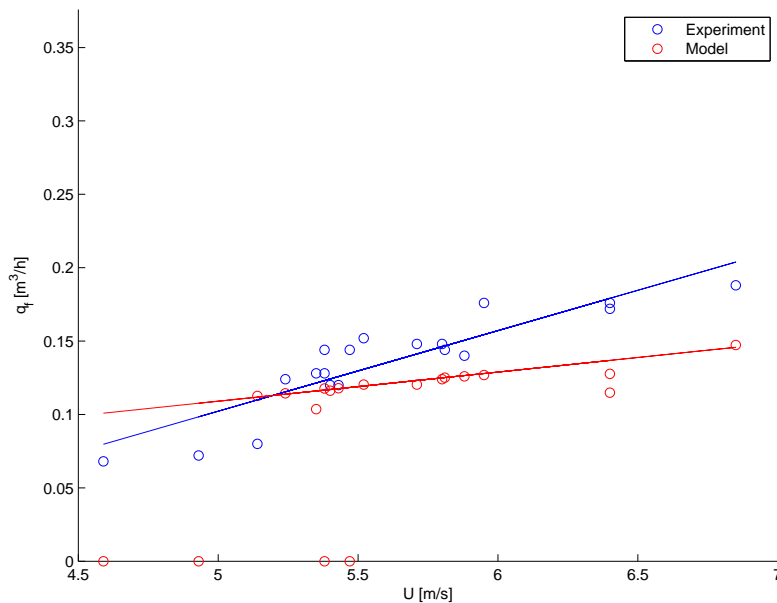


Figure 4-4: Comparison of permeate flow over wind speed of the model with data from the Curacao experiment

It turned out that the base configuration actually provided good results. The permeate flow around mean wind speed is relatively close to the experimental data and decreasing the feed pressure does not really affect that. Increasing the efficiency results in slightly better results, but an efficiency of 98% is not likely and due to the minor effect on permeate flow at mean wind speed it was decided to keep the efficiency at 88%. The base case was therefore considered to be the optimal

configuration. Figure 4-4 shows the permeate flow over wind speed from which the conclusion is drawn that around mean wind speed the permeate flow is approximating the water output sufficiently.

Figure 4-3(a) shows the required pump torque and the pump torque obtained from the SIMULINK model and the experiment. The data from the experiment was however not completely reliable. In the report difficulties with the torque measurements were described. The different results for the model and experimental torque are therefore not considered a problem. The torque obtained from the model is converging to the required pump torque under the variable wind input. It shows a realistic pattern.

4-2 Validation by means of Hatenoer configuration

In the summer of 2009 Hatenoer-Water built a pilot of a reverse osmosis system electrically driven by wind energy. They used a 5 kW Fortis Montana turbine. This turbine has a synchronous generator to convert the wind energy to 48 VDC. Hatenoer coupled the wind turbine and 5.25 m² of solar panels to a 400 Ah battery to provide enough energy for the reverse osmosis system in low wind speed.

From Augustus 26th till September 14nd Hatenoer measured the power produced by the solar cells, the permeate outflow and the wind speed. In the Simulink model the configuration of Hatenoer was modeled. How the Fortis Montana wind turbine model was defined is described in section 3-2. The electrical coupling was approximated by introducing efficiency factors for the generator, the battery (charging and discharging) the inverter and the motor. The capacity of the battery was calculated by multiplying the voltage with the electrical charge (Ah). Variation of voltage over time and the charging/discharging rates effect on the rated battery capacity were neglected, so the capacity is approximated as a constant value. Other influences on capacity that were neglected for the sake of simplicity are the age and history of the battery and the temperature. At higher temperatures the capacity is higher, but this comes at the cost of the battery lifetime.

Figure 4-5 shows the wind profile experienced by the system during the Hatenoer test. This wind profile was implemented in the Simulink model to compare the test results with the model. During the experiment the total generated power, so from solar cells as well as wind turbine, was not measured. The power from the solar cells was obtained however and is added to the wind power model. The wind turbine power and the solar cell power combined form the total generated power. The total generated power will experience some losses before it can drive the pump. The losses included are inverter loss, generator loss, battery losses and motor losses. The total generated power minus the losses is called the power delivered. The advantage of the electrical coupling is that the pump speed can be chosen independently from the wind turbine speed. It was fixed at a speed of 2900 rpm. The power required is a function of the feed pressure and the pump speed. According to Hatenoer the Danfoss APP1.0APM0.8 does not need to have the start up torque based on the APP1.0 alone. The system starts running as soon as the APP1.0/APM0.8 requirements are met and build up pressure and speed until the feed pressure is reached at the fixed rotational speed. The model does not include the time delay needed to build up pressure, since this will not have a large impact on the final results.

Figure 4-6 shows the pump load and power delivered over time for configuration 2. The power delivered is the wind turbine power with losses, but without the influence of the battery. The figure gives an idea of how much power is generated at a certain moment and how much power is needed. With configuration 2 the system with the efficiencies and battery set up as given in table

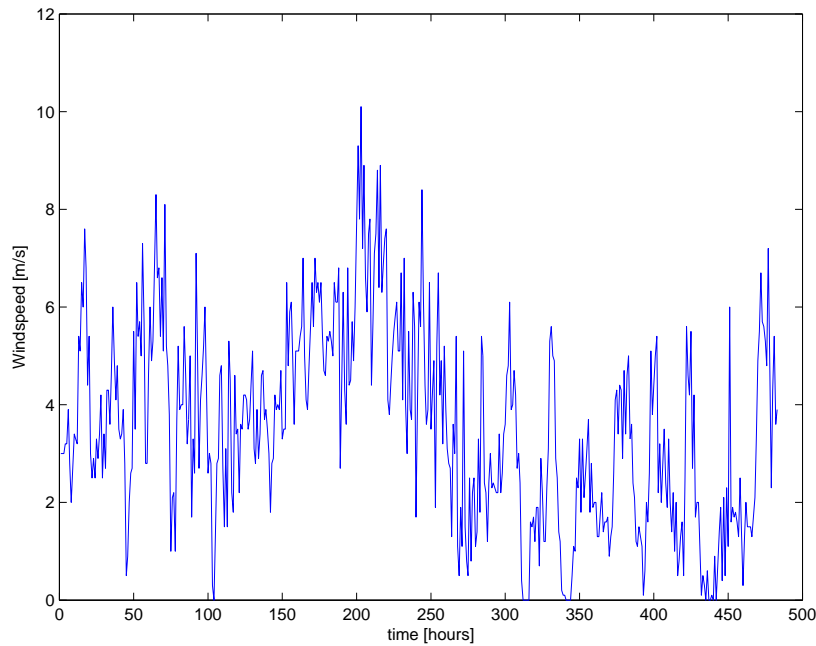


Figure 4-5: Wind profile of Hatenoer test

4-3 is meant. The variable 'battery' indicates how much of the theoretical capacity (i.e. 400 Ah * 48 VDC) is used in the model. This is varied to see the influence of the battery capacity on the output. From the Hatenoer report it is known that due to some problems the battery was not working at its full capacity during the tests. The capacity of the battery was varied to see how much influence this had on the output. If the battery is set to 1, this means it is operating at its full capacity. Zero means there is no battery and 0.5 indicates the battery operating at half its capacity, 1000 is used to model an infinitely big battery. In many type of batteries the full energy stored in the battery cannot be withdrawn without causing serious damage to the battery. The depth of discharge (DOD) is the term used to describe the fraction of the power that can be withdrawn from the battery.

Table 4-3: Influence of model parameters on water output

Configuration	1	2	3	4	5	6	7	8	9	10	11
$\eta_{generator}$	1	0.95	1	1	0.95	0.85	0.95	0.95	0.95	0.9	0.95
$\eta_{inverter}$	1	0.95	1	1	0.95	0.85	0.95	0.95	0.95	0.9	0.95
battery	0	0	1	1	1	1	1	0.5	1000	0.5	2.5
DOD	-	-	1	0.75	1	1	0.75	0.75	0.75	0.75	0.75
$\eta_{battery}$	-	-	1	1	0.95	0.85	0.85	0.85	0.85	0.8	0.85
$q_p [m^3/day]$	0.40	0.34	1.74	1.67	1.71	1.46	1.62	1.55	6.83	1.40	1.89

The water output flow is the variable that can be used to verify the behavior of the model compared to the experimental data. Figure 4-7 shows the permeate flow according to the Hatenoer test and the model for configuration 6. Figure 4-8 zooms in on the permeate flow at the first 70 hours. The frequent stops that were measured are also present in the model. The do however not start on exactly the same moment in time and the model seems to respond somewhat quicker, resulting

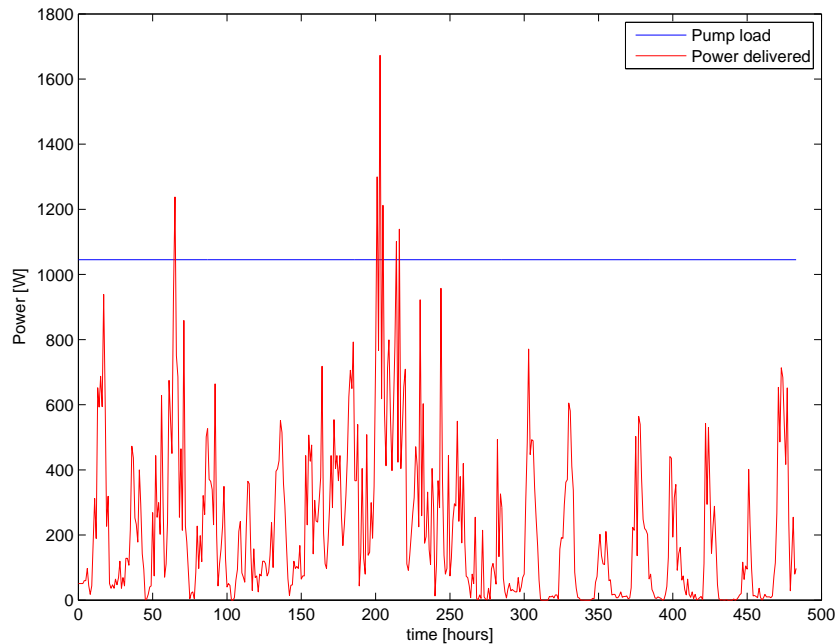


Figure 4-6: Power delivered and required for coupling configuration 2 (without battery)

in more peaks for shorter periods of time. In general it can however be stated that the model is a good approximation of the reality.

In order to understand the behavior of the system better the different powers in the coupling are plotted as can be seen in figure 4-9. In this figure the power available in the battery, the power delivered by the generator (minus losses) and the power needed by the load are plotted. The power needed is constant. The extra power delivered is saved in the battery (until the battery is fully charged). The maximum battery capacity is $48 \cdot 400 = 19200 \text{ V Ah} = 19.2 \text{ kWh}$. With required pump power of almost 2 kW, this means that the system can run for approximately 10 hours when the wind turbine is not running.

The variables that may be changed for comparison with the test data are the efficiencies, the battery capacity and depth of discharge. The model was run for the configurations as given in table 4-3. Configuration 6 is the one we have seen. Reducing the depth of discharge basically means that less of the energy in the battery can be used to run the pump, which leads to a shortage of power sooner and thus stops the system in an earlier stage and starts later after a stop. The water output per day is indeed a bit smaller as can be seen in table 4-3 if you compare configuration 3 with 4, but the influence is limited. It will depend on the size of the battery however. Reducing the efficiencies will reduce the water output and the different configurations in table 4-3 provide an idea of the extent to which the efficiencies have an effect on the water output. In the model the inverter loss increases the required load, since the inverter will come right before the pump after the battery and is therefore defined as part of the load. The generator loss will reduce the power delivered.

Configuration 8 is similar to configuration 7 (which is comparable to configuration 6, but with more efficient generator and inverter) except for the fact that the battery was assumed to be only working at half its capacity. During the Hatenoer tests it was noticed that the battery was not working at full capacity after some time, due to some charging/discharging issues at the start of the test. The effect of having a battery with less capacity is that it can store less energy to

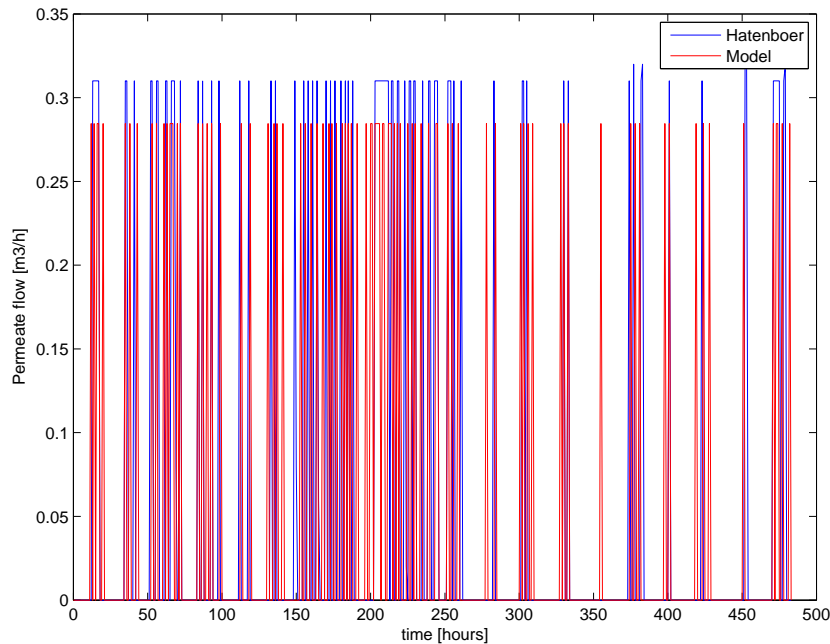


Figure 4-7: Permeate flow of model compared with the Hatlenboer test data for coupling configuration 6

overcome low wind speed periods. Provided that the wind turbine delivers enough power to store, a system with a larger battery will deliver more water as it can run for a longer period of time during low wind speed periods.

In configuration 3 the battery is modeled as a 100 % efficient one, so without experiencing any losses while gaining the benefits of the stored power. Configuration 1 is a similar system except that there is no battery included and the energy is used directly. Comparing these two configurations shows that adding a battery significantly increases the water output for this combination of wind turbine and pump. This is because, as we have seen in figure 4-6, the generator power is usually not enough to deliver the pump load. Adding a larger windmill or placing it at a location with higher wind speeds can result in a better performance of the system without battery.

Applying a battery with more capacity than the one used by Hatlenboer will result in more water output and also decreases the negative effects of charging and discharging, since that will happen over a smaller range of the total capacity (i.e. 2 kWh is of less influence on a 200 kWh battery than on a 20 kWh battery). Configuration 9 shows what happens if we assume an extremely large battery (in this case 1000x the original one). The battery is so large that it offers enough energy to drive the pump constantly for a long period of time. Batteries are however costly and increasing the battery bank size to deal with long periods of small wind speeds should be viewed from a cost per cubic meter point of view (see appendix H). It should also be noted that if the wind turbine is continuously delivering less power than the load requires (as is the case for this Hatlenboer experiment), the battery will eventually be empty independent of the size, because it does not get sufficient opportunity to charge.

In table 4-4 the total water output per day for a selection of the configurations and of the Hatlenboer test is given. The selection does not contain the configurations without a battery or with a larger battery since it should approximate the Hatlenboer test best. The Hatlenboer test consists of two

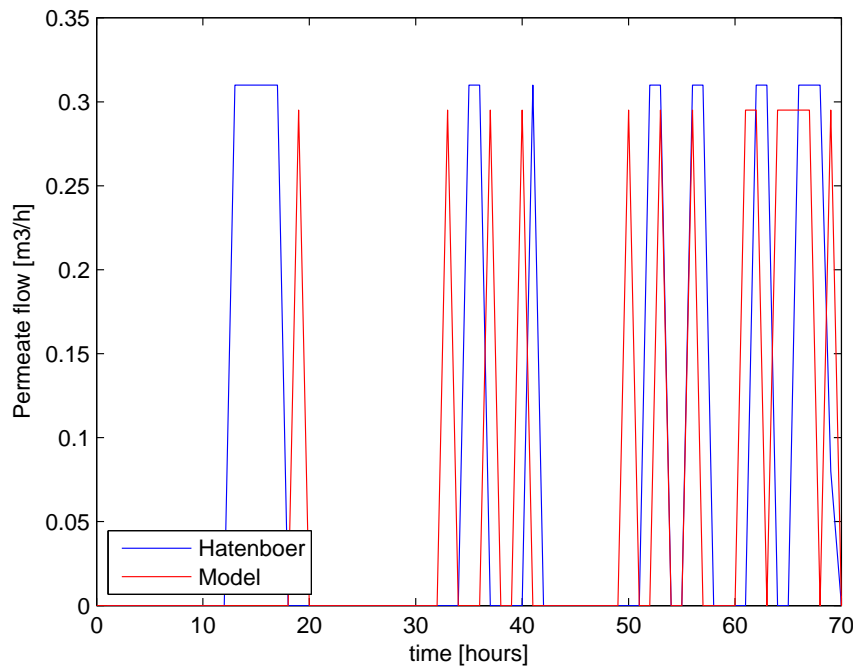


Figure 4-8: Zoom of the permeate flow of model compared with the Hatenboer test data for coupling configuration 6

types, the average water output for an subset of the test data (i.e. the hourly test samples) and the average water output for the total test data set. The difference is approximately 2% and can therefore be neglected. The water output of the model is in all cases relatively close to the test results. The ideal cases offer too much water as expected. Configuration 6 and 10 provide the best results. Since Hatenboer described that the performance of the battery was not working properly, configuration 10 is likely to be more realistic resulting in lower efficiencies.

Table 4-4: Water output of selected model configurations and Hatenboer test

	Hatenboer Test		Model Configuration			
	Total	Subset	3	6	8	10
$q_p [m^3/day]$	1.42	1.39	1.74	1.46	1.55	1.40

Summarizing, it can be said that the Simulink model of the Hatenboer configuration does match the test results properly. For analysis of future electrical systems the model can be used to estimate the system behavior and water output. According to these results the efficiencies should be set similar to the values for configuration 10. The values can always be changed in order to evaluate the influence, but configuration 10 (with a full battery) promises to be a realistic starting point.

4-3 Conclusion of Wind2Water model validation

The mechanical Wind2Water model was validated by means of the data from the experiments done on Curaçao. It was shown that for sea water desalination the feed pressure could be assumed constant. Theoretically this should result in the permeate flow being a direct function

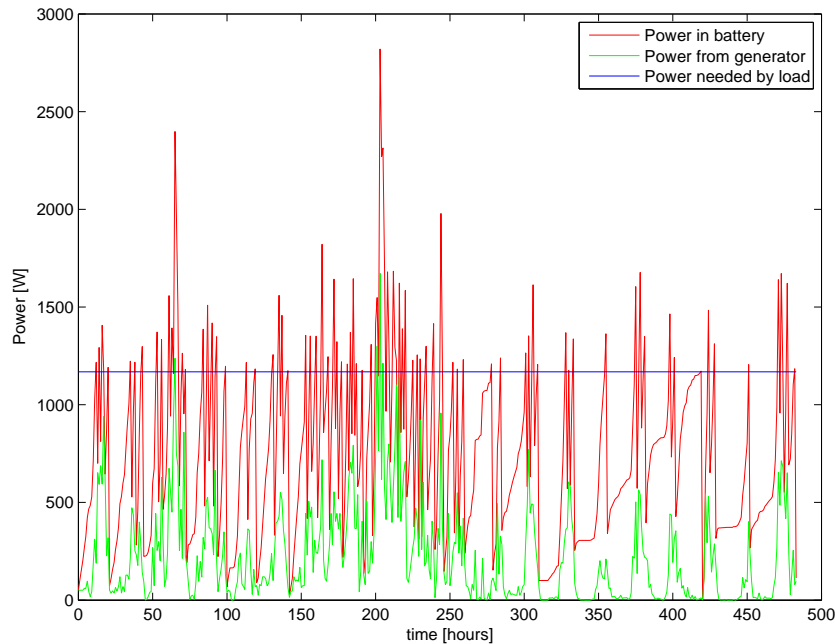


Figure 4-9: Power required and delivered for coupling configuration 6

of the rotational angular velocity of the pump. If the model provides a good match with the experimental data for the permeate outflow it is expected to match similarly well with the pump rotational angular velocity. This is however not the case. The most likely explanation is a consistent measurement error.

The experimental data were used to validate the assumptions made for the creation of the mechanical Wind2Water model. The data set was however small and the quality of the angular velocity output questioned. Because of this it was decided to focus on a match for the permeate outflow around mean wind speed. This match was found and proved that with the assumptions done for the mechanical Wind2Water model the modeled permeate flow is a good approximation of reality. The mechanical efficiency of 88% and the neglected pump inertia can therefore be used to estimate the performance of other mechanical configurations.

The electrical Wind2Water model was validated by means of the prototype of Hatlenboer Water. Due to the low wind speed the wind turbine continuously delivered less power than the load required, resulting in an intermittent pump performance (i.e. with many starts and stops). The efficiencies of the components in the electrical configuration were varied to find an electrical coupling that best matched the experimental results. This configuration was found and the characteristics of this configuration can be used for the evaluation of future electrical couplings.

Part III

Selection for configuration Somaliland

Promising configurations

In this chapter a selection of brackish water configurations and sea water configurations is made. These configurations are analyzed over constant wind input between 3 and 9 m/s (section 5-3 and section 5-4). Based on those results the most promising configurations are selected and evaluated for sites with a mean velocity of 5.9 m/s and/or 7 m/s. For these configurations also the weighted score on the four design criteria (cost, maintenance, life and reliability) is obtained and based on this the 5 best configurations are selected for brackish water and for sea water desalination.

5-1 Design criteria and weighting factors

The selection of the optimal configuration for the wind driven desalination system does not only depend on cost per cubic meter of water output. Although this is an important criterion, other criteria of importance are the reliability of the system, the lifetime and the maintenance. Furthermore it matters if the system is built of standard parts or custom made parts. Custom made parts are not easy to replace and might have some teething troubles. Also a local manufacturer is an advantage, since that makes the replacement and repair of parts easier. It is decided to evaluate the wind driven desalination system only on the four most important criteria, namely the reliability, cost, lifetime and maintenance as will be explained later in this chapter.

Not every criterion is as critical as the other. Therefore weighting factors for each criterion are introduced. They are defined by comparing one criterion with the other and grading the importance. For example, if we compare Cost with Reliability, then Cost is less important than Reliability and a zero is assigned to Cost. If the criteria are equally important a one is assigned and if the criterion is more important a two will be given. Table 5-1 shows the resulting weighting factors and how they are defined.

The wind driven desalination system is meant to operate in developing countries. It will be placed in coastal regions, implying that the materials should be able to withstand a salty environment and sand. There will be guidance and support during the operation of the system by The Windrinker Holding, but daily operations have to be done by the local entrepreneurs. This means that the system should be easy to maintain. For this reason, standard parts and local manufacturing are preferred. By using standard parts replacement is easier and with local manufacturers new parts can be transported quicker. Even better than using standard parts and local manufacturers is reducing maintenance to a minimum. Simple and quick maintenance activities can be performed by the local entrepreneur and are therefore not considered a problem. Maintenance is thus important

Table 5-1: Weighting factor definition by comparing the importance of the criteria with each other. Assign a zero if the criterion is less important, one is for equally important criteria and a two is assigned if a criterion is valued more important

	C	M	L	R	S	LM	I	Total Score	Weighting Factor
Maximum	-	2	2	2	2	2	2	12	4
Cost (C)	-	1	2	0	2	2	2	9	3.0
Maintenance (M)	1	-	1	0	2	1	2	7	2.3
Life (L)	0	1	-	0	2	2	2	7	2.3
Reliability (R)	2	2	2	-	2	2	2	12	4
Standard Parts (S)	0	0	0	0	-	1	1	2	0.7
Local Manufacturing (LM)	0	1	0	1	-	1	2	3	1.0
Initial Investment (I)	0	0	0	0	1	1	-	2	0.7

but not as important as the relative cost (i.e. the cost per m^3 of desalinated water) . In the relative cost the lifetime is already slightly present, because the cost will increase when the lifetime is shorter than the payback time. This results in cost being more important than lifetime. One thing is more important than relative price and that is reliability. No unexpected and frequent stand stills should occur. The system is a basis for a water selling business and the entrepreneurs should be able to count on it, otherwise it will not be used at all.

5-2 System configurations used for evaluation

Table 3-1 gives an overview of all parts available in the SIMULINK model. It can be seen that theoretically it is possible to make 240 different configurations. A selection was made of these configurations, resulting in the 19 configurations given in table 5-2. The motivation for selecting these configurations is based on the following points:

1. **Danfoss pumps only for sea water desalination:** Danfoss pumps are high pressure pumps and are therefore suitable for desalination of sea water. They can desalinate brackish water as well, but for the desalination of brackish water medium pressure pumps are more efficient.
2. **Orbit pumps only for brackish water desalination:** Orbit pumps can deliver up to 30 bar and are therefore not suitable for sea water desalination.
3. **Evaluate the largest and the smallest Orbit pump:** Orbit GW1304 not for sale anymore, making the GW0904 the largest. The smallest Orbit pump is the GW0504.
4. **Pearson pump unreliable:** Although the model showed similar results with the experimental data (see appendix G), it was found that the model produced unrealistic results. The reason for that is that the start up torque could not be included correctly (due to a lack of data from the manufacturer)
5. **M5015 and Fortis Montana too small:** From the preliminary study as described in appendix B it followed that windmills with small rotor diameters are usually not able to deliver sufficient water output.
6. **Turbex only for mechanically coupled systems:** The advantageous start up torque of the multi-bladed windmill is not needed in electrical systems. More efficient three bladed turbines are therefore considered for the electrical configurations.

7. **Fortis Alize and Bergey Excel evaluated in both mechanical and electrical coupled systems:** Although these windmills are designed for electricity generation it was part of this research to find out what the effect of using these windmills with a mechanical coupling would be.
8. **Only a RO array with 4 membranes is considered:** The number of membranes has influence on the recovery of the array. With low fluxes less membranes can be used because of the risk of fouling. This fouling risk is not concluded in the model

Table 5-2: Selected system combinations for brackish water desalination and sea water desalination

	Brackish water	Sea water
Mechanical	Turbex - Orbit GW0504 Turbex - Orbit GW0904 Fortis Alize - Orbit GW0504 Fortis Alize - Orbit GW0904 Bergey Excel - Orbit GW0504 Bergey Excel - Orbit GW0904	Turbex - Danfoss APP1.0/APM0.8 Turbex - Danfoss APP1.5/APM1.2 Turbex - Danfoss APP2.5/APM1.8 Fortis Alize - Danfoss APP1.5/APM1.2 Fortis Alize - Danfoss APP2.5/APM1.8 Bergey Excel - Danfoss APP1.5/APM1.2 Bergey Excel - Danfoss APP2.5/APM1.8
Electrical	Fortis Alize - Orbit GW0504 Fortis Alize - Orbit GW0904 Bergey Excel - Orbit GW0504 Bergey Excel - Orbit GW0904	Fortis Alize - Danfoss APP1.0/APM0.8 Fortis Alize - Danfoss APP1.5/APM1.2 Fortis Alize - Danfoss APP2.5/APM1.8 Bergey Excel - Danfoss APP1.0/APM0.8 Bergey Excel - Danfoss APP1.5/APM1.2 Bergey Excel - Danfoss APP2.5/APM1.8

Table 5-3 shows the costs of the different parts. The costs are rounded and the custom mechanical coupling is the roughest approximation. The price of an Orbit GW0504 pump was known and based on that the price for GW1304 was assumed to be €500 higher. The APP1.0/APM1.8 price was approximated based on the total RO cost of the Hatlenboer system which included the pump. The price of the larger Danfoss pumps was then set a factor higher. The price of the electrical coupling consists of inverter and battery, which was found with the retail prices of the Alize wind turbine.

Table 5-3: Approximated cost of selected system parts

Wind turbine		Coupling	
Turbex	€20000	Custom mechanical coupling	€5000
Fortis Alize	€25000	Electrical coupling	€15000
Bergey Excel	€30000	Extra transmission	€500
Pump		RO	
Danfoss APP1.0/APM0.8	€6000	4 membranes	€20000
Danfoss APP1.5/APM1.2	€7200		
Danfoss APP2.5/APM1.8	€9000		
GW0504	€7500		
GW0904	€8000		

5-3 Brackish water system

Desalinating brackish water reduces the energy requirement of the windmill, because the feed pressure needed to desalinate brackish water is far lower than the feed pressure needed for sea water desalination. Bas Heijman, researcher of the TU Delft, designed a system consisting of off-the-shelf components for implementation in regions with sufficient brackish water resources. He selected the Turbex windmill and combined it with an Orbit pump. The SIMULINK model was used to estimate the water output of the current design and to give recommendations on the preferred pump type and transmission ratio. Also combinations with three bladed wind turbines mechanically coupled to the Orbit pumps were evaluated as well as the electrical configuration for the brackish water system.

5-3-1 Mechanical configuration

The Turbex windmill is a multi-bladed windmill from a manufacturer from South Africa. It is interesting for our application since it already has a rotating vertical axis that can be coupled to a rotating pump axis relatively easy. Together with the 90 degrees rotation of the shaft, a transmission ratio of 1:6.67 is applied. The Turbex windmill is designed to drive an helical rotary pump. This pump is however not suitable for sea- or brackish water, since it cannot withstand the salt properly. The Orbit positive displacement pump made by Franklin is a pump with good salt protection and can easily be coupled to the rotating axis of the windturbine. This is preferably done without any extra transmission. Two types of Orbit pumps were evaluated as explained in the previous section: the smaller GW0504 and the GW0904.

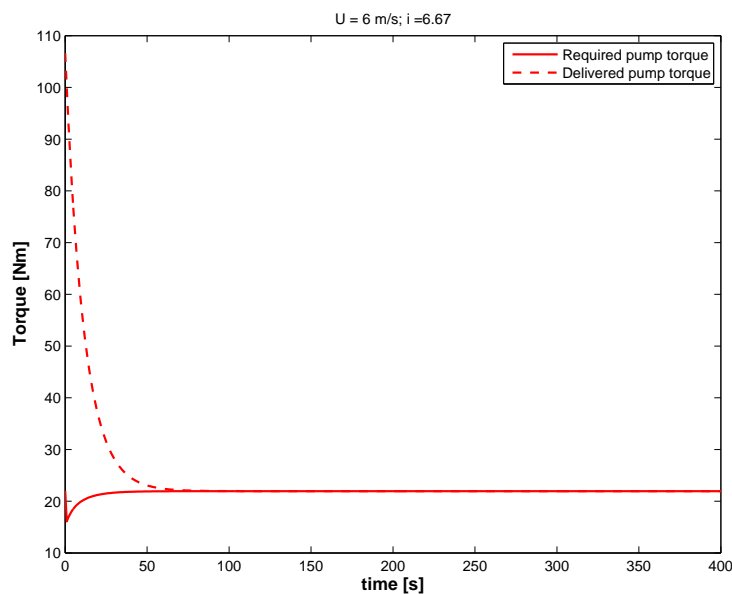
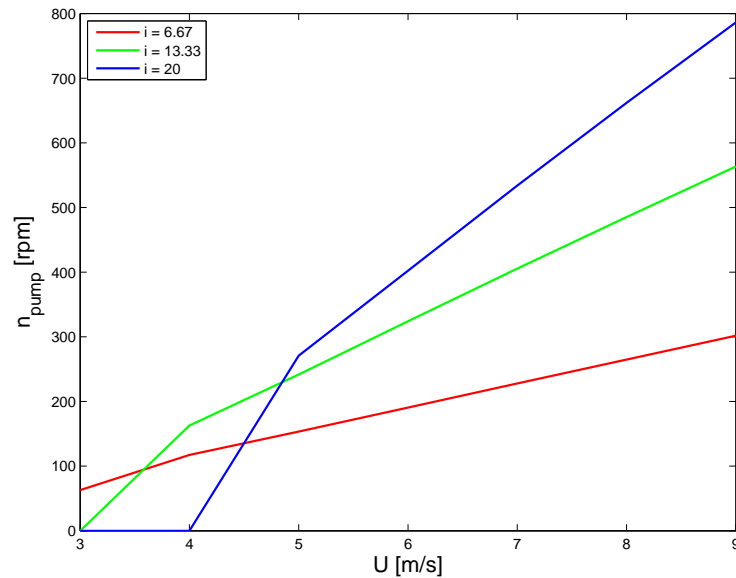
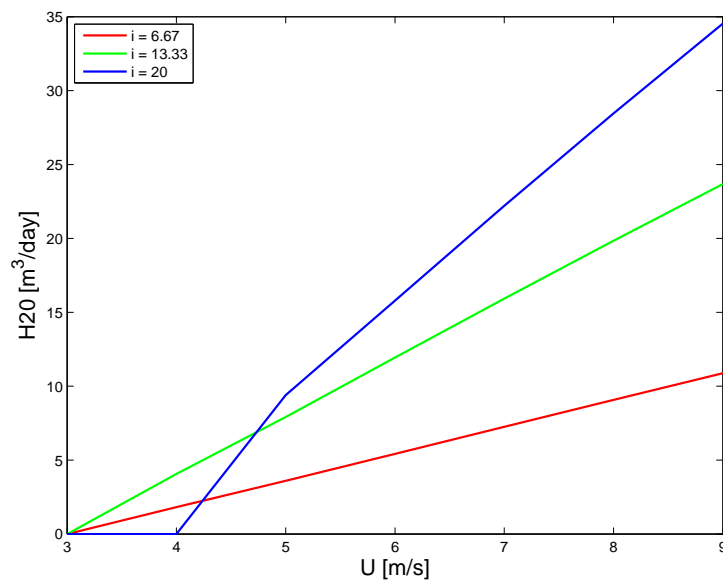


Figure 5-1: Torque over time for Turbex windmill with GW0504 Orbit pump; dotted line is the delivered pump torque and the straight line the required pump torque; $i = 6.67$ and $U = 6$ m/s



(a) Pump rotational velocity (n) over wind speed (U)



(b) Daily water output (H2O) over wind speed (U)

Figure 5-2: Turbex windmill with GW0504 Orbit pump for brackish water desalination

In figure 5-1 the torque delivered by the windmill and the torque required by the pump at a mean wind speed of 6 m/s is shown. The torque delivered is much higher than the required pump torque, resulting in an increase of the angular velocity until the delivered and required torque are equal. What happens is that the increase in angular velocity increases the tip speed ratio of the wind turbine (according to equation 5-1). This leads to another result for the torque coefficient by means of the C_q - λ -curve, changing the delivered torque. A representation of this behavior is given in figure 5-3. For the calculation of the daily water output the time is taken sufficiently long,

such that the effect of the convergence to the operating point at the beginning of the simulation is limited. The time frame shown in figure 5-1 is only a small part of the total simulation.

$$\lambda = \frac{\Omega R}{U} \quad (5-1)$$

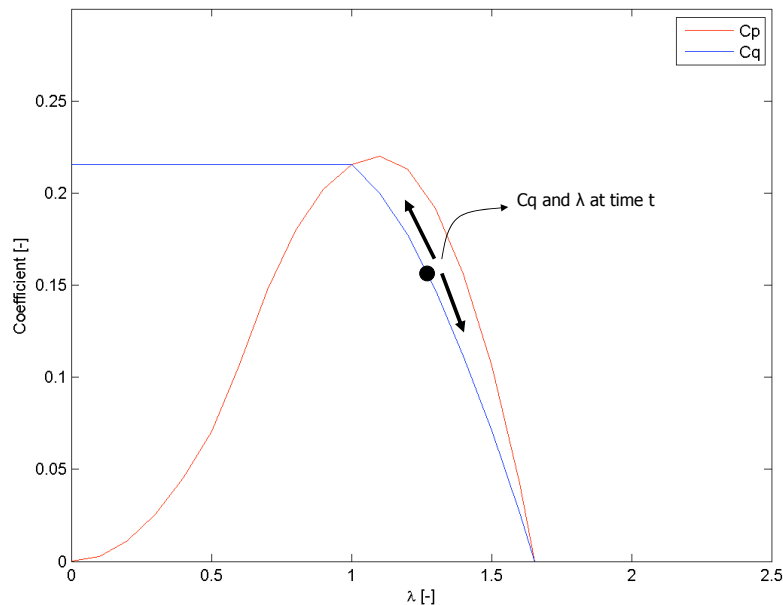


Figure 5-3: Movement over the C_q - λ -curve to find the operating point. A change of angular velocity changes the tip speed ratio, resulting in a different torque coefficient (and torque).

Preferably no extra transmission is attached to the vertical axis of the Turbex windmill, since that will increase the complexity of the design and makes it more prone to problems. It might however be the case that the production is so much higher with an extra transmission that it justifies the drawbacks. With that in mind, the water production is also calculated for systems with an extra transmission. The extra transmission is either one or two times the standard Turbex transmission of $i = 6.67$. Higher transmission ratios resulted in start up problems and lower transmission ratios allow for remaking the standard Turbex transmission, which is undesirable. According to Turbex the system operates with an angular velocity between 100 and 400 rpm. In figure 5-5(a) the angular velocity of the Turbex windmill with the GW0504 pump is given and it can be seen that indeed the pump will not rotate faster than 400 rpm without an extra transmission.

The permeate flow based on 4 membranes and 10 % recovery per membrane is a direct function of the angular velocity. In figure 5-2(b) the daily water output per transmission ratio is given. The advantage of the Turbex design is that it can be applied directly to the pump, because it already has a rotating vertical axis. Installing an extra transmission will make the system more complex. It increases the water output however significantly.

What the transmission does is that it reduces the torque delivered and increases the angular velocity. As long as the delivered torque meets the required torque a higher transmission ratio results in more water output, since the pump angular velocity directly increases. If the transmission ratio is too high however, the delivered torque is not sufficient and the system will not start until it is slowed down enough to meet the torque requirements. In figure 5-4 the angular velocity of the pump is shown for the system with a transmission ratio of $i = 20$. It shows that the system is slowed down when the mean wind speed is 3 or 4 m/s in order to meet the torque requirements. In reality the system is not running until the operating point is found, this is incorporated by not

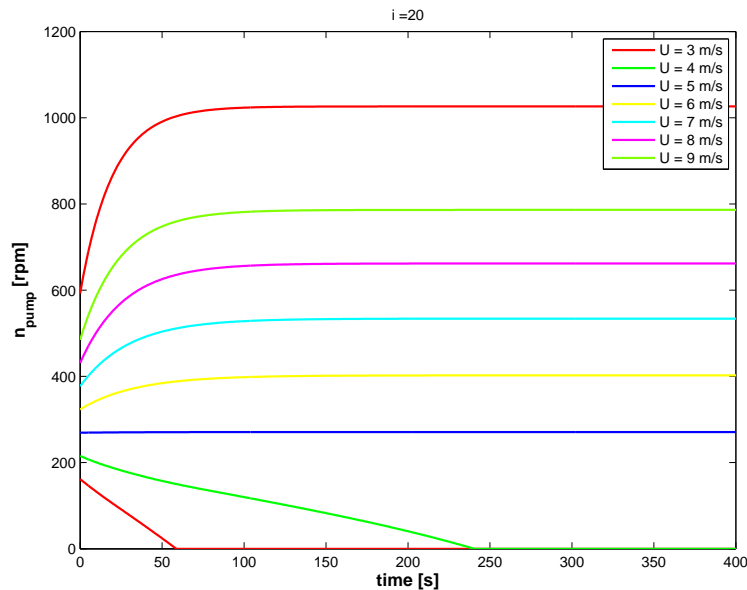


Figure 5-4: Angular velocity of Turbex-GW0504 system for different mean wind speeds and transmission ratio $i = 20$

letting the system produce any water in that case. At 3 and 4 m/s the torque requirement cannot be met as can be seen in figure 5-4 where the lines of 3 and 4 m/s mean wind speed go to zero angular velocity. No water will be produced in those cases.

The Orbit GW0904 is a larger pump than the Orbit GW0504, implying that the permeate flow is more for a specific angular velocity. The required torque is however also larger. The average daily water output for different wind speeds and transmission ratios is given in figure 5-5.

The Turbex-GW0904 combination operates best at $i = 13.33$ for wind speeds between 4.5 and 6.3 m/s. At wind speeds above 6.3 m/s a transmission ratio of $i = 20$ is preferable. For wind speeds smaller than 4.5 m/s the production the Turbex-GW0504 configuration without any extra transmission is optimal. The production in that case does however not exceed the $4 \text{ m}^3/\text{day}$. Adding a larger transmission is not beneficial, since the system will have difficulty meeting the torque requirement and will not produce more water compared to the system without extra transmission until wind speeds above 7 m/s are reached.

Three bladed wind turbines are generally built for generating electricity and need to be customized for direct mechanical use. The difference with a multi-bladed windmill is that the three bladed wind turbine produces less torque at small tip speed ratios, which seems to be a disadvantage for applying them directly to a pump with high start up torque.

Table 5-4 shows the result of connecting the Fortis Alize and the Bergey Excel windturbines directly to a GW0504 pump and a GW0904 pump. The entire coupling will be custom made and a transmission ratio can be chosen freely. The transmission ratio can not be too large, because that will result in issues with the required torque versus the delivered. For example, at a transmission ratio of $i = 5$ the Fortis Alize - GW0504 configuration does not start before a wind speeds of 7 m/s is reached. At the moment the wind turbine did meet the torque requirement, a higher transmission ratio does result in more water output, due to the increased pump shaft speed. The difference between the performance of the Fortis Alize and Bergey Excel both coupled mechanically to the Orbit pumps is small. An advantage of the Bergey Excel is that it does start at a lower wind speed than the Fortis Alize.

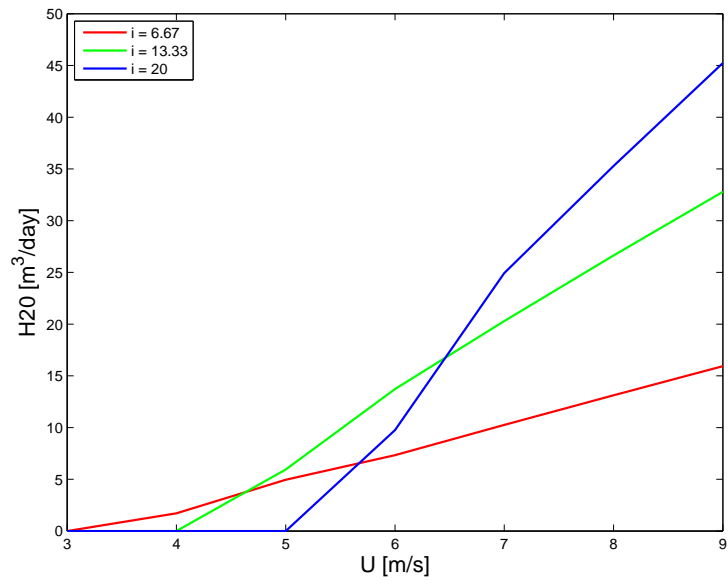
(a) Pump rotational velocity (n) over wind speed (U)(b) Daily water output (H_{2O}) over wind speed (U)**Figure 5-5:** Turbex windmill with GW0904 Orbit pump for brackish water desalination

Table 5-4: Water output [m^3/day] for the three bladed wind turbines combined with the Orbit pumps for different constant wind speed inputs and transmission ratio, i

U [m/s]	Fortis Alize				Bergey Excel			
	GW0504		GW0904		GW0504		GW0904	
	i = 2	i = 5	i = 2	i = 5	i = 2	i = 5	i = 2	i = 5
3	0.0	0.0	0.0	0.0	0.0	0.0	0.0	0.0
4	3.4	0.0	0.0	0.0	3.8	0.0	2.9	0.0
5	6.1	0.0	5.4	0.0	6.4	0.0	7.6	0.0
6	8.8	0.0	11.4	0.0	9.1	17.3	12.3	0.0
7	11.4	25.2	15.8	0.0	11.7	28.0	16.5	0.0
8	14.0	33.7	20.0	0.0	14.3	35.7	20.6	42.8
9	16.6	41.2	24.1	51.6	16.8	42.8	24.6	56.7

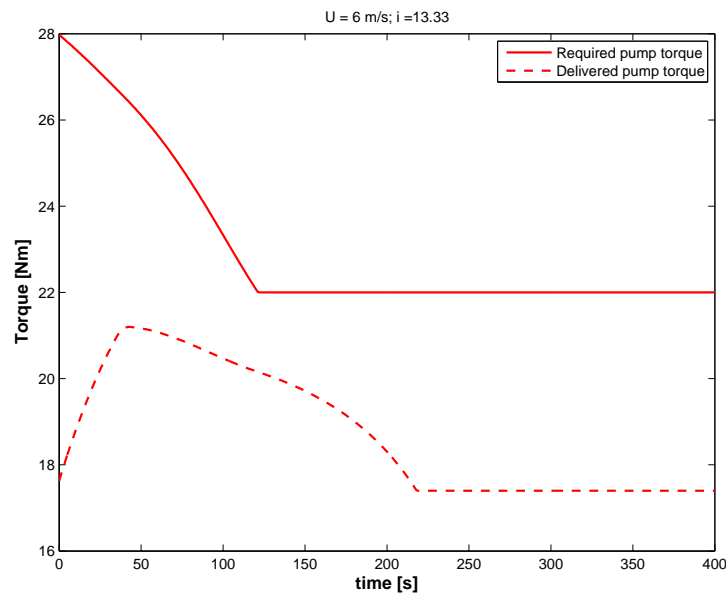


Figure 5-6: Torque for $V = 6 \text{ m/s}$ of the Alize-GW0504 system with $i = 13.33$; straight line is the required pump torque and the dotted line the delivered pump torque

Figure 5-6 illustrates what happens with the torque when the torque requirement is not met. The Alize-GW0504 combination with a transmission ratio of $i = 13.33$ does not start at wind speeds of 6 m/s . The model starts with assuming that the wind turbine rotates at the design tip speed ratio. The mean wind speed of 6 m/s therefore results in a certain virtual delivered torque and angular velocity. The required pump torque depends on this angular velocity. It is found that at a mean wind speed of 6 m/s the wind turbine at the design tip speed ratio delivers an angular velocity too high and/or a torque too low to meet the requirement. The pump therefore exerts a moment on the wind turbine, decreasing the speed and in the same time the required pump torque (due to its dependency on the angular velocity). Also the decrease in angular velocity changes the tip speed ratio of the turbine and thus the delivered torque. The required pump torque at stand still can however not be smaller than the start up torque as provided by the pump manufacturer. This is indicated by the horizontal 'required pump torque' line. For a centrifugal pump the start up torque can be zero, but due to the variability of the feed pressure for brackish water applications these pumps were not selected for the wind driven reverse osmosis system (chapter 2-3). When the

required pump torque is higher than the delivered pump torque the system will be slowed down and the torque coefficient (C_q) delivered by the windturbine changes. At a wind speed of 6 m/s the delivered torque will however never match the required torque and the system will not start rotating.

5-3-2 Electrical configuration

In this section the Orbit pumps electrically coupled to the Bergey Excel and Fortis Alize are evaluated. The pump speed was fixed at 300, 500 or 700 rpm and the results are shown in figure 5-7, figure 5-8(a) and figure 5-8(b) respectively. The electrical system has to deal with losses in the generator, in the converter and in the battery. The losses for these systems are set as the ones defined in chapter 4-2 for configuration 10. Configuration 10 was the one that matched the Hatzenboer test results best.

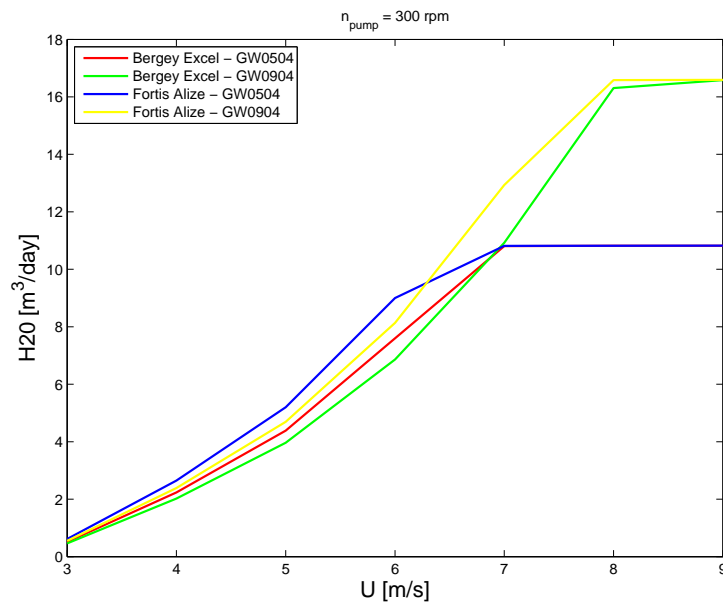
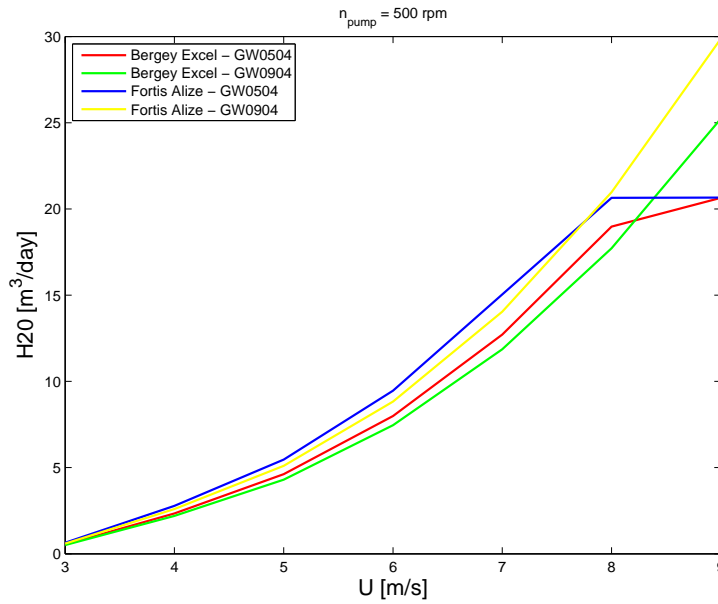


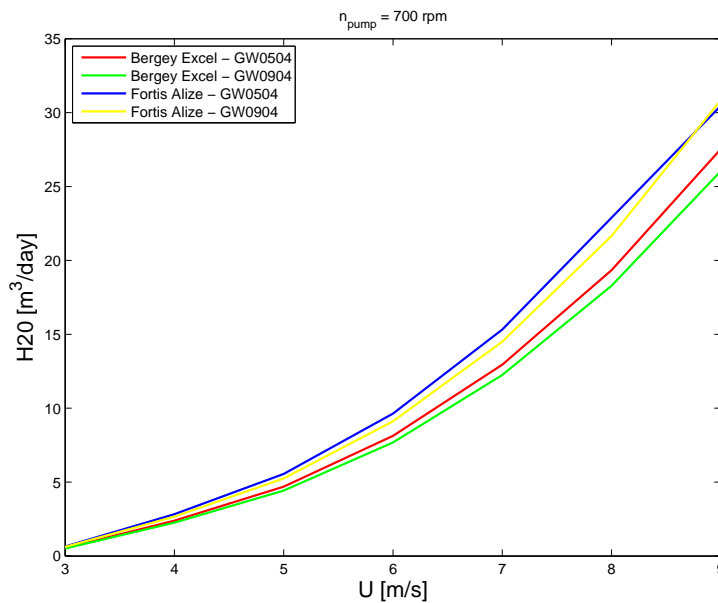
Figure 5-7: Daily water output (H2O) over wind speed (U) of the Fortis Alize with Orbit pumps for electrically driven brackish water desalination with a pump shaft speed of 300 rpm

The advantage of an electrical system is that the speed of the pump is independent of the wind speed as long as the battery can provide enough power. If the battery does not provide enough power the system simply stops running. In this evaluation we assume constant wind speed which implies that the delivered power to the battery by the generator is constant. Also the power required by the pump is constant.

If the generator power is smaller than the required pump power the system will behave with a constant start-stop rhythm. The battery is loaded until enough power is present. It immediately uses that power until it can not supply enough anymore and starts charging again after that. This pattern is then repeated. At higher pump speeds the permeate flow is larger when it starts running, but the required load is also larger, resulting in more time needed to charge the battery sufficiently. Since this time delay and amount of permeate flow are proportional, increasing the pump speed does not result in more water output. This would only be the case when the generator power is constantly higher than the pump load, resulting in continuous water output at the required pump speed.



(a) Pump shaft speed of 500 rpm



(b) Pump shaft speed of 700 rpm

Figure 5-8: Daily water output (H20) over wind speed (U) of the Fortis Alize with Orbit pumps for electrically driven brackish water desalination

This is for example true for the Fortis Alize and Bergey Excel combined with the GW0504 pump at 300 rpm at wind speeds above 6.5 m/s. The water output is in those cases constant which is illustrated by the horizontal line in figure 5-7. The same configurations at a pump speed of 500 rpm do not deliver continuous water output before a wind speed of 8 m/s is reached, but then, as expected, the flow rate is larger than for the 300 rpm case. Also at 7 m/s the system at 500 rpm does have a similar flow rate as was the case for the system at 300 rpm. The same holds for

the system at 700 rpm as can be seen in figure 5-8(b). So for combinations where the continuous wind speed is not enough to provide the needed pump torque the pump speed setting does not influence the water output significantly.

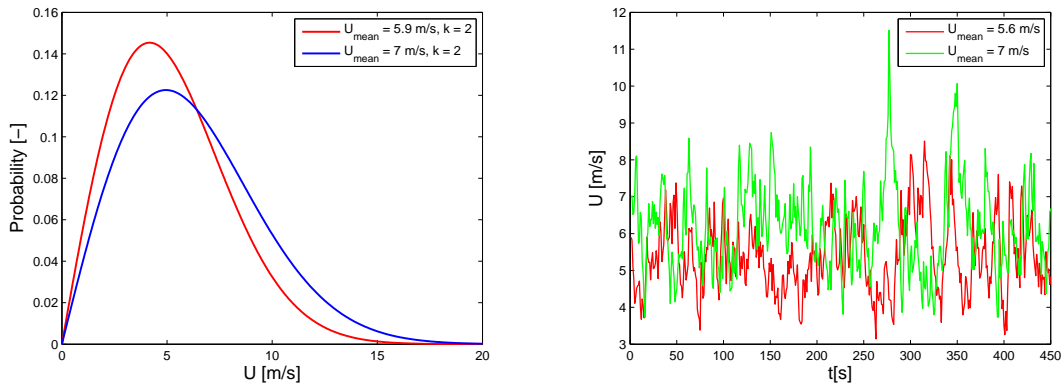
The situations in which the power delivered is less than the power required, are characterized by the gradually increasing lines in the three figures. This corresponds with the start stop behavior as described previously. The difference between the power delivered and the power required decreases with increasing wind speed. This results in increased water output with increasing wind speed until the power delivered matches the power required.

The difference between the performance of the Bergey Excel and the Fortis Alize is small. This makes sense, because the wind turbines are of similar size, generating more or less equal amount of power and due to the electrical coupling the wind turbines operates independent of the reverse osmosis system.

The wind input for this evaluation was constant in order to clearly see the reaction of the system on the difference in torque while getting an idea of the water output at those wind speeds. In reality however wind speed is not constant. That is the reason why batteries are interesting. They can be used to overcome the periods of low wind speeds while charging the battery during periods with sufficient wind speed. Matching the wind turbine to a pump that meets the torque requirement at mean wind speed is therefore desirable. At sites with a mean wind speed of 7 m/s the Fortis Alize combined with the Orbit GW0504 at 300 rpm would be a good option for example. Is the mean wind speed however 8 m/s the Fortis Alize can better be combined with the Orbit GW0904. At mean wind speeds of 5 m/s the system will most of the time operate with the intermittent character. A larger wind turbine could solve that problem, since the power of the turbine is proportional to the rotor radius squared. In appendix B a short study already showed the importance of the rotor radius on the water output.

5-3-3 Configuration selection for $U_{mean} = 5.9$ m/s and $U_{mean} = 7$ m/s

In the previous sections we evaluated the water output for different brackish water system configurations under constant wind speed. In this section we will select the best configurations for two different sites. The selection is based on the weighted score of each configuration on different design criteria as described in section 5-1.



(a) Weibull distribution with shape factor $k = 2$

(b) Part of the wind input for the SIMULINK model

Figure 5-9: Wind input for evaluation of configurations with U_{mean} is 5.9 m/s and U_{mean} is 7 m/s. Wind in figure 5-9(b) is defined by selecting random variables from the Weibull distribution with shape factor $k = 2$ (figure 5-9(a)) and 80% dependence on the value of the previous time step

The first site to be evaluated is a site with a mean wind speed of 5.9 m/s. This is the average yearly wind speed in Somaliland, see table 6-1. The second site has a mean wind speed of 7 m/s. This is the mean wind speed we first assumed for Somaliland and due to the limited wind data it was decided to evaluate this original assumption as well. The wind input was based on the Weibull distribution with the mean wind speeds at 5.9 m/s and 7 m/s and a shape factor of $k = 2$ as shown in figure 5-9(a). The Weibull principle is explained in appendix C-1. At time t the wind speed is a function of a randomly selected value from the Weibull distribution and the wind speed at time $t-1$. At time $t = 0$ the wind speed equals the mean wind speed. Equation 5-2 shows how the wind speed per time step is calculated. The resulting wind input is used in the SIMULINK model to calculate the average daily water output for different system configurations and is given for a selection of configurations in table 5-5.

$$U(t) = 0.2 \cdot U_{Weibull} + 0.8 \cdot U_{t-1} \quad (5-2)$$

From the results in section 5-3-1 and 5-3-2 the configurations with the most water output per configuration type were selected. For example from figure 5-2(b) it followed that the Turbex windmill with the Orbit GW0504 pump with a transmission ratio of $i = 20$ produces most water at 5.9 m/s (and also at 7 m/s). For the Turbex windmill with the GW0904 pump the water output for a transmission ratio of $i = 13.33$ and $i = 20$ at 5.9 m/s is almost similar. Also a transmission ratio of $i = 20$ performs better with wind speeds above 5.9 m/s and vice versa for wind speeds below 5.9 m/s. No clear winner was found for this configuration type and both configurations were selected for further evaluation. The electrical configurations all showed very similar results. It was decided to select the configuration with the highest water output at mean wind speed for one of the configurations with the Fortis Alize and one of the configurations with the Bergey Excel. Table 5-5 gives a summation of the selected configurations.

For each configuration the system cost were defined by means of adding the cost of the different components as given in table 5-3. For larger transmission ratios 1 to 4 times the cost of the 'Extra transmission' were added on the total system cost depending on the ratio (i.e. $i = 60$ got 4 times the 'Extra transmission' cost and $i = 13.33$ only one time). With the total system cost the cost of the water for different payback times were calculated by means of equation 5-3 with $t_{payback}$ in years, C_{water} in €/m³ and q_f in m³/day. The cost of the water does not include any operational cost such as maintenance or replacement of parts. The water costs given in table 5-3 do however give a good feeling for the minimal water cost and how one configuration perform sin comparison to the other. The table also shows that with a mean velocity of 5.9 m/s only one configuration is likely to get a water cost price of 1 €/m³ with a payback time of 10 years. The water is thus relatively expensive.

$$C_{water} = \frac{C_{system}}{365 \cdot q_f \cdot t_{payback}} \quad (5-3)$$

The water cost is only one of the design criteria. Six other design criteria were mentioned in section 5-1. For each of these criteria weighting factors were defined by comparing the importance of one criterion with the other. Cost, Maintenance, Life and Reliability turned out to be the most important criteria and are used in this section to select the best configuration for each site. Each configuration was given a score on the four criteria. The score had to be a value between 0 and 4 in which 0 indicates poor performance and 4 excellent performance. The following logic was applied in defining the score for each configuration:

- **Cost:** Three cost ranges of equal size were defined, they account for the score 1 to 3; Score of zero correspond with water costs higher than the highest cost within the ranges and a score of four with a cost lower than the lowest cost within the ranges. The water costs were taken from table 5-5, table 5-7, table 5-10 or table 5-11

Table 5-5: Comparison of the water cost in a region with a mean wind speed of 5.9 m/s

				Water cost (€/m ³)		
				Payback time (years)		
	Description	System Cost	Water output [m ³ /day]	3	5	10
A-I (B-I)	Turbex-GW0504, i = 20, mechanical	€48500	12.9	3.43	2.06	1.03
A-II (B-II)	Turbex-GW0904, i = 13.33, mechanical	€48500	9.4	4.71	2.83	1.41
A-III (B-III)	Turbex-GW0904, i = 20, mechanical	€49000	4.9	9.13	5.48	2.74
A-IV (B-IV)	Fortis Alize-GW0504, i = 2, mechanical	€57500	7.7	6.82	4.09	2.05
A-V (B-IV)	Fortis Alize-GW0904, i = 2, mechanical	€58000	7.4	7.16	4.29	2.15
A-VI	Bergey Excel-GW0504, i = 2, mechanical	€62500	8.0	7.13	4.28	2.14
A-VII (B-VII)	Bergey Excel-GW0504, i = 5, mechanical	€62500	3.5	16.31	9.78	4.89
A-VIII (B-III)	Bergey Excel-GW0904, i = 2, mechanical	€63000	9.2	6.25	3.75	1.88
A-IX (B-IX)	Fortis Alize-GW0504, n _{pump} = 700 rpm, electrical	€67500	10.8	5.71	3.42	1.71
A-X (B-V)	Bergey Excel-GW0504, n _{pump} = 700 rpm, electrical	€72500	12.4	5.34	3.20	1.60

- **Maintenance:** Turbex with mechanical coupling was assumed to be good to maintain (i.e. score of 3), due to the experience of Turbex with operation in developing countries and rural areas. Furthermore the extra transmission is located on the ground and easy to reach. The three bladed wind turbines with a mechanical coupling were assigned a score of 1. The entire coupling need to be custom made, making it more prone to problems and also hard to repair since no standard parts are available. Normally the electrical coupled system would get a good score on maintenance. In developing countries however there are only few people experienced with maintaining electrical system. For rural areas an maintaining an electrical system can therefore be a problem. For this reason the electrically coupled systems were given a 1 for maintenance.
- **Life:** The lifetime of the different systems is expected to be around 20 years, assuming the system is maintained properly. The systems that needed little customization (the Turbex mechanically coupled system and the electrically coupled systems) were assigned a score of 3 and the system with the custom made coupling was expected to have a slightly worse lifetime and therefore assigned a score of 2.
- **Reliability:** The reliability of the electrically coupled systems was assumed to be good and even better for the configuration with the Bergey Excel wind turbine due to the manufacturers experience in rural areas and with water pumping. Also the reliability of the

configurations with the Turbex windmill were expected to be reliable, due to the many years of experience of Turbex with water pumping in Africa. The extra customized coupling is a small risk on the reliability resulting in a score of 3 for these systems. The reliability of the mechanically coupled three bladed wind turbines is expected to be less, due to the entire customized coupling and lack of experience with this new coupling in developing countries.

Table 5-6: Score of selected configurations on each design criterion; values between 0 and 4 in which 0 indicates poor and 4 good performance and multiplied by the weighting factor

	Cost	Maintenance	Life	Reliability	Total Score	Total score as % of ideal case
Weighting factor	3	2.3	2.3	4.0		
Ideal case	12.0	9.2	9.2	16.0	46.4	100%
A-I	12	6.9	6.9	12	37.8	81 %
A-II	12	6.9	6.9	12	37.8	81 %
A-III	3	6.9	6.9	12	28.8	62 %
A-IV	6	2.3	4.6	8	20.9	45 %
A-V	6	2.3	4.6	8	20.9	45 %
A-VI	6	2.3	4.6	8	20.9	45 %
A-VII	0	2.3	4.6	8	14.9	32 %
A-VIII	9	2.3	4.6	8	23.9	52 %
A-IX	9	2.3	6.9	12	30.2	65 %
A-X	9	2.3	6.9	16	34.2	74 %

Table 5-6 shows the results of the selected configurations for the site with a mean wind speed of 5.9 m/s and brackish water. The scores for each criterion were multiplied with the weighting factor of that criterion, resulting in the weighted scores. The summation of the weighted scores were compared with the weighted score of in the ideal case, resulting in a total score of each configuration as a percentage of the ideal case. For brackish water desalination in areas with a mean wind speed of 5.9 m/s it turned out that the Turbex windmill with the Orbit GW0504 with transmission ratio $i = 20$ or the the Turbex windmill with the Orbit GW0904 and transmission ratio $i = 13.33$ performed best. Also the Electrical Bergey Excel with the Orbit GW0504 performed reasonably well.

A similar evaluation was done for a brackish water site with a mean wind speed of 7 m/s. Table 5-7 shows the water cost as a function of the payback time. The configurations were selected in the same way as the selection for the site with a mean wind speed of 5.9 m/s, so basically by looking at the configurations with the highest flow rate for each configuration type. Most of the selected configurations were also selected for the 5.9 m/s case and the corresponding configuration is given between the brackets in table 5-7. The system cost was again obtained by combining the cost of the different parts given in table 5-3. The water output was retrieved by running the SIMULINK model with a wind input as defined by means of equation 5-2. With this the relative water cost was calculated (equation 5-3) and from that the score on the Cost design criterion for each configuration was assigned. The scores on the other criteria were obtained by means of the same logic as explained before. Table 5-12 shows how the different configurations compare to each other based on the weighted scores on the four design criteria. The same configurations as for the site with a mean wind speed of 5.9 m/s perform well, namely the Turbex-GW0504 system with $i = 20$, the Turbex-GW0904 with $i = 13.33$ and the Bergey Excel- GW0504 electrical system. For the site with a mean wind speed of 7 m/s the system with the Turbex-GW0904 with $i = 20$ is however also one of the best performing configurations.

Table 5-7: Comparison of the water cost at a site with a mean wind speed of 7 m/s

				Water cost		
				Payback time (years)		
	Description	System Cost	Water output [m^3/day]	3	5	10
B-I (A-I)	Turbex- GW0504, i = 20, mechanical	€48500	19.5	2.27	1.36	0.68
B-II (A-II)	Turbex- GW0904, i = 13.33, mechanical	€48500	18.2	2.43	1.46	0.73
B-III (A-III)	Turbex- GW0904, i = 20, mechanical	€49000	19.5	2.29	1.38	0.69
B-IV (A-IV)	Fortis Alize- GW0504, i = 2, mechanical	€57500	9.8	5.36	3.21	1.61
B-V	Fortis Alize- GW0504, i = 5, mechanical	€57500	19.9	2.64	1.58	0.79
B-VI (A-V)	Fortis Alize- GW0904, i = 2, mechanical	€58000	13.9	3.81	2.29	1.14
B-VII (A-VII)	Bergey Excel - GW0504, i = 5, mechanical	€62500	23.1	2.47	1.48	0.74
B-VIII (A-III)	Bergey Excel - GW0904, i = 2, mechanical	€63000	12.3	4.68	2.81	1.40
B-IX (A-IX)	Fortis Alize- GW0504, $n_{pump} = 700$ rpm, electrical	€67500	19.3	3.19	1.92	0.96
B-X (A-X)	Bergey Excel - GW0504, $n_{pump} = 700$ rpm, electrical	€72500	22.2	2.98	1.79	0.89

5-3-4 Conclusions for brackish water desalination

In terms of water output it can be concluded that the best configuration type depends on the mean wind speed at the wind turbine location. The three bladed wind turbines, either mechanically or electrically coupled are only favorable at high mean wind speeds (> 7 m/s). In that case they deliver $23.1 m^3/day$ (mechanical) and $22.2 m^3/day$ (electrical) compared to $19.5 m^3/day$ of the mechanical multi-bladed configuration. At mean wind speeds lower than 6 m/s the mechanically coupled three bladed wind turbines are not such a good option (maximum of $9.2 m^3/day$). The electrical machines are performing better (maximum of $12.4 m^3/day$), but a well chosen mechanical coupling with a multi-bladed wind turbine was able to deliver the highest water output at lower mean wind speed (i.e. maximum of $12.9 m^3/day$).

By looking at the water cost it is found that for both a mean wind speed of 5.9 m/s and of 7 m/s the multi-bladed mechanical configuration is the best option. At higher mean wind speed the three bladed mechanical configurations and the electrical configurations can however become cost competitive.

The most important design criteria for the system for Somaliland were found to be cost, maintenance, life and reliability. Taking into account all these criteria results in the mechanically coupled multi-bladed windmill being the best solution for both evaluated mean wind speed cases. Assuming the reliability of the Bergey Excel is indeed as high as the assigned score in the analysis, the

Table 5-8: Score of selected configurations for brackish water desalination at a mean velocity of 7 m/s on each design criterion; values between 0 and 4 in which 0 indicates poor and 4 good performance and multiplied by the weighting factor

	Cost	Maintenance	Life	Reliability	Total Score	Total score as % of ideal case
Weighting factor	3	2.3	2.3	4.0		
Ideal case	12.0	9.2	9.2	16.0	46.4	100%
B-I	12	6.9	6.9	12	37.8	81 %
B-II	12	6.9	6.9	12	37.8	81 %
B-III	12	6.9	6.9	12	37.8	81 %
B-IV	0	2.3	4.6	8	14.9	32 %
B-V	12	2.3	4.6	8	26.9	58 %
B-VI	6	2.3	4.6	8	20.9	45 %
B-VII	12	2.3	4.6	8	26.9	58 %
B-VIII	3	2.3	4.6	8	17.9	39 %
B-IX	9	2.3	6.9	12	30.2	65 %
B-X	9	2.3	6.9	16	34.2	74 %

electrical configuration with the Bergey Excel wind turbine is a configuration to consider as well.

5-4 Sea water system

The system changes significantly when it has to desalinate sea water. The Orbit pumps can not be used, since they will not deliver enough pressure to overcome the osmotic pressure of sea water. In this chapter the configurations for the desalination of sea water as given in table 5-2 are evaluated. Three types of Danfoss pumps with energy recovery were considered and coupled to either the Turbex (for a mechanical coupling), the Fortis Alize (for both mechanical and electrical coupling) and the Bergey Excel (for both mechanical and electrical coupling).

5-4-1 Mechanical configurations

Figure 5-10 shows the water output for the Turbex windmill with the APP1.0/APM0.8 Danfoss pump for different transmission ratios. The water output for transmission ratios of $i = 20$ or smaller is not exceeding $3 \text{ m}^3/\text{day}$ even for large wind speeds. This can be improved by adding a significant transmission, but still with a transmission ratio of $i = 60$ the daily water production at a wind speed of 7 m/s is only around $6 \text{ m}^3/\text{day}$. Higher transmission ratios will result in a pump shaft speed that is exceeding the pump limitations (i.e. maximum of around 3000 rpm). Figure 5-11 gives the pump speed of the system at different transmission ratios and shows that the system with a transmission ratio of $i = 60$ the pump shaft speed is well below the maximum pump shaft speed.

Figure 5-12 shows the permeate flow rate of the Turbex windmill combined with the Danfoss APP1.5/APM1.2 and with the Danfoss APP2.5/APM1.8. The APP2.5/APM1.8 is the largest Danfoss pump considered in the evaluation and delivers more water at the same pump angular velocity. The required pump torque is however also larger. This results in start up issues for the system with higher transmission ratios as can be seen in figure 5-12(b) where for example the APP2.5/APM1.8 pump with a transmission ratio of $i = 60$ only starts producing water at a wind

speed between 5 and 6 m/s. Once running the water output is larger than for the smaller pump types.

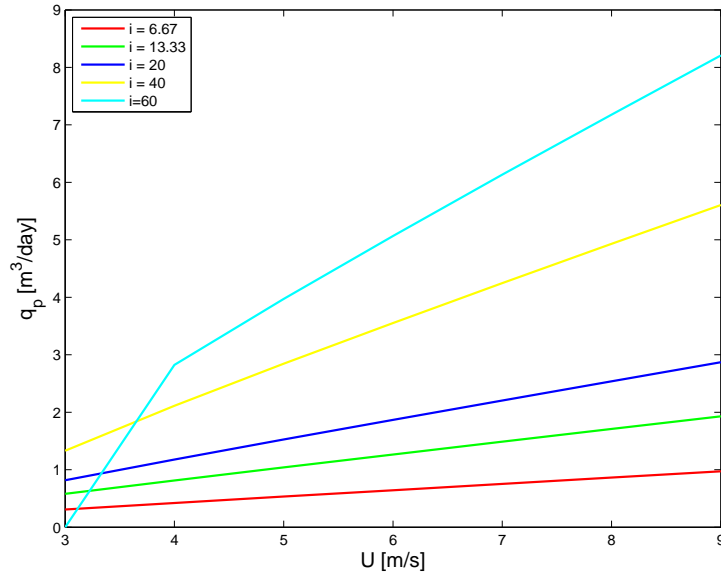


Figure 5-10: Daily water output (q_p) over wind speed (U) of the Turbex windmill with the Danfoss APP1.0/APM0.8 pump for mechanically driven sea water desalination

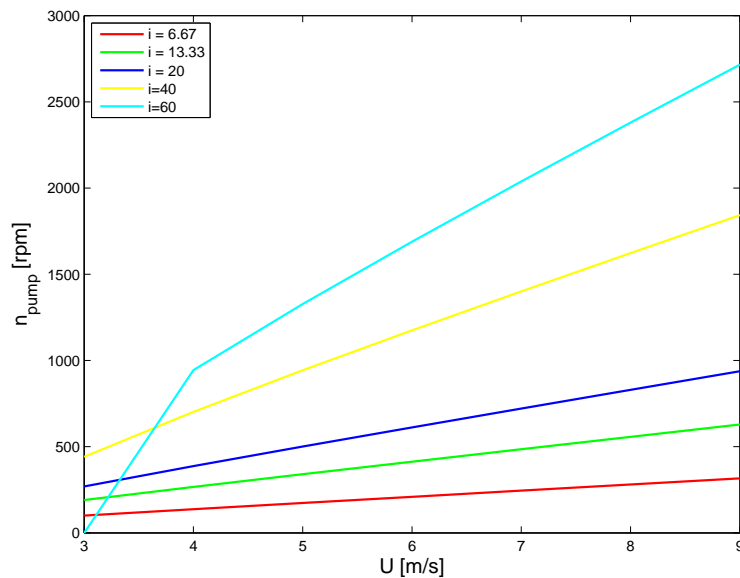
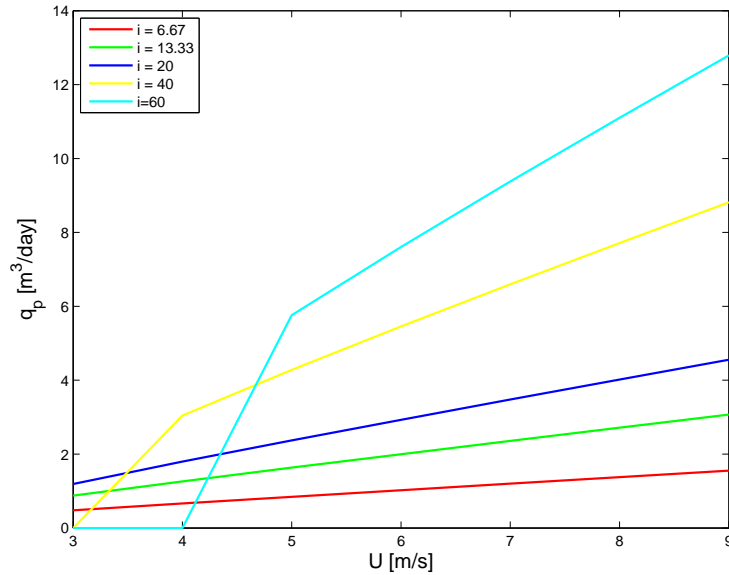


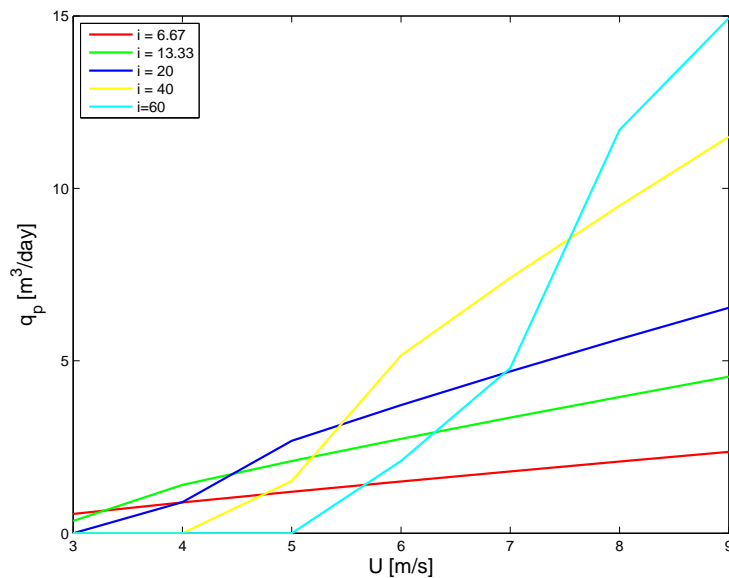
Figure 5-11: Pump angular velocity (n_{pump}) over wind speed (U) of the Turbex windmill with the Danfoss APP1.0/APM0.8 pump for mechanically driven sea water desalination

The Danfoss pumps were also mechanically coupled to the three bladed windturbines, Fortis Alize and Bergey Excel. The smallest Danfoss pump, the APP1.0/APM0.8 was disregarded since the

water output of this pump is small. The pump is interesting in regions with low wind speed when the other pumps have difficulty with starting. From figure 5-13(a) and figure 5-14(a) it follows however that the APP1.5/APM1.2 pump with small transmission ratios can start at lower wind speeds as well, making the evaluation of the APP1.0/APM0.8 pump in this case unnecessary.



(a) Danfoss APP1.5/APM1.2 pump

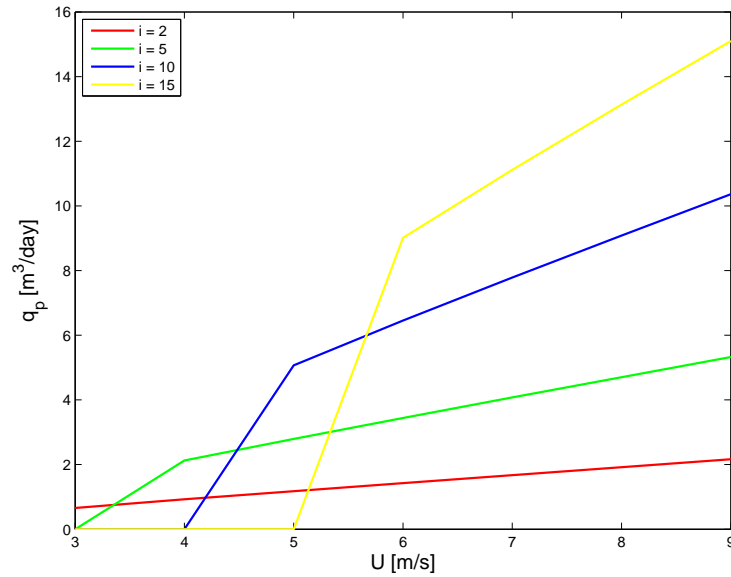


(b) Danfoss APP2.5/APM1.8 pump

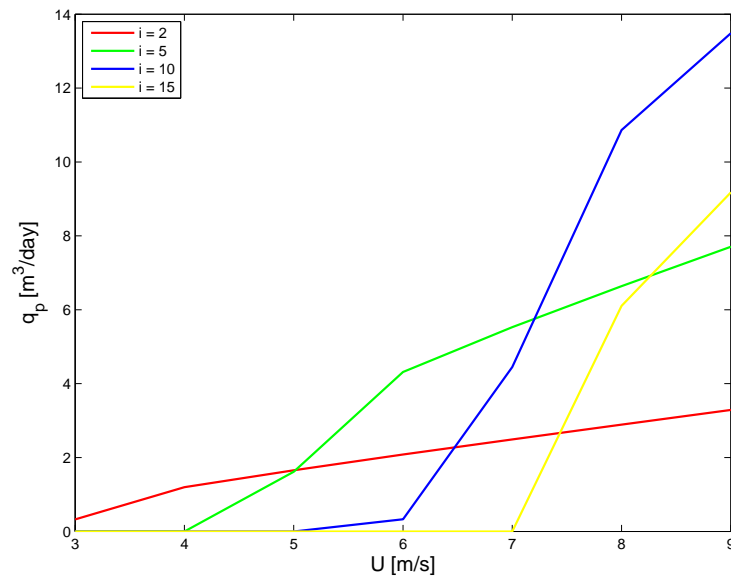
Figure 5-12: Daily water output (q_p) over wind speed (U) of the Turbex windmill with a Danfoss pump for mechanically driven sea water desalination.

As expected the three bladed wind turbines mechanically coupled to the Danfoss pumps have more

start up issues than the configurations with the Turbex windmill. Once running the configurations do however produce similar or even larger quantities of water. The selection of the transmission ratio should be done carefully, because the selected ratio has a large impact on the start up wind speed (see figure 5-13 and figure 5-14).

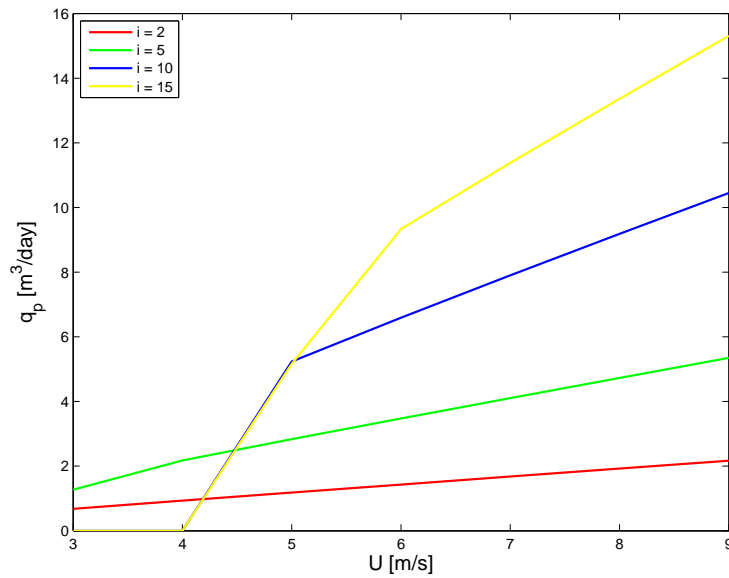


(a) Danfoss APP1.5/APM1.2 pump

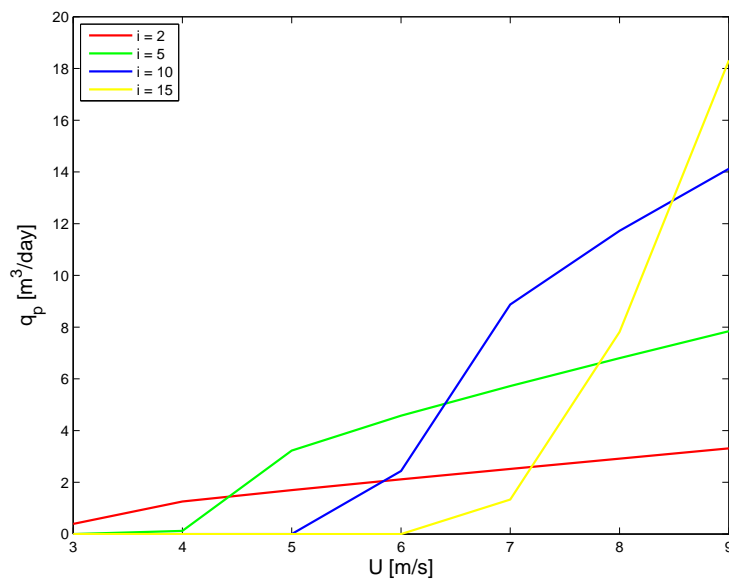


(b) Danfoss APP2.5/APM1.8 pump

Figure 5-13: Daily water output (q_p) over wind speed (U) of the Fortis Alize with a Danfoss pump for mechanically driven sea water desalination.



(a) Danfoss APP1.5/APM1.2 pump



(b) Danfoss APP2.5/APM1.8

Figure 5-14: Daily water output (q_p) over wind speed (U) of the Bergey Excel with the a Danfoss pump for mechanically driven sea water desalination.

5-4-2 Electrical configurations

For the electrical coupling six configurations are evaluated. The Fortis Alize and Bergey Excel wind turbines were combined with the Danfoss APP1.0/APM0.8, the Danfoss APP1.5/APM1.2, the Danfoss APP2.5/APM1.8.

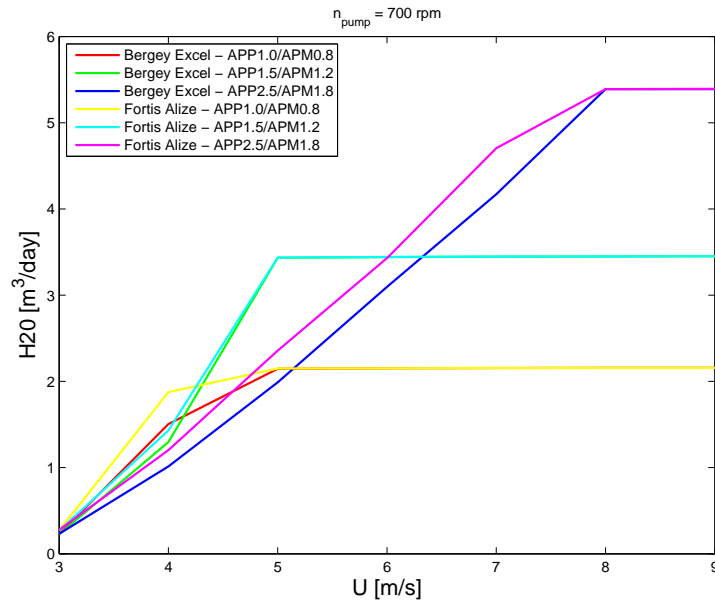


Figure 5-15: Daily water output (H2O) over wind speed (U) for the electrically driven sea water desalination with a fixed pump speed of 700 rpm

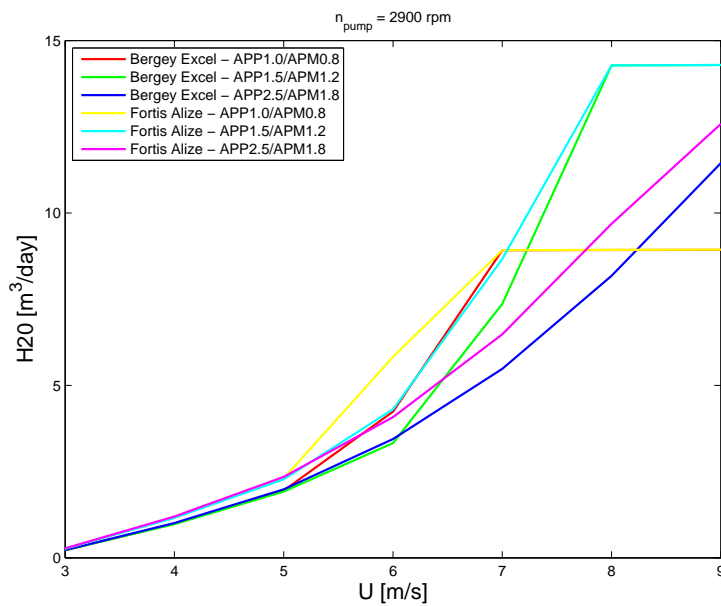


Figure 5-16: Daily water output (H2O) over wind speed (U) for electrically driven sea water desalination with a fixed pump speed of 2900 rpm

In figure 5-15 the average daily permeate flow rate for the six configurations at a fixed pump shaft speed of 700 rpm is given. In section subsec:elecconfig it was explained that the horizontal line indicate that the power delivered to the pump is higher than the required pump power resulting in continuous operation. The gradually increasing lines correspond with the situations in which the power delivered at the corresponding constant wind speed is lower than the required power

resulting in a constant start-stop operation mode. At 700 rpm the wind turbine is generally provides enough power at wind speeds above 5 m/s. Only for the larger Danfoss APP2.5/APM1.8 the power requirement is continuously met at wind speeds higher than 8 m/s. At 700 rpm the water output will never exceed the $5.5 \text{ m}^3/\text{day}$. Increasing the pump angular velocity increases this maximum water output.

In figure 5-16 the water output of the electrical configurations with a pump shaft speed of 2900 rpm is shown. Even the configuration with the smallest pump does not reach the point where the power required matches the power delivered directly before 7 m/s. Below this wind speed the system operates intermittently for every configuration. The water output is however similar at these lower wind speeds. The best configurations with a fixed angular velocity of 2900 rpm are therefore selected for further evaluation (section 5-4-3). It should be noted however that the intermittent operation of the system will have an impact on the performance of the battery. The battery performance will probably decrease quicker with continuous start stop behavior than with a system that meets the power requirement most of the time.

5-4-3 Configuration selection for $U_{mean} = 5.9 \text{ m/s}$ and $U_{mean} = 7 \text{ m/s}$

Table 5-10 and table 5-11 give the water cost for 3, 5 or 10 years of system payback time for the sea water site with a mean wind speed of 5.9 m/s and 7 m/s respectively. The configurations were selected based on the same reasoning as applied to the brackish water systems. Also the total system cost, the average daily water output and the water cost for the different payback times were obtained similarly (see section 5-3-3).

The desalination of sea water results in significantly higher water cost as compared to brackish water desalination. The smallest cost for sea water desalination with 10 years of payback time at a site with a mean wind speed of 5.9 m/s is 1.69 €/m^3 . For brackish water desalination this was 1.03 €/m^3 . At a site with a mean wind speed of 7 m/s the smallest cost of desalinating sea water is 1.30 €/m^3 compared to 0.68 €/m^3 for desalinating brackish water.

Table 5-9: Score of selected configurations for sea water desalination at a mean velocity of 5.9 m/s on each design criterion; values between 0 and 4 in which 0 indicates poor and 4 good performance and multiplied by the weighting factor.

	Cost	Maintenance	Life	Reliability	Total Score	Total score as % of ideal case
Weighting factor	3	2.3	2.3	4.0		
Ideal case	12.0	9.2	9.2	16.0	46.4	100%
C-I	9	6.9	6.9	12	34.8	75 %
C-II	12	6.9	6.9	12	37.8	81 %
C-III	3	6.9	6.9	12	28.8	62 %
C-IV	0	6.9	6.9	12	25.8	56 %
C-V	9	2.3	4.6	8	23.9	52 %
C-VI	12	2.3	4.6	8	26.9	58 %
C-VII	0	2.3	4.6	8	14.9	32 %
C-VIII	12	2.3	4.6	8	26.9	58 %
C-IX	0	2.3	4.6	8	14.9	32 %
C-X	6	2.3	6.9	12	27.2	59 %

Table 5-10: Comparison of the water cost for sea water desalination in a region with a mean wind speed of 5.9 m/s.

				Water cost		
				Payback time (years)		
	Description	System Cost	Water output [m^3/day]	3	5	10
C-I (D-I)	Turbex-APP1.0/APM0.8, i = 60, mechanical	€ 48000	5.9	7.43	4.46	2.23
C-II (D-II)	Turbex-APP1.5/APM1.2, i = 60, mechanical	€ 49200	7.6	5.91	3.55	1.77
C-III (D-III)	Turbex-APP2.5/APM1.8, i = 40, mechanical	€ 50500	3.7	12.46	7.48	3.74
C-IV	Turbex-APP2.5/APM1.8, i = 20, mechanical	€ 50000	3.4	13.43	8.06	4.03
C-V	Fortis Alize-APP1.5/APM1.2, i = 10, mechanical	€ 57200	7.3	7.16	4.29	2.15
C-VI (D-IV)	Fortis Alize-APP1.5/APM1.2, i = 15, mechanical	€ 57200	9.3	5.62	3.37	1.69
C-VII	Fortis Alize-APP2.5/APM1.8, i = 5, mechanical	€ 59000	3.9	13.82	8.29	4.14
C-VIII (D-VII)	Bergey Excel-APP1.5/APM1.2, i = 15, mechanical	€ 62200	9.0	6.31	3.79	1.89
C-IX	Bergey Excel-APP2.5/APM1.8, i = 5, mechanical	€ 64000	4.5	12.99	7.79	3.90
C-X (D-IX)	Fortis Alize-APP1.0/APM0.8, $n_{pump} = 2900$ rpm, electrical	€ 66000	5.9	10.22	6.13	3.06

Table 5-11: Comparison of the water cost for sea water desalination in a region with a mean wind speed of 7 m/s.

				Water cost		
				Payback time (years)		
	Description	System Cost	Water output [m^3/day]	3	5	10
D-I (C-I)	Turbex-APP1.0/APM0.8, i = 60, mechanical	€ 48000	7.0	6.26	3.76	1.88
D-II (C-II)	Turbex-APP1.5/APM1.2, i = 60, mechanical	€ 49200	9.8	4.58	2.75	1.38
D-III (C-III)	Turbex-APP2.5/APM1.8, i = 40, mechanical	€ 50500	7.6	6.07	3.64	1.82
D-IV (C-VI)	Fortis Alize-APP1.5/APM1.2, i = 15, mechanical	€ 57200	11.7	4.46	2.68	1.34
D-V (C-VII)	Fortis Alize-APP2.5/APM1.8, i = 5, mechanical	€ 59000	6.3	8.55	5.13	2.57
D-VI	Fortis Alize-APP2.5/APM1.8, i = 10, mechanical	€ 59000	6.0	8.98	5.39	2.69
D-VII (C-VIII)	Bergey Excel-APP1.5/APM1.2, i = 15, mechanical	€ 62200	13.1	4.34	2.60	1.30
D-VIII	Bergey Excel-APP2.5/APM1.8, i = 10, mechanical	€ 64000	8.3	7.04	4.23	2.11
D-IX (C-X)	Fortis Alize-APP1.0/APM0.8, $n_{pump} = 2900$ rpm, electrical	€ 66000	11.2	5.38	3.23	1.61
D-X	Fortis Alize-APP1.5/APM1.2, $n_{pump} = 2900$ rpm, electrical	€ 67200	10.2	6.02	3.61	1.80

Table 5-12: Score of selected configurations for sea water desalination at a mean velocity of 7 m/s on each design criterion; values between 0 and 4 in which 0 indicates poor and 4 good performance and multiplied by the weighting factor.

	Cost	Maintenance	Life	Reliability	Total Score	Total score as % of ideal case
Weighting factor	3	2.3	2.3	4.0		
Ideal case	12.0	9.2	9.2	16.0	46.4	100%
D-I	6	6.9	6.9	12	31.8	69 %
D-II	12	6.9	6.9	12	37.8	81 %
D-III	6	6.9	6.9	12	31.8	69 %
D-IV	12	2.3	4.6	8	26.9	58 %
D-V	3	2.3	4.6	8	17.9	39 %
D-VI	0	2.3	4.6	8	14.9	32 %
D-VII	12	2.3	4.6	8	26.9	58 %
D-VIII	6	2.3	4.6	8	20.9	45 %
D-IX	9	2.3	6.9	12	30.2	65 %
D-X	6	2.3	6.9	12	27.2	59 %

Table 5-9 and table 5-12 give the score of the different configurations on each design criteria. The scores were assigned based on the logic as described in section 5-3-3 and multiplied by the corresponding weighting factors. A summation of the scores per configuration and comparing these with the ideal case results in the relative score of the configuration as a percentage of the ideal case. At a site with a mean wind speed of 5.9 m/s the configurations with the Turbex windmill coupled mechanically to the either the Danfoss APP1.0/0.8 or the Danfoss APP1.5/1.2 both with a transmission ratio of $i = 60$ perform best. Also at a site with a mean velocity of 7 m/s the configurations with the Turbex windmill perform good. The Turbex windmill with the Danfoss APP1.5/APM1.2 and a transmission ratio of $i = 60$ gives the highest score. Also the electrical configuration with the Fortis Alize wind turbine and the Danfoss APP1.0/APM0.8 pump has a relatively good score.

5-4-4 Conclusion for sea water desalination

In terms of water output the three bladed wind turbines mechanically coupled with a well chosen transmission are outperforming the others at a mean wind speed of 7 m/s as well as 5.9 m/s. The best configurations at a mean wind speed of 5.9 m/s gives a water output of $9.3 \text{ m}^3/\text{day}$, compared to $7.6 \text{ m}^3/\text{day}$ for the best multi-bladed mechanical configuration and $5.9 \text{ m}^3/\text{day}$ for the best electrical configuration. At a mean wind speed of 7 m/s the electrical configurations show better results than the multi-bladed mechanical configurations (i.e. $11.2 \text{ m}^3/\text{day}$ compared to $9.8 \text{ m}^3/\text{day}$). With $13.1 \text{ m}^3/\text{day}$ the mechanically coupled Bergey Excel delivers however the highest water output.

From a water cost point of view the multi-bladed configurations show similar results as the three bladed mechanical configurations for a mean wind speed at 5.9 m/s as well as 7 m/s. The water cost for the electrical configurations is high for mean wind speeds at 5.9 m/s. At the higher mean wind speed of 7 m/s the water cost are still higher, but the gap with the other configurations has become smaller.

The most important design criteria for the system for Somaliland were found to be cost, maintenance, life and reliability. Applying these four design criteria to the sea water configurations show that using mechanical bladed configurations is the best solution. So despite the high score on the

water output and cost, mechanically coupled three bladed wind turbines were not found to be the optimal solution. The customized mechanical coupling reduced the score on maintenance, life and reliability compared to the multi-bladed windmill with an off-the-shelf coupling that needs only limited modification. The difference in water output was not high enough to overcome these drawbacks.

Configuration for Somaliland

In this chapter the optimal solution for brackish water desalination and for sea water desalination in Berbera, Somaliland, is selected. This is done by evaluating the promising configurations selected in chapter 5 with the monthly wind conditions of Berbera.

6-1 Wind input for Somaliland configuration

In table 6-1 the mean monthly wind speed is given. The measurements were done at the airport of Berbera in 2003. It gives an indication of the environment in Berbera, Somaliland. The Winddrinker will be placed in an empty area just outside of Berbera. No presence of buildings or surrounding trees will disturb the wind, making the location similar to the one where the wind data was obtained (i.e. the airport). One difference is that the wind turbine rotor hub will have a height of 18 meter above ground level compared to a height of 10 meter for the wind speed measurement location. This might result in a slightly higher wind speed for the wind turbine. The available wind data is however limited, and the wind input for the SIMULINK model is therefore a rough estimation of the reality. It was decided to work with the data from the measurements directly and not account for the height difference, because a conservative approach was preferred.

Table 6-1: Mean monthly wind speeds in Berbera, Somaliland [m/s]

	Jan	Feb	Mar	Apr	May	Jun	Jul	Aug	Sep	Oct	Nov	Dec
0600 UTC	1.4	1.5	2.4	2.7	2.2	11.7	14.5	13.3	8.8	2.0	1.9	1.2
1200 UTC	7.2	6.6	6.8	7.7	6.4	6.4	6.7	6.3	6.0	5.9	5.0	6.5

The wind varies per time of year and also per day. A Weibull distribution was used to simulate the wind speed in Berbera Somaliland. The rough estimation was made that half of the day the mean wind speed is the 0600 UTC value and the other half of the day it is the 1200 UTC value. 0600 UTC is 9 am local time and 1200 UTC is 3pm local time. In MATLAB a vector of 900 data points was constructed to model the daily wind speed by means of the 'wblrnd'-function, which creates a vector of random numbers from the specified Weibull distribution. The vector starts at the mean wind speed and the next point is 80% of the previous wind speed plus 20% of the randomly selected wind speed from the Weibull distribution (equation 5-2). The mean 0600 UTC value was used for the first 450 datapoints and the 1200 UTC mean for the next 450 datapoints. In figure 6-1 the wind speed curve, obtained as described above, for January and July is shown.

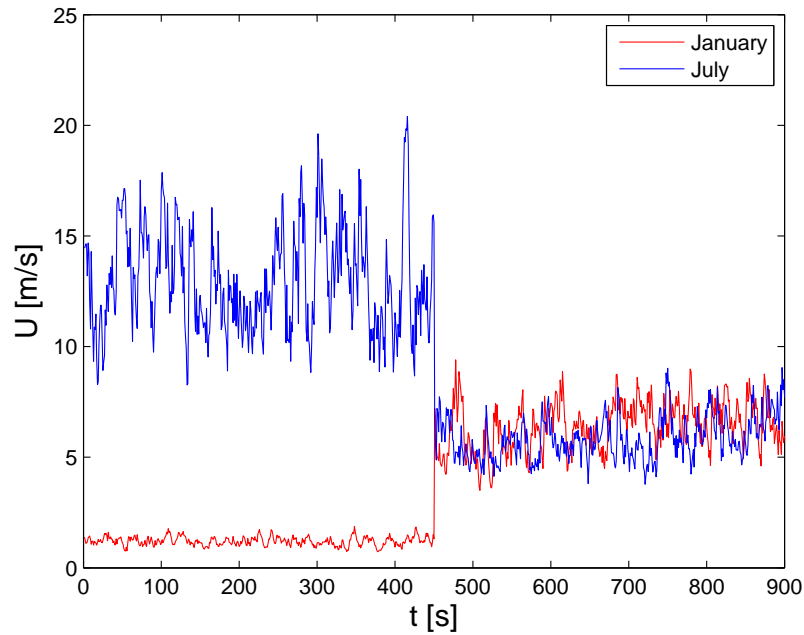


Figure 6-1: Windspeed model for Berbera, Somaliland

6-2 Brackish water system

Table 6-2 shows the mean daily water output for each month for a selection of the configurations as described in section 5-3-3. The five best configurations for the 5.9 m/s mean wind speed site were selected as well as the five best configurations for the 7.0 m/s site. They turned out to be the same configurations resulting in five configurations to be evaluated for Somaliland. The results given in the table are based on the wind speed model as described in section 6-1. Figure 6-2 shows how the water output changes during the year.

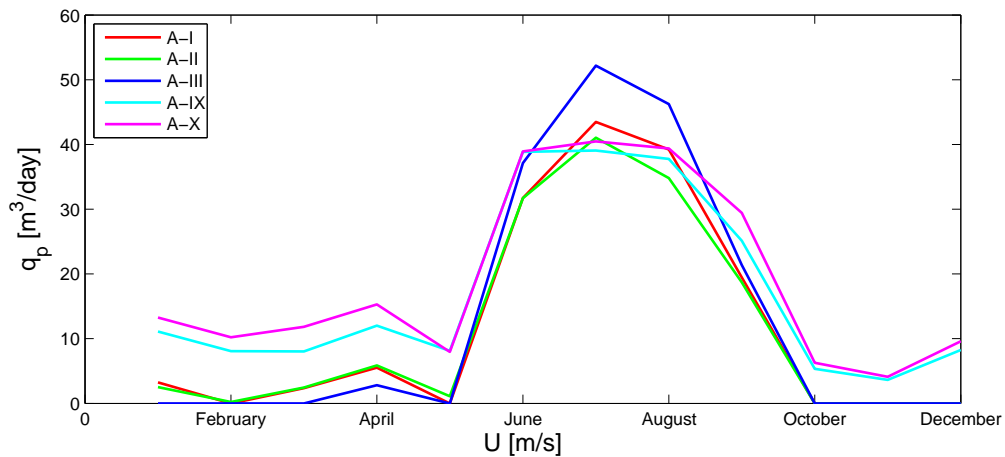


Figure 6-2: Daily water output of different system configurations for brackish water desalination (i.e. $P_f = 14.7$ bar) in Berbera, Somaliland

Table 6-2: Comparison of the water cost for brackish water desalination in Berbera Somaliland based on wind input as given in figure 6-1

				Water cost (€/m ³)		
				Payback time (years)		
	Description	System Cost	Water output [m ³ /day]	3	5	10
A-I (B-I)	Turbex-GW0504, i = 20, mechanical	€ 48500	12.1	3.66	2.20	1.10
A-II (B-II)	Turbex-GW0904, i = 13.33, mechanical	€ 48500	11.5	3.85	2.31	1.16
A-III (B-III)	Turbex-GW0904, i = 20, mechanical	€ 49000	13.3	3.36	2.20	1.01
A-IX (B-IX)	Fortis Alize- GW0504, n _{pump} = 700 rpm, electrical	€ 67500	17.1	3.60	2.16	1.08
A-X (B-V)	Bergey Excel - GW0504, n _{pump} = 700 rpm, electrical	€ 72500	18.9	3.50	2.10	1.05

Table 6-3: Score on each design criterion for selected configurations for brackish water desalination in Berbera Somaliland based on wind input as given in figure 6-1; values between 0 and 4 in which 0 indicates poor and 4 good performance and multiplied by the weighting factor

	Cost	Maintenance	Life	Reliability	Total Score	Total score as % of ideal case
Weighting factor	3	2.3	2.3	4.0		
Ideal case	12.0	9.2	9.2	16.0	46.4	100%
A-I	12	6.9	6.9	12	37.8	81 %
A-II	12	6.9	6.9	12	37.8	81 %
A-III	12	6.9	6.9	12	37.8	81 %
A-IX	12	2.3	6.9	12	33.2	72 %
A-X	12	2.3	6.9	16	37.2	80 %

6-2-1 Conclusion for brackish water desalination in Somaliland

In terms of water output the electrical configurations outperform the multi-bladed mechanical configurations. The best electrical system produces an average water output of 18.9 m³/day and the best mechanical system a water output of 13.3 m³/day.

Due to the lower system cost of the mechanical configuration the water costs of the selected configurations are similar. Also the differences between the total scores based on the four design criteria are small. The mechanical multi-bladed configuration is the winner, but with a close finish. The difference with the electrical system with the Bergey turbine is only 1%.

The mean wind speed in Somaliland varies highly per month and even per day (see table 6-1). Half the year the average daily water output is around 4 m/s. From figure 5-6 and 5-5 it follows that with the transmission ratios of the selected multi-bladed mechanical configurations the

system has difficulty meeting the torque requirement at these low wind speeds. This results in the fact that the selected configurations are barely producing water in those months. Decreasing the transmission ratio will increase the water output in the low wind speed months, but decreases the water output in the high wind speed months significantly due to the lower pump angular velocity. When choosing for a system with a fixed transmission ratio it is therefore recommended to stick with the higher transmission ratio configurations.

Introducing a multi-bladed mechanical system that is able to switch between different transmission ratios during the year promises to be the best solution for brackish water desalination in Somaliland. The variable transmission will allow for more water production in the low wind speed months, resulting in a higher average daily water output. With this higher water output the water cost will be decreased and the weighted score of the multi-bladed mechanical configuration will increase.

6-3 Sea water system

Selecting the best five configurations for sea water desalination resulted in the selection of six configurations for the site with a mean wind speed of 5.9 m/s due to a shared fifth place for configuration C-VI and C-VIII. From the five best configurations at a wind speed of 7 m/s the B-X was the only one not already selected. In table 6-4 the average daily water output for each configuration in Berbera, Somaliland, is given. Figure 6-3 shows how the water output for the selected configurations is spread over the year.

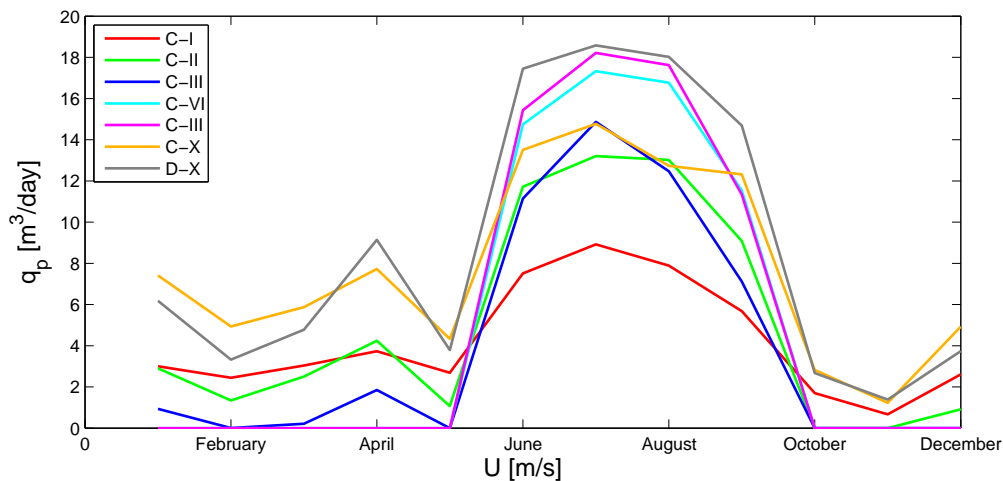


Figure 6-3: Daily water output of different system configurations for sea water desalination (i.e. $P_f = 14.7$ bar) in Berbera, Somaliland

6-3-1 Conclusion for sea water desalination in Somaliland

For sea water desalination the electrical configurations have the highest average water output. The best electrical system produces an average water output of $8.6 \text{ m}^3/\text{day}$ compared to an average water output of $5.2 \text{ m}^3/\text{day}$ for the best mechanical system with a three bladed wind turbine and $5.0 \text{ m}^3/\text{day}$ for the best mechanical system with a multi-bladed windmill.

Table 6-4: Comparison of the water cost for sea water desalination in Berbera Somaliland based on wind input as given in figure 6-1

				Water cost		
				Payback time (years)		
	Description	System Cost	Water output [m^3/day]	3	5	10
C-I (D-I)	Turbex-APP1.0/APM0.8, i = 60, mechanical	€ 48000	4.2	10.44	6.26	3.13
C-II (D-II)	Turbex-APP1.5/APM1.2, i = 60, mechanical	€ 49200	5.0	8.99	5.39	2.70
C-III (D-III)	Turbex-APP2.5/APM1.8, i = 40, mechanical	€ 50500	4.0	11.53	6.92	3.46
C-VI (D-IV)	Fortis Alize-APP1.5/APM1.2, i = 15, mechanical	€ 57200	5.0	10.45	6.27	3.46
C-VIII (D-VII)	Bergey Excel-APP1.5/APM1.2, i = 15, mechanical	€ 62200	5.2	10.92	6.55	3.28
C-X (D-IX)	Fortis Alize-APP1.0/APM0.8, $n_{pump} = 2900$ rpm, electrical	€ 66000	7.7	7.83	4.70	2.35
D-X	Fortis Alize-APP1.5/APM1.2, $n_{pump} = 2900$ rpm, electrical	€ 67200	8.6	7.14	4.28	2.14

Table 6-5: Score on each design criterion for selected configurations for sea water desalination in Berbera Somaliland based on wind input as given in figure 6-1 ; values between 0 and 4 in which 0 indicates poor and 4 good performance and multiplied by the weighting factor.

	Cost	Maintenance	Life	Reliability	Total Score	Total score as % of ideal case
Weighting factor	3	2.3	2.3	4.0		
Ideal case	12.0	9.2	9.2	16.0	46.4	100%
C-I	6	6.9	6.9	12	31.8	69 %
C-II	9	6.9	6.9	12	34.8	75 %
C-III	3	6.9	6.9	12	28.8	62 %
C-VI	6	2.3	4.6	8	20.9	45 %
C-VIII	3	2.3	4.6	8	17.9	39 %
C-X	12	2.3	6.9	12	33.2	72 %
D-X	12	2.3	6.9	12	33.2	72 %

Also from a water cost point of view the electrical configurations are showing the best results.

The water cost of the best mechanically coupled multi-bladed configuration is also relatively good. The three bladed wind turbines with mechanical coupling have a significantly higher water cost.

After evaluation with the other design criteria, the mechanically coupled multi-bladed configuration with the lowest water cost was found to be the optimal configuration for desalinating sea water in Somaliland. The difference compared to the electrical configurations is however small.

The water output of the multi-bladed configurations can be increased by applying different transmission ratios over the year as explained in section [6-2-1](#). This will result in a lower water cost and a higher weighted score for these configurations.

Conclusions and recommendations

7-1 Conclusions

The research objective defined two main tasks. The first was to design a tool to evaluate and optimize wind driven reverse osmosis desalination configurations for specific sites and the second task was to apply this tool to find the best configuration for Berbera, Somaliland.

Objective 1: Design a tool to evaluate and optimize wind driven reverse osmosis desalination configurations for specific sites

The Wind2Water model was the tool developed for the evaluation of wind driven reverse osmosis systems and can be used to find optimal configurations for specific sites. The model is organized in such a way that it allows easy implementation of additional components (such as a new wind turbine or pump).

The assumptions that were made for the creation of the mechanical Wind2Water model were validated by means of the experimental data from the prototype of Delft University of Technology built on Curaçao. The validation focussed on the permeate outflow around mean wind speed. With this focus the model matched the experimental results, proving that the assumptions were valid. The electrical Wind2Water model was validated by means of the prototype of Hatendoer Water. The efficiencies of the components in the electrical configuration were varied to find an electrical coupling that best matched the experimental results. This configuration was found and the characteristics of this configuration were used for the evaluation of other electrical configurations.

Objective 2: Apply the tool to find the best configuration for Berbera, Somaliland

With the Wind2Water model brackish water configurations and sea water configurations were first analyzed for regions with a mean wind speed of 5.9 m/s, which is the average yearly wind speed in Somaliland, and 7 m/s, which is the mean wind speed that was originally assumed. With the Wind2Water model multi-bladed and three-bladed wind turbines with a mechanical coupling, and three bladed wind turbines with an electrical coupling were evaluated. The effect of different pump sizes and, for the mechanical systems, transmission ratios were also taken into

account. The water output for each configuration was estimated and from that the water cost were defined. The total score of each configuration was based on the weighted score of the cost-, maintenance-, life- and reliability- criteria. From this analysis the five configurations with the highest weighted score for brackish water and for sea water desalination were selected. These configurations were evaluated to find the optimal configuration for Somaliland.

The selected configurations were analyzed with the monthly wind conditions of Berbera, Somaliland. For both brackish water and for sea water desalination, the mechanically coupled multi-bladed windmill configuration was found to be the optimal solution. The electrical configurations did show a higher average water output, but for brackish water desalination the water cost score was similar to the multi-bladed configuration. For sea water desalination however the score on the cost criterion was higher for the electrical machine than for the multi-bladed configuration. For application in a developing country the score on the ease of maintenance for the electrical system was however assumed to be lower than for the multi-bladed mechanical configuration, resulting in a slightly lower overall score for the electrical configuration.

The mean wind speed in Somaliland varies highly per month and even per day. Introducing a multi-bladed mechanical system that is able to switch between different transmission ratios during the year promises to be the best solution for both brackish water desalination as well as for sea water desalination in Somaliland. The variable transmission will allow for more water production in the low wind speed months, resulting in a higher average daily water output. With this higher water output the water cost will decrease and the weighted score of the multi-bladed mechanical configuration will increase.

7-2 Recommendations

The Wind2Water model forms a good basis for future research on wind driven reverse osmosis desalination. The model is highly adaptable, which makes it easy to add additional components. The main recommendations for continuation of the research on wind driven reverse osmosis desalination are:

1. **Test, test, test:** At the moment the Wind2Water model is validated with limited available experimental data. The electrical configuration of Hatenboer has been installed in Indonesia. Evaluating the operation of this system over a longer period of time and comparing the experimental results with the Wind2Water model will be an interesting contribution to the current research. The same holds for the mechanical system that will be placed in Somaliland in the end of 2011. Also it is recommended to evaluate the operation of the Pearson pump in more detail with a specific focus on the start up behavior. By doing that future configurations with the Pearson pump can be evaluated with the Wind2Water model.
2. **Direct electrical coupling:** By using a direct electrical coupling the losses of the battery are bypassed, thereby reducing one of the big disadvantages of an electrical coupling. With a direct coupling the wind speed should be high enough to drive the motor directly most of the time. At what conditions this configuration becomes cost competitive and if the configuration will obtain a higher weighted score is an interesting topic for a follow-up study.
3. **Pressure variation for brackish water configurations:** From the data of the Curaçao experiment it followed that the feed pressure could be assumed constant for sea water desalination. The same assumption was applied to brackish water desalination, which probably resulted in somewhat conservative results for the brackish water configurations. By adding the variability of the feed pressure especially the brackish water model will be improved.

4. **Include the risk of fouling in the SIMULINK model:** At the moment the quality over time of the membranes is not taken into account. Using too many membranes at a low flux will for example result in fouling which decreases the performance of the membranes. Adding this effect to the model will make it more accurate.
5. **Evaluate configurations with larger wind turbines:** The power delivered by a wind turbine is a function of the rotor radius squared. Increasing the radius therefore results in significantly more water output (see appendix B). Adding a larger wind turbine and comparing the water cost with the configurations with a smaller wind turbine will be a valuable addition to the current work. Especially for the electrical systems increasing the rotor radius is expected to be beneficial. The electrically coupled configurations are now most of the time operating with the continuous start stop behavior, because the power delivered to the pump is less than the power required. Operating a system like this is not beneficial for the performance of the battery and better matching of wind turbine with the pump is therefore recommended. Decreasing the pump size and the pump shaft speed is one way of matching the power delivered with the power required. This however results in relatively low water outputs. Another solution is to increase the wind turbine rotor diameter, which increases the total system cost, but might decrease the relative water cost. It is recommended to add a larger wind turbine in the Wind2Water model to find out if the water output can really result in decrease of the relative system cost and, more importantly, in an improved total weighted score compared to other configurations.

Bibliography

- [MDG, 2006] (2006). *Meeting the MDG drinking water and sanitation target: the urban and rural challenge of the decade*. WHO, UNICEF.
- [Corbus and Meadors, 2005] Corbus and Meadors (2005). Small wind reserach turbine. Technical report, National Renewable Energy Laboratory.
- [Danfoss, 2007] Danfoss (2007). Datasheet 'sea water pump with energy recovery'.
- [Essam et al, 2004] Essam et al (2004). Design, simulation and economic analysis of a stand-alone reverse osmosis desalination unit powered by wind turbines and photovoltaics. *Elsevier - Desalination*, 164:87–97.
- [Feron, 1984] Feron, P. (1984). *Seawater desalination and windenergy: a system analysis*. Technische Hogeschool Eindhoven.
- [Forstmeier et al, 2006] Forstmeier et al (2006). Feasibility study on wind-powered desalination. *Elsevier - Desalination*, 203:463–470.
- [Garcia-Rodriguez et al, 2000] Garcia-Rodriguez et al (2000). Economic analysis of wind-powered desalination. *Elsevier - Desalination*, 137:259–265.
- [Habali et al, 1994] Habali et al (1994). Design of stand-alone brackish water desalination wind energy system for jordan. *Elsevier - Solar Energy*, 52(6):525–532.
- [Heijman et al, 2010] Heijman et al (2010). Sustainable seawater desalination: Stand-alone small scale windmill and reverse osmosis system. *Elsevier - Desalination*, 251:114–117.
- [J.A. de Ruijter, 2010] J.A. de Ruijter (2010). Eind rapportage 'drinking with the wind'. Technical report, Hatendoer Water.
- [J.F. Manwell, J.G. McGowan, A.L. Rogers, 2002] J.F. Manwell, J.G. McGowan, A.L. Rogers (2002). *Wind Energy Explained*. John Wiley and Sons.
- [Kalogirou, 2005] Kalogirou, S. (2005). Seawater desalination using renewable energy sources. *Progress in Energy and combustion Science*, 31:242–281.
- [Kentfield, 1996] Kentfield, J. A. (1996). *The Fundamentals of Wind-Driven Water Pumpers*. Gordon and Breach Science Publishers.

- [Kiranoudis, 1996] Kiranoudis, C. (1996). Wind energy exploitation for reverse osmosis desalination plants. *Elsevier*.
- [Larsen, 2006] Larsen (2006). Water hammer in pumped sewer mains. Technical report, Aalborg University.
- [Liu et al, 2002] Liu et al (2002). Experiments of a prototype wind-driven reverse osmosis desalination system with feedback control. *Elsevier - Desalination*, 150:277–287.
- [Miranda, 2002] Miranda, M. (2002). A wind-powered seawater reverse-osmosis system without batteries. *Elsevier - Desalination*, 153:9–16.
- [Moreno et al, 2004] Moreno et al (2004). Preliminary experimental study of a small reverse osmosis wind-powered desalination plant. *Elsevier - Desalination*, 171:257–265.
- [Nando Timmer,] Nando Timmer. Technical report, Delft University of Technology.
- [Ocean Pacific Technologies,] Ocean Pacific Technologies. Ocean x-pumps.
- [Rabinovitch, 2008] Rabinovitch, E. (2008). Drinking with the wind, small scale swro-installation mechanically driven by wind energy. Master’s thesis, TU Delft, Faculty of Civil Engineering and Geosciences.
- [Robinson et al, 1992] Robinson et al (1992). Development of a reliable low-cost reverse osmosis desalination unit for remote communities. *Elsevier - Desalination*, 86:9–26.
- [Spectra Watermakers, 2009] Spectra Watermakers (2009). Pearson high pressure pump application guide.
- [Thomson, 2003] Thomson, M. (2003). *Reverse-Osmosis Desalination of Seawater Powered by Photovoltaics Without Batteries*. PhD thesis, Loughborough University.
- [Thomson et al, 2002] Thomson et al (2002). A small-scale reverse-osmosis system with excellent energy efficiency over a wide operating range. *Elsevier*.
- [van Dijk, 2008] van Dijk, J. (2008). *Drinking water, Water treatment technology*.
- [Witte et al, 2003] Witte et al (2003). Winddesalter technology. *Elsevier - Desalination*, 156:275–279.

Part IV

Appendices

Appendix A

Research and development on small scale wind turbines and desalination

Wind powered desalination is one of the most promising alternatives of renewable energy desalination [Kalogirou, 2005]. It can be competitive with other desalination systems, providing safe and clean drinking water efficiently in an environmentally responsible manner [Forstmeier et al, 2006].

Garcia-Rodriguez presented a preliminary cost evaluation of wind-powered RO [Garcia-Rodriguez et al, 2000]. This research was done for relatively large scale systems with windturbines ranging from 600 to 750 kW nominal power. The total plant capacity was in the order of 200-3000 m³/day. The study showed that the levelized cost of the system could be significantly reduced by improvements in technology. Reducing the energy requirement by means of using the energy of the wind turbines directly might be one way. Improvement of energy recovery was mentioned as a second option and the development of membrane technology as the third. Nowadays energy recovery indeed reduces the energy requirement significantly. Also membrane technology has developed and currently only slight improvements are observed. The coupling of a reverse osmosis system to a wind turbine is however still under research. Direct mechanical couplings were only scarcely installed and are not developed far enough to use commercially.

Kiranoudis performed a detailed analysis of a wind-powered RO plant by considering both different wind turbines and membranes [Kiranoudis, 1996]. The wind turbines used in the analysis were the Vestas 59kW wind turbine and the Floda 170 kW wind turbine. The Vestas wind turbine is suitable for capacities up to 400 Km³ per year for brackish water desalination and up to 100 Km³ a year for seawater desalination. The size of this plant is much larger than the intended system size for this research. What is however interesting is that the study showed that with wind energy the water cost price of RO desalination can be reduced up to 20% at mean wind speeds higher than 5 m/s provided that the plant size is determined correctly. This result promises that at least for large scale applications wind power can significantly reduce the unit cost of produced water by RO desalination plants.

The previous mentioned large scale reverse osmosis units used an electrical coupling. Witte described how a windturbine of 1MW could be used to drive a sea water reverse osmosis system directly with the WindDesalter technology [Witte et al, 2003]. The WindDesalter promises to deliver 2400 m³/day of desalinated sea water. All the system elements are included in the tower and

some wind energy is converted to electricity to drive the lifting pump and regulating and control devices. The rotating axis furthermore drives the high pressure pump directly. The technology was published in 2003. By looking at the website of WindDesalter the technology, although promising, does not seem to be developed to a commercial point yet.

In 1984 Feron studied the feasibility of RO desalination in combination with wind energy for small scale applications. He considered three possible configurations of wind-powered RO-plants, namely a RO plant driven at constant conditions, an RO plant operating at varying conditions and an RO plant operating with varying membrane area [Feron, 1984]. In figure A-1 an overview of the three configurations and the corresponding power output curves are shown.

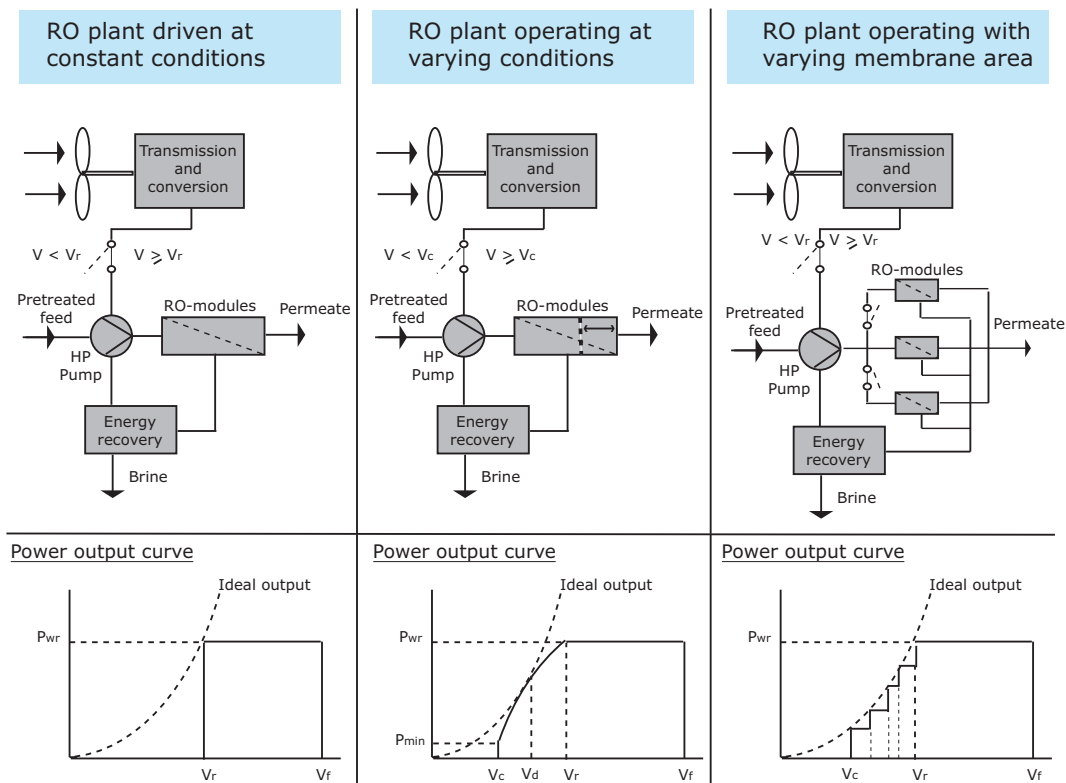


Figure A-1: Wind powered desalination configurations and the corresponding power output curves

The wind turbine starts to deliver power at the cut-in wind-speed, V_c . Above the rated wind-speed, V_r , the power output is limited and above the furling wind-speed, V_f the turbine is shut down. The design wind-speed, V_d is the wind-speed at which the wind turbine reaches its highest efficiency (i.e. $C_{p_{max}}$). The ideal wind-turbine always runs at its maximum efficiency and is shown by the dashed line in the power output curves in figure A-1. Feron concluded that although the prospects for reverse osmosis in seawater desalination are very good, the feasibility of windpowered RO-plants is poor compared to dieselpowered plants due to the low availability of the windturbine and the difficulty of membrane modules to work under variable loads. Recent developments have however shown that membranes can operate under variable loading and with rising diesel prices and attention to sustainability wind powered RO can be competitive in regions with sufficient wind.

In table A-1 an overview of different small scale wind powered RO studies is given. The systems were all installed for research objectives. U_{mean} is the mean wind speed at the site and TDS stands for total dissolved solids, a way of describing the salt content of the water. A TDS of 35000-40000 ppm indicates sea water and the sites with 1500 - 6000 TDS are brackish water sites. A difference

is made between a mechanical (M) and an electrical (E) coupling. The cost of the water is not always given and is also a difficult variable to compare. For a valid comparison a similar cost structure should be applied. If a water price is given it is usually not mentioned how they exactly got to this price. Does it include investment cost only or also operational cost? And what is the lifetime over which the costs are spread? The values mentioned in the table do however give a good feeling for the price range. The cost price for the mechanical brackish water system of Robinson is very high compared to the others [Robinson et al, 1992]. The mean wind speed at Robinson's site was however only 3 m/s and the water production around 200 liters per day. Robinson made an clear overview of the cost structure. The water price included investment cost, running cost and the amortization of the capital cost of the system was based on a 15 year life span. The cost price of the water could be reduced to 2.5 \$/m³ when a production of 1000 liter per day is realized (which can be true at sites with higher mean wind speeds). The study showed that for remote communities in Australia the system becomes economically viable at production levels of 500 liters per day. It also stated that for good system acceptance in these communities the human factor should not be neglected. The community members have to get familiarized with the technology and therefore consultation from the start, training and ensuring that the technology is compatible with their lifestyle is of great importance. Also the reliability of supply and maintenance are important criteria. A back-up source of pumping energy and a servicing agency are essential for reliable and constant operation of the system.

Table A-1: Wind powered RO studies

Author	Year	Location	U_{mean} [m/s]	TDS [ppm]	E/M*	Output [m ³ /day]	Cost [\$/m ³]	Comments
Heijman et al	2008	Curacao	7	sea	M	5-10	na	Multi-bladed 5m diameter windmill
Habali et al	1994	Jordan	4.7	1500-4000	E	22 - 33	0.99-1.71	Aeroman 15 kW windturbine
Miranda et al	2002	UK	8.3	40000	E	8.5	-	2.2 kW wind turbine, no batteries
Robinson et al	1991	Australia	3	2000-6000	M	0.2	20	Multi-bladed 4 m diameter windmill
Essam et al	2003	Greece	5.7	40000	E	8.5	7.2	10kW wind turbine and 35 % PV system
Liu et al	2002	Hawaii	5	3000	M	3.7	na	Multi-bladed 4.3 m diameter windmill
Moreno et al	2004	Colombia	7 - 9	35000	E	0.4	na	1.5kW wind generator

Liu also investigated a brackish water system with a direct mechanical coupling [Liu et al, 2002]. The system consisted of four major subsystems: a multi-vaned windmill/pump, a flow/pressure stabilizer, a reverse osmosis module and a control mechanism. The control mechanism allowed the system to operate satisfactorily under an average wind speed of 5 m/s. At 5 m/s and a TDS of 3000 mg/L the experiments showed a feed water flow of 13 L/min. At the average recovery ratio of 20% the product flow is then 3.7 m³/day.

The most recent publication on a direct mechanical coupling concerned the sea water desalination system tested on Curacao in 2008 [Heijman et al, 2010]. Sea water desalination requires a higher feed pressure and therefore high pressure pumps are needed which have a higher power requirement. The 5 meter diameter windmill was directly coupled to a high pressure piston pump with energy recovery. Due to the energy recovery the power requirement was reduced significantly. A transmission of $i = 1:40$ was applied to increase the pump shaft speed. In the same time the

transmission reduced the torque delivered to the pump. The start up torque did however remain high resulting in start up only at high wind speeds (in the order of 7 m/s). The system produced 5 to 10 m³ of permeate per day at a mean wind speed of 7 m/s.

Wind powered sea water desalination was also studied by Miranda [Miranda, 2002], Essam [Essam et al, 2004] and Moreno [Moreno et al, 2004]. The systems they proposed all had an electrical coupling. Miranda evaluated a system with a 2.2 kW wind turbine connected to a RO system without the use of any batteries. The output estimated at a mean wind speed of 8.3 m/s was 8.5 m³/day. The system contained a model-based control strategy to independently maximize the energy extracted from the wind and the water output of the RO unit. The Clark pump was used as the energy recovery device. Essam presented a method for sizing and simulating a hybrid wind-PV system to power RO desalination based on a technical and economical analysis. The cost of the system contained investment cost, running cost and included the life-span of the different components. Compared to an autonomous PV system the hybrid wind-PV system results in lower water production cost. The study also showed that it is more cost effective to store fresh water rather than to store electrical energy. At the same time however the battery bank should be kept at an appropriate size in the pursuit of constant operating conditions. Moreno just like Miranda developed a system that reduced the need for an energy storage system. The most appropriate configuration found was the high-voltage wind generator, connected directly to the motor. Although the DC electricity supply allows for the control of speed and it offers flexibility in operating characteristics, it is also more expensive than the AC equivalent. Furthermore it needs a rectifier, reducing the simplicity of this solution.

Electrical wind powered RO desalination systems for brackish water applications are also studied. Habali designed a stand-alone system for Jordan and concluded that the wind-RO pumping-desalination system can be considered technically and economically feasible. The water production cost were based on investment cost, annual operating cost and the economic life of the equipment and drastically decreases with larger wind turbine capacities and/or higher annual mean wind speeds. Also it was found that over the lifetime of the system the diesel-RO system costs more per unit production than the wind driven RO system.

The different theoretical analysis and prototype experiments show that with careful design and site selection small scale wind powered reverse osmosis desalination can be both technically and economically feasible. Robinson emphasized the importance of other criteria besides the cost effectiveness. The reliability of supply which Essam improved by designing a hybrid wind-PV system is one of the criteria mentioned. The variable character of the wind causes a variable water output for the directly coupled mechanical or electrical system. This variable water supply might make the acceptance of the technology in remote areas difficult. Also a workable maintenance schedule is key to success and should be considered in the water production cost. Furthermore the community should be acquainted with the technology before the operation starts. Simplicity of the system is therefore advantageous. This will make it easier to understand, making it more likely that the remote community keeps the system running.

The choice between a mechanical or an electrical coupling remains difficult. The disadvantage of an electrical coupling are the losses due to changing from mechanical energy to electrical energy and vice versa. Especially adding a battery bank increases the energy losses considerably. This is the main reason for Miranda, Habali and Moreno to design an electrical coupling without any batteries. Heijman decided to get rid of the conversion losses completely by moving to a completely mechanical coupling. The difficulty with this design is the matching of the available power with the optimal shaft speed. Including a higher transmission ratio means a higher pump shaft speed and therefore more water, but at the same time it implies less torque at the pump. This can result in difficulty with providing enough torque to drive the pump especially at start up. Another disadvantage is that due to the high start up torque required by the pump the windturbine selection is limited to multi-bladed windmills. These windmills provide high start up torque at the cost of low angular velocities. Also their size is limited compared to the wide range of sizes of three bladed wind-turbines, which reduces the possibilities for increasing scale.

Appendix B

Preliminary research into a wind driven RO system

To get a first insight into the effect of wind turbine characteristics, pump, RO characteristics and wind profile on the water output a matlab model was developed. The general overview is shown in B-1. With this model the effect of wind turbine variations on the water output are evaluated. Variations in airfoil type, number of blades and radius of the blade are considered.

With the airfoil known the design angle of attack (α_{design}) and the design lift coefficient ($C_{l,design}$) are determined. From this the blade properties can be retrieved as described in appendix C. The blade properties are the chord distribution c , the blade twist angle θ_T , lambda λ and inflow angle ϕ distribution. These parameters function as input for the blade element momentum (BEM) model. The BEM model of this preliminary study is also used in the SIMULINK model. The power and torque generated by the wind turbine and the power coefficient at start up serve as input for the coupling module. The coupling induces certain losses on the wind turbine power and the turbine angular velocity needs to be increased to a suitable pump shaft velocity by means of a transmission system. The water output of this preliminary model depends on the wind, the energy consumption of the RO membrane(s) and the power and pressure delivered by the windmill-pump combination.

The system configuration of the preliminary model was based on the prototype built on Curacao in 2008 [Rabinovitch, 2008]. The windturbine was not kept the same in order to evaluate the influence of the wind turbine design on the water output. The rotor radius R was varied between 3 and 8 meters and the number of blades was either 3 or 9. The airfoils considered were the DU-91-W2-250, normally used for high tip speed ratio machines and the curved plate airfoil with a tube at 0.25 chord, commonly used for multi-bladed windmills. The coupling losses in the model were obtained from the report on this prototype and are given in table B-1. The values might be different from reality. The goal of this model is however to get a rough idea of the effects of the wind turbine configuration and the variation in coupling losses will not have a large impact on the general understanding. It was therefore decided to work with these values.

The pump used for the prototype and therefore the matlab model was the Danfoss APP1.5 pump. The Danfoss APP1.5 high pressure pump used in this design needs a minimum rotational speed of 700 rpm. The transmission should thus be able to convert the turbine angular velocity to at least 700 rpm. At cut in wind speed the angular velocity is smallest, so dividing the required pump velocity by the angular velocity at U_{cutin} results in the necessary transmission ratio (i). The angular velocity is a function of the tip speed ratio λ_{design} , rotor radius R and wind speed

U. Table B-2 gives the minimum required transmission ratios for different number of blades and radius [m].

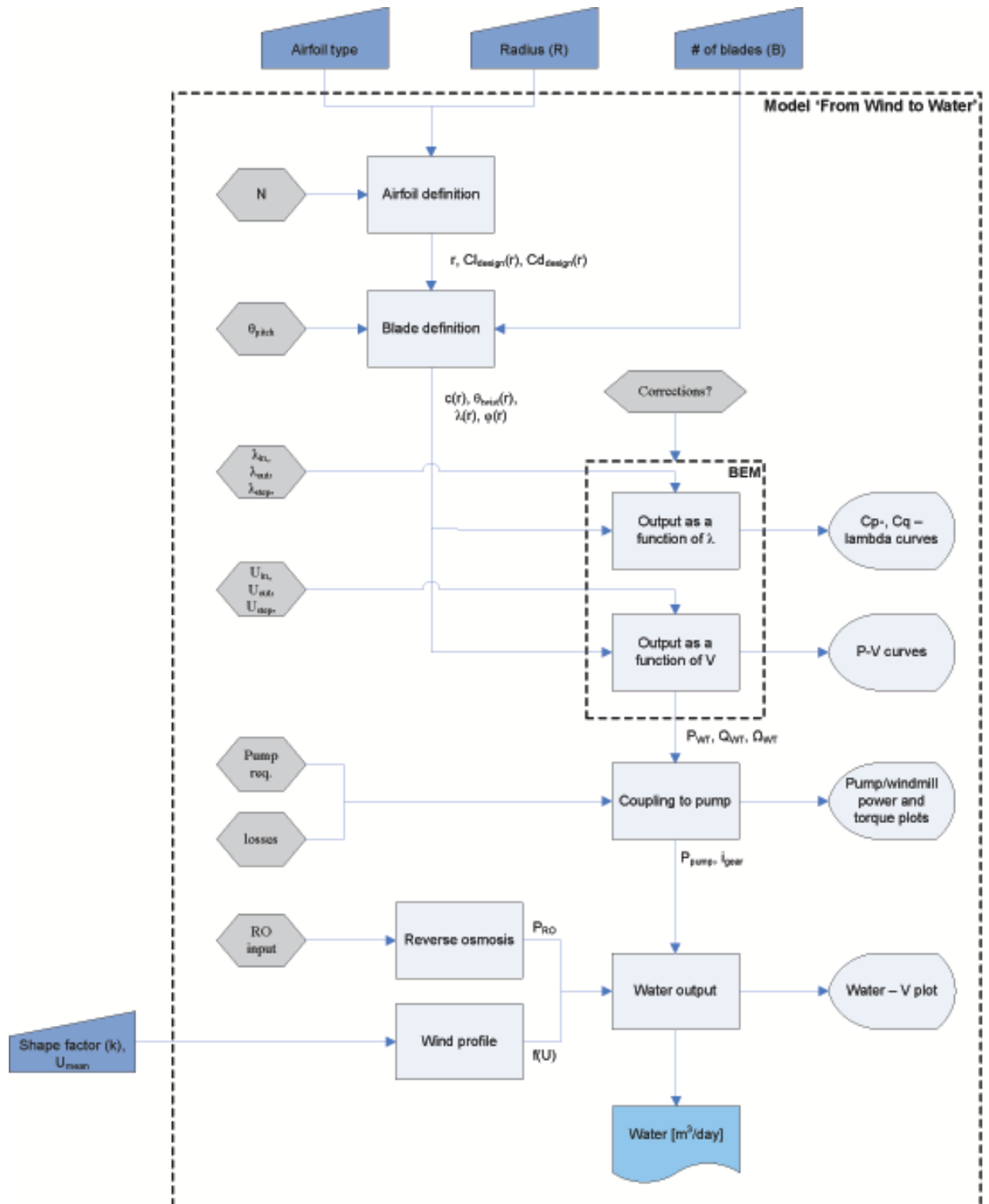


Figure B-1: Overview of the 'Wind to water' matlab model

Table B-1: Energy losses of the mechanical coupling of the prototype built on Curacao[Rabinovitch, 2008]

Component	Energy loss [%]
Gear box	6
V-belt	1
Bearing	5
Total	12

Table B-2: Minimum required transmission ratio (i) for Danfoss APP1.5 pump; B is number of blades, R is rotor radius

	B = 3	B = 9
R = 3	1:13	1:39
R = 5	1:22	1:66
R = 8	1:35	1:105

Besides the angular velocity criterion, the torque/power criterion should be taken into account. The pump will not start to run if the power (P) and torque (Q) delivered by the wind turbine are not sufficient. The trick now is to find a wind turbine configuration for which the pump starts running at a wind speed close to and preferable somewhat below U_{cutin} . The wind speed at which the pump starts running is called U_{start} , which is calculated by means of formula B-1. Table B-3 gives an overview of the required wind speeds for the different wind turbine configurations.

$$U_{start} = \sqrt{\frac{Q_{pump,start} i}{\frac{1}{2} \rho C_{q,start} \pi R^3}} \quad (\text{B-1})$$

Table B-3: Wind speed at which the APP1.5 pump ($Q_{start} = 11 \text{ Nm}$) starts running with the minimum required transmission ratio (see table B-2)

[m/s]		B = 3	B = 9
DU-91-W2-250	R = 3	6.4	5.7
	R = 5	3.8	3.4
	R = 8	2.4	2.5
Curved plate with tube at 0.25 chord	R = 3	7.1	5.7
	R = 5	4.3	3.4
	R = 8	2.7	2.1

Figure B-2 gives a graphical overview of the location of U_{start} for the wind turbine with 9 blades, a rotor radius of 3 meter and the curved plate airfoil with a tube at a quarter chord. The power and torque requirements of the APP1.5 high pressure pump and the APP1.5/APM1.2 pump/recovery combination is shown with the blue and green lines respectively. At start up, when the energy recovery system does not provide pressurized water yet, the wind turbine output should meet the APP1.5 requirements but once running only the APP1.5/APM1.2 requirements have to be met. U_{start} is the wind speed at the intersection of the APP1.5 line with the wind turbine at zero tip speed ratio.

The energy consumption of the RO membrane(s) is calculated in the 'RO'-module and is dependent on the feed pressure, the recovery and the efficiency of the energy recovery. The same values

as for the experiment on Curacao are used [Rabinovitch, 2008]. That implies a feed pressure of 42.5 bar and efficiency of energy recovery of 33%. The recovery of 20% is chosen to prevent concentration polarization from happening. In today's model the energy consumption is 4.38 kWh/m³.

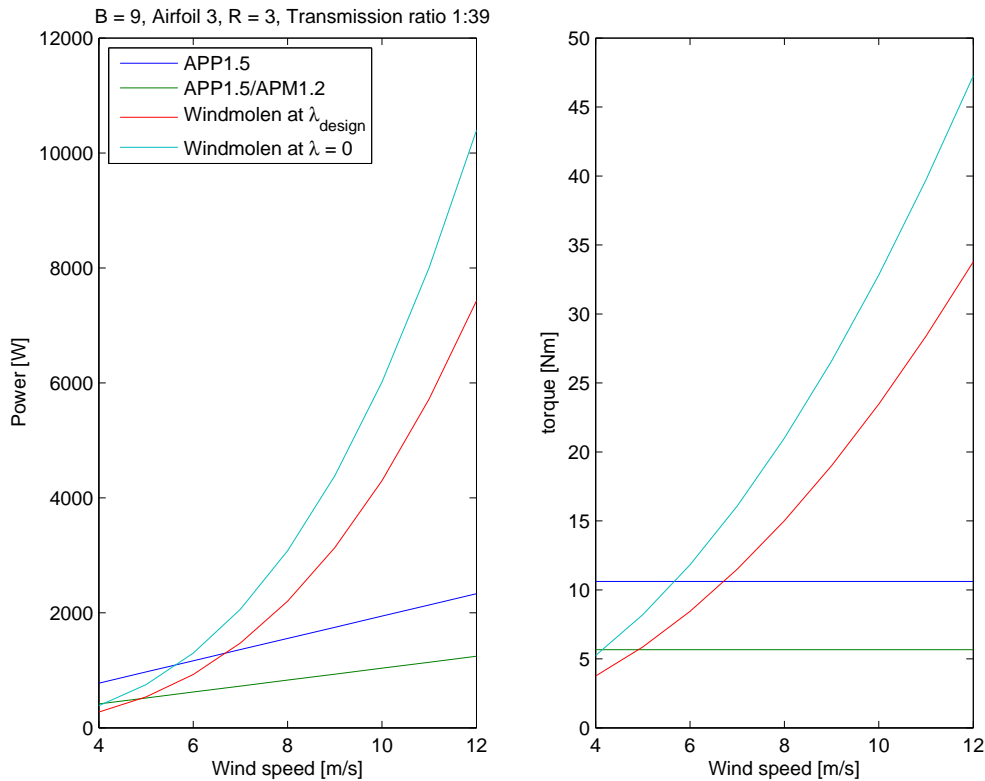


Figure B-2: Wind turbine and pump torque and power curves for B = 9 and R = 3 and the curved plate (with tube at 0.25 chord) airfoil

The wind is modeled by means of the Weibull function in the 'Wind'-module. The scale parameter, k, and the mean velocity are varied to see the influence on the water output.

The specific energy and the wind profiles are fed into the water module in which the water output is calculated. The following rules are applied for the simulation of the water output:

- Under cut-in wind speed the system does not deliver any water; the cut-in wind speed is set at 4 m/s
- The wind speed at which the torque provided by the rotor is less than the torque needed by the APP/APM combination is less than U_{cut-in}

Table B-4 gives the calculated water output for the system with the APP1.5/APM1.2 Danfoss pump and for a mean wind speed of 5 m/s and a shape factor of 2 to define the Weibull distribution. The values are given for different airfoils, number of blades and radii. The water output is strongly related with U_{start} , the wind speed at which the pump is receiving enough torque. If U_{start} is below cut-in wind speed the water output is at its maximum for that wind profile.

Generally, it can be said that for the coupling of a wind turbine to a RO pump system the wind speed at which the rotor delivers enough torque to start the pump (i.e. U_{start}) is of great

Table B-4: Water output for mean wind speed $U_{mean} = 5$ m/s and Weibull shape factor $k = 2$; R is rotor radius, B is number of blades; the pump applied is the APP1.5/APM1.2 Danfoss pump; feed pressure is 42.5 bar and recovery 33%

	DU-91-W2-250		Curved plate with tube at 0.25 chord	
[m ³ /day]	B = 3	B = 9	B = 3	B = 9
R = 3	3.1	3.2	2.9	3.2
R = 5	4.6	4.6	4.5	4.6
R = 8	4.6	4.6	4.6	4.6

Table B-5: Influence of wind profile on water output; airfoil is DU-91-W2-250, R is rotor radius, B is number of blades; the pump applied is the APP1.5/APM1.2 Danfoss pump; feed pressure is 42.5 bar and recovery 33%

	$U_{mean} = 7$ m/s; $k = 2$		$U_{mean} = 5$ m/s; $k = 1.5$	
[m ³ /day]	B = 3	B = 9	B = 3	B = 9
R = 3	5.2	5.7	2.1	2.5
R = 5	6.7	6.7	4.1	4.1
R = 8	6.7	6.7	4.1	4.1

importance regarding the water output. From the figures it follows that changing the blade radius has the largest influence on U_{start} , followed by increasing the number of blades. The airfoil type does not seem to make that much of a difference, but needs to be selected based on structural and cost considerations.

Appendix C

Wind turbine selection

For the selection of a proper windmill first some basic calculations are done to define for what wind turbine capacity we are looking. With the results of these calculations a market research was performed in order to select the most interesting wind turbines for the desalination of sea water.

C-1 Wind approximation with the Weibull distribution

The Weibull distribution is a flexible model that estimates how often winds of different speed will occur at a location with a certain mean wind speed. The Weibull cumulative distribution is formulated by equation C-1 with A as given in equation C-2.

$$F(U) = 1 - \exp\left(-\left(\frac{U}{A}\right)^k\right) \quad (\text{C-1})$$

$$A = \frac{U_{avg}}{\Gamma(1 + 1/k)} \quad (\text{C-2})$$

The probability of the wind being in a certain wind interval $[U_1, U_2]$ can be calculated by means of equation C-3.

$$P(U_1 \leq U \leq U_2) = F(U_2) - F(U_1) = \exp\left(-\left(\frac{U_1}{A}\right)^k\right) - \exp\left(-\left(\frac{U_2}{A}\right)^k\right) \quad (\text{C-3})$$

The windregime can thus be described by two parameters, the average windspeed U_{avg} and the shapefactor k. For many sites a value of $k=2$ is representative. Using this value for the shape parameter will result in a simplification of the Weibull distribution which is commonly known as the Rayleigh distribution. With $k = 2$, A can be simplified to equation C-4. Most regions in the world know however other shapefactors. Trade winds for example can have a shape factor of around 5.

$$A = \frac{U_{avg}}{\Gamma(1 + 1/k)} = \frac{2}{\sqrt{\pi}} U_{avg} \quad (\text{C-4})$$

C-2 Basic calculations to define needed capacity

The goal of the new wind powered desalination system is to deliver 25 m³ a day. Spectra Watermakers claims that the energy consumption of their Pearson pump is 2.1 kWh/m³. Adding a margin of 10% results in an energy consumption of 2.3 kWh/m³ for sea water desalination with the Spectra Pearson pump. In order to get the desired output of 25 m³/day the pump needs 2.3·25 = 57.5 kWh per day. The average power it needs per hour will be 75/24 = 2.4 kW. The system also has to deal with transmission losses, which are for this rough estimation assumed to be 20%. This leads to an average energy consumption of 2.9 kWh.

$$P = P_{rat} \left(\frac{U}{U_{rat}} \right)^3 \quad (\text{C-5})$$

Wind turbines are categorized by their rated power (which is stated on the generator). The power a wind turbine delivers at a certain wind speed can be approximated by means of equation C-5. The probability that that wind speed occurs is commonly estimated by means of a Weibull distribution, as explained in section C-1. With this information the energy production can be found (see equation C-6).

$$E = T \int_0^{U_{out}} P(U) f(U) dU \quad (\text{C-6})$$

To get an idea of what wind turbine is needed, the energy production for different P_{rated} and varying mean wind speed are calculated. The results are given in table C-1 and provide the theoretical energy production. It follows that appropriate wind turbines should be in the range of 15 - 20 kW. However, the theoretical data may be somewhat different in reality, therefore it is important to look at the power specifications provided by the manufacturer.

Table C-1: Energy production in kWh

[kWh]		Mean wind speed [m/s]		
		5	6	7
P_{rated} [kW]	10	1.34	2.16	3.03
	15	2.01	3.23	4.55
	18	2.42	3.88	5.46
	20	2.69	4.31	6.06


The Fortis Alize 10kW wind turbine of Fortis for example has a higher energy production than the theoretical wind turbine with the same configuration (see table C-2). The power curves show that in the region between 4 and 12 m/s wind speed the Fortis Alize has a higher power output (see figure 2-2). These are the wind speeds which occur most, resulting in the higher energy output. Although a production of 2.5 kWh at a mean wind speed of 6 m/s is still not enough for the production of 25 m³/day, it is not far off. The Fortis Alize 10kW turbine is one to consider even though the energy output of a 10kW theoretical turbine is not that promising.

Table C-2: Energy production in kWh for 10kW wind turbine and $U_{rated} = 12$ m/s

[kWh]	Mean wind speed [m/s]		
	5	6	7
Theoretical	1.34	2.16	3.03
Fortis Alize	1.66	2.52	3.32

C-3 Wind turbine specifications


Molins de Vent, Tarrago	
Diameter	1.8 -10m
Height	4-18m
Cost (approximation)	€ 13000? for M-1015
Cut in wind speed	4 m/s
Cut out wind speed	
Rated wind speed	12 m/s
Purpose	Water pumping
Experience	25 years
Installation	Easy
Lifetime expectancy	+/- 10 year
Comment	Windmill of 1 st prototype was M-5015





Molins de Vent TARRAGO


www.tarrago.es


Spain


Turbex		
Diameter	7.8m	
Height	18-30 m	
Cost (approximation)	€ 20000	
Cut in wind speed	3	
Cut out wind speed	20	
Rated wind speed	11.7	
Purpose	Water pumping	
Experience		
Installation		Turbex
Lifetime expectancy		www.turbex.co.za
Comment	Rotary principle	South Africa


Kijito			
Diameter	3.7 - 7.9m		
Height	9.1 - 12.2m		
Cost (approximation)	€ 10000 for D7.9m		
Cut in wind speed	2.5 m/s		
Cut out wind speed	(Survival windspeed: 45 m/s)		
Rated wind speed	5 m/s		
Purpose	Water pumping		
Experience	25 years - 400 windmills		
Installation	Winch		Bobs Harries Engineering Ltd
Lifetime expectancy	Medium		www.kijitowindpower.com
Comment		Kenya	

Southern Cross		
Diameter	2.5 - 7.5m	
Height	6 - 18 m	
Cost (approximation)	€5300 for D7.5m	
Cut in wind speed	3 m/s	
Cut out wind speed		
Rated wind speed	11 m/s	
Purpose	Water pumping	
Experience	>50 years	
Installation	Winch (although not designed for it)	
Lifetime expectancy	>30 years (good)	
Comment		Southern Cross Industries LTD www.southx.co.za South Africa

Eco - 10kW		
Diameter	8m	
Height	18m	
Cost (approximation)	€20000	
Cut in wind speed	2 m/s	
Cut out wind speed	20 m/s	
Rated wind speed	12 m/s	
Purpose	Electricity generation	
Experience	15 years	
Installation	Hydraulic tower	
Life expectancy	-	
Comment	easy maintenance; how to drive hydraulic tower?	Eco Wind Turbine www.ecowindturbine.com US

TML - 15kW		
Diameter	9.5m	
Height	18m	
Cost (approximation)	€-	
Cut in wind speed	2.5 m/s	
Cut out wind speed	25 m/s	
Rated wind speed	12 m/s	
Purpose	Electricity generation	
Experience	30 years - >500 windturbines	
Installation	Anticyclonic tilting tower (down in 40 min.)	
Life expectancy	-	
Comment	direct drive; permanent magnet; for isolated, rural locations	TML SA www.tml-windenergy.com Belgium

Bergey Excel		
Diameter	7m	
Height	18-43 m	
Cost (approximation)	€20000	
Cut in wind speed	3.5 m/s	
Cut out wind speed	None	
Rated wind speed	15 m/s	
Purpose	-	
Experience	-	
Installation	-	
Life expectancy	-	
Comment	-	Bergey Windpower www.bergey.com US

Fortis Alize - 10kW		
Diameter	7m	
Height	30.5m	
Cost (approximation)	€37000	
Cut in wind speed	3 m/s	
Cut out wind speed	25 m/s	
Rated wind speed	12 m/s	
Purpose	Electricity generation	
Experience	25 years - 6000 windturbines	
Installation	Possible without crane	
Life expectancy	20 years	
Comment	a-synchronous generator 3 phase permanent magnet	Fortis Wind Energy www.fortiswindenergy.com Netherlands

C-4 Obtaining $C_q - \lambda$ and λ_{design} for each wind turbine

The following steps should be followed to get an estimation of the $C_q - \lambda$ curve and the design tip speed ratio:

1. Select the airfoil
2. Find $C_{l,design}$ and α_{design}
3. Define the blade shape
4. Apply the BEM code to get $C_q - \lambda$ and λ_{design}

C-4-1 Select the airfoil

A wind turbine blade consists of N blade elements. Figure C-1 illustrates the important variables of a blade. The blade has a length R , also called the rotor radius. The radius, or length from the hub is defined by r and Ω is the angular velocity in rad/s. The chord, c , is the length of the blade element and dr the blade element width.

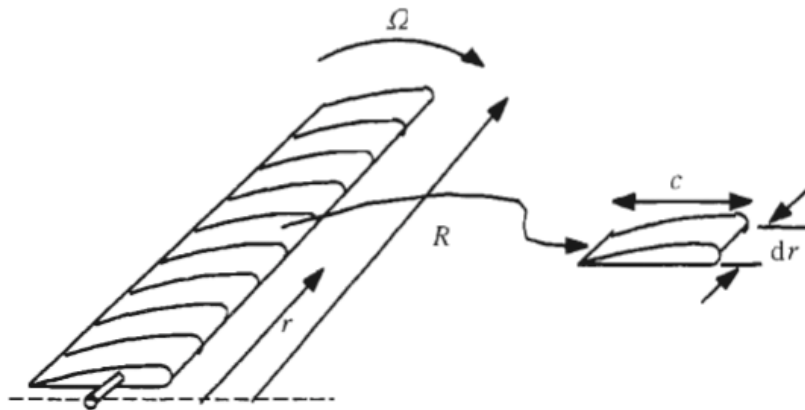


Figure C-1: Definition of the blade variables. Ω is the rotor angular velocity [rad/s], R is the rotor radius [m], r is the local rotor radius [m], c is the airfoil chord [m] and dr is the blade element width [m] [J.F. Manwell, J.G. McGowan, A.L. Rogers, 2002]

The airfoil is the aerodynamic cross section of the blade and creates lift as it moves through the air. The shape of the airfoil strongly affects the amount of lift it produces. The airfoil may vary from root to tip. The SIMULINK model assumes only one airfoil type per wind turbine. Figure C-2 gives a schematic overview of the airfoil geometry.

It shows that the angle of attack, α is a function of the angle of relative wind ϕ and the pitch angle, θ_P . The pitch angle is the summation of the blade twist angle θ_T and the pitch angle at the tip $\theta_{P,0}$. dF_L is the incremental lift force and dF_D the incremental drag force. dF_N is the incremental force contributing to the thrust and normal to the plane of rotation and dF_T is the incremental force creating useful torque and tangential to the circle swept by the rotor. The relationships determined from this figure form the basis of the blade element theory and will be explained in more detail in section C-4-4.

C-4-2 Find $C_{l,design}$ and α_{design}

The aerodynamic properties of the airfoil, i.e. the $C_l - \alpha$ and the $C_d - \alpha$ curves, can be obtained from literature or by means of the program Xfoil. This study uses data from literature. The multi-bladed windmills were assumed to consist of curved plates with a tube at a quarter chord. The empirical curves were obtained from the experimental results of Timmer [Nando Timmer,]. The relations for the $C_l - \alpha$ and the $C_d - \alpha$ curves for the NACA 4415 airfoil used in the Fortis Alize and Fortis Montana windmill came from Wind Energy Explained [Nando Timmer,]. The Bergey Excel turbine contains the SH3052 airfoil and the curves were obtained from a report of the National Renewable Energy Laboratory [Corbus and Meadors, 2005]. The design aerodynamic conditions (α_{design} and $C_{l,design}$) were chosen such that $C_{l,design}/C_{d,design}$ is maximum. Table C-3 provides the design conditions for the wind turbines used in the SIMULINK model.

Table C-3: Airfoil characteristics and the wind turbines in the SIMULINK model that use the particular airfoil. $C_{l,design}$ and α_{design} are the lift coefficient and angle of attack at maximum C_l/C_d

Airfoil	Wind turbine	α_{design} [°]	$C_{l,design}$ [-]
Curved plate with tube at 1/4-chord	M5015; Turbex	8	1.2
NACA 4415	Fortis Alize; Fortis Montana	6	0.9
SH3052	Bergey Excel	4	1.4

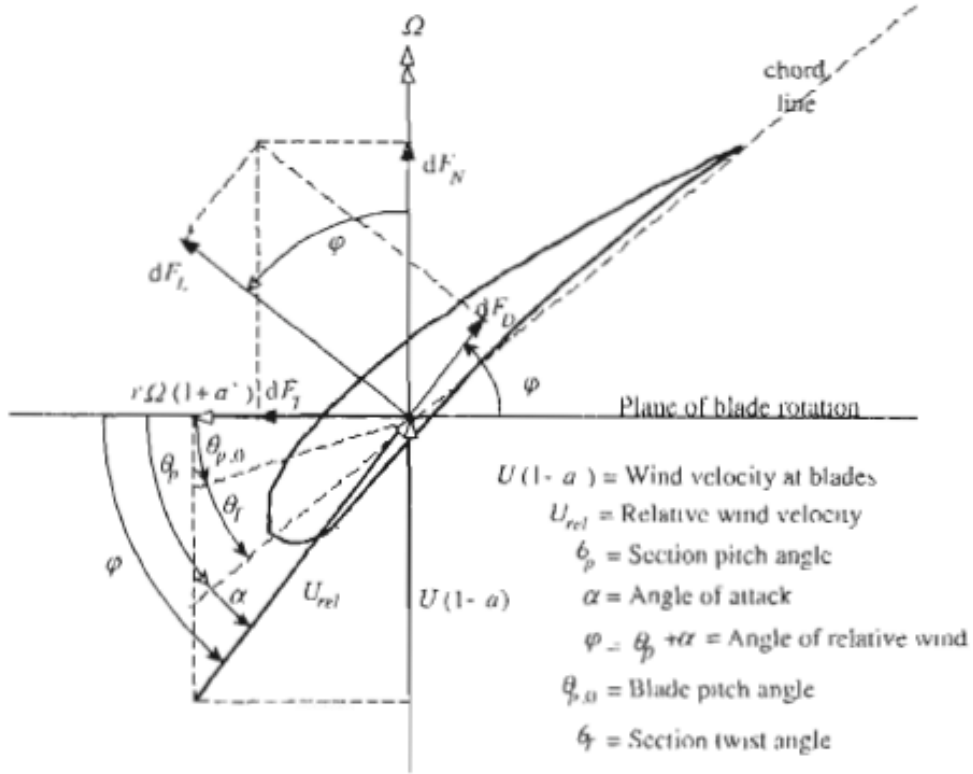


Figure C-2: Airfoil geometry for analysis of a horizontal axis wind turbine; for definition of variables, see text [J.F. Manwell, J.G. McGowan, A.L. Rogers, 2002]

C-4-3 Define the blade shape

As described previously the blade is divided into N elements. With equation C-7, C-10, C-11 and C-9 the local tip speed ratio (λ_r), local pitch ($\theta_{P,r}$), local twist angle ($\theta_{T,r}$) and the local chord (c_r) can be obtained to estimate the shape of the blade at each element. In these equations R is the rotor radius, r is the local rotor radius and B is the number of blades. $C_{l,design}$ and α_{design} are found as described in the previous section. The optimum shape is used to select the final blade shape that is an approximation of the optimum shape but is also easy to manufacture.

$$\lambda_r = \lambda \left(\frac{r}{R} \right) \quad (C-7)$$

$$\phi_r = (2/3) \text{atan}(1/\lambda_r) \quad (C-8)$$

$$c_r = \frac{8\pi r}{BC_{l,design}} (1 - \cos(\phi_r)) \quad (C-9)$$

$$\theta_{P,r} = \phi_r - \alpha_{design} \quad (C-10)$$

$$\theta_{T,r} = \theta_{P,r} - \theta_{P,0} \quad (C-11)$$

The blade shape of the other wind turbines that are implemented in the SIMULINK model were retrieved with the same method Table C-4 gives the selected chord and twist distribution for these wind turbines. The selected blade shapes were in accordance with what literature prescribed. The slower machines are expected to have the most twist and the largest and roughly constant chord [J.F. Manwell, J.G. McGowan, A.L. Rogers, 2002].

Table C-4: Selected blade shape for each wind turbine used in the SIMULINK model. c is the airfoil chord length, $\theta_{P,0}$ the pitch angle at the hub, θ_T the twist angle, λ_d the design tip speed ratio, B is the number of blades, r the local rotor radius and R is the blade radius

	M5015		Turbex		Fortis Montana		Fortis Alize		Bergey Excel	
	$\lambda_d = 1.4$	$B = 12$	$\lambda_d = 1.1$	$B = 18$	$\lambda_d = 5$	$B = 3$	$\lambda_d = 6$	$B = 3$	$\lambda_d = 6$	$B = 3$
	$\theta_{P,0} = -10$		$\theta_{P,0} = -10$		$\theta_{P,0} = -1$		$\theta_{P,0} = -1$		$\theta_{P,0} = -1$	
r/R	c/R	θ_T	c/R	θ_T	c/R	θ_T	c/R	θ_T	c/R	θ_T
0.05	0.28	38.4	0.25	52	0.19	13.6	0.11	9.6	0.08	11.6
0.15	0.27	36.8	0.25	50	0.18	12.7	0.11	8.8	0.08	10.8
0.25	0.27	35.2	0.25	47	0.17	11.8	0.10	8.0	0.08	10.0
0.35	0.26	33.6	0.24	45	0.16	10.9	0.09	7.2	0.07	9.2
0.45	0.26	32.0	0.24	42	0.15	10.0	0.09	6.4	0.07	8.4
0.55	0.26	30.4	0.24	40	0.13	9.1	0.08	5.6	0.06	7.6
0.65	0.25	28.8	0.23	37	0.12	8.2	0.08	4.8	0.06	6.8
0.75	0.25	27.2	0.23	34	0.11	7.3	0.07	4.0	0.05	6.0
0.85	0.24	25.6	0.23	32	0.10	6.4	0.07	3.2	0.05	5.2
0.95	0.24	24.0	0.22	29	0.09	5.5	0.06	2.4	0.05	4.4

C-4-4 Apply the blade element momentum method to get $C_q - \lambda$ and λ_{design}

The blade element momentum (BEM) theory is a combination of momentum theory and blade element theory. Momentum theory refers to a control volume analysis of the forces at the blade based on the conservation of angular and linear momentum. Blade element theory refers to an analysis of forces at a section of the blade.

Momentum theory

A wind turbine extracts kinetic energy from the wind. The presence of the wind turbine causes the approaching air to slow down. The mass flow rate is the same everywhere along the streamtube. To compensate for the slowed down air, the streamtube must expand as illustrated in figure C-3. The axial induction factor or inflow angle, a , is the fractional decrease in wind velocity between the free stream and the disc plane. The pressure difference across the actuator disc causes a change of momentum equal to the overall change of velocity times the mass flow rate. From the conservation of linear momentum to the control volume of radius r and thickness dr an expression for the differential contribution of the thrust can be obtained (see equation C-12).

$$dT = \rho U^2 4a(1-a)\pi r dr \quad (C-12)$$

Similarly, from the conservation of angular momentum the differential torque imparted to the blades can be determined (see equation C-13). In this equation a' is the angular induction factor and is defined as $a' = \omega/2\Omega$.

$$dQ = 4a'(1-a)\rho U \pi r^3 \Omega dr \quad (C-13)$$

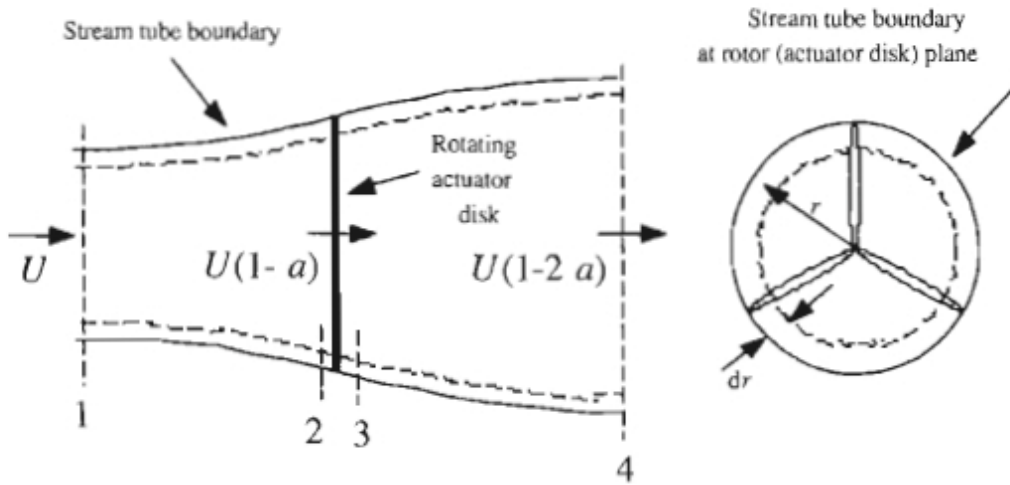


Figure C-3: Geometry for rotor analysis; U , velocity of undisturbed air; a , induction factor; r , radius

The momentum theory results thus in two equations that are a function of the axial and angular induction factors. One defines the thrust and the other the torque on an annular section of the rotor. For a detailed description of how to derive equation C-12 and C-13 the reader is referred to the book 'Wind energy explained' [J.F. Manwell, J.G. McGowan, A.L. Rogers, 2002].

Blade element theory

Blade element theory refers to an analysis of forces at a section of the blade. The geometry of the blade and is shown in figure C-2. The angle of relative wind, ϕ , can be calculated by means of equation C-14 and the relative velocity itself by means of equation C-15 in which a and a' are the axial and angular induction factors respectively.

$$\tan\phi = \frac{U(1-a)}{\Omega r(1+a')} \quad (\text{C-14})$$

$$U_{rel} = \frac{U(1-a)}{\sin\phi} \quad (\text{C-15})$$

The angle of attack for each element is a function of the local pitch angle and the local angle of relative wind. The local pitch angle is the sum of the local twist angle and the pitch angle at the hub. These parameters were fixed after the blade shape selection. With the angle of attack the local lift and drag coefficients can be found. With these coefficients and the relative velocity the local lift and drag forces can be calculated as shown in equation C-16 and C-17.

$$dF_L = C_l \frac{1}{2} \rho U_{rel}^2 c dr \quad (\text{C-16})$$

$$dF_D = C_d \frac{1}{2} \rho U_{rel}^2 c dr \quad (\text{C-17})$$

With these equations and the angle of relative wind the local normal and tangential force can be obtained. If the rotor has B blades, the total normal force on the section at a distance, r , from the center can be calculated by means of equation C-18.

$$dF_N = B \frac{1}{2} \rho U_{rel}^2 (C_l \cos \phi + C_d \sin \phi) c dr \quad (C-18)$$

The differential torque due to the tangential force is given by equation C-19.

$$dQ = BrdF_T = B \frac{1}{2} \rho U_{rel}^2 (C_l \cos \phi + C_d \sin \phi) c r dr \quad (C-19)$$

Just as for the momentum theory the blade element theory also results in two equations that define the normal force (thrust) and the tangential force (torque) on the annular rotor section. For the blade element theory the equations are a function of the flow angles at the blades and airfoil characteristics. For the momentum theory the equations are a function of the axial and angular induction factors.

The BEM code

As stated before combining the momentum theory and the blade element theory results in the BEM method. This method can be used for generalized rotor design and is used in the SIMULINK model for the calculation of rotor performance based on basic rotor parameters such as the radius, number of blades, airfoil and the tip speed ratio λ . First these basic parameters need to be determined, then the blade shape needs to be defined and finally the rotor performance can be calculated.

In *Wind Energy Explained* ([J.F. Manwell, J.G. McGowan, A.L. Rogers, 2002]) the detailed description of the BEM method is given. Also in the BEM code used in the SIMULINK model the iterative solution for a and a' can be found. The steps which are taken for each blade section are as follows:

- Guess values for a and a'
- Calculate the angle of relative wind by means of equation C-14
- Calculate the blade sectional angle of attack and the effective wind speed
- Calculate the Prantl tip correction and Glauert correction for heavily loaded wind turbines if desired
- Get C_l and C_d with the found angle of attack
- Calculate the new induction factors which are functions of the effective wind speed, the lift coefficient, the angle of relative wind and the correction factors

When the new induction factor differs too much from the old one the process is repeated. The induction factors will converge and when the difference is small enough, the process is stopped. The local lift and drag are used to calculate the local torque, thrust and bending moment. Summing these local parameters will result in the total blade thrust, torque and bending moment with which the power-, torque- and thrust coefficient can be calculated.

C-4-5 The $C_q - \lambda$ curve and λ_{design}

The BEM code results in a power and torque coefficient that describe the performance of the wind turbine at the selected tip speed ratio. The code is used iteratively for a range of tip speed ratios from $\lambda = 0$ to at least the tip speed at which the coefficients are zero. From this the $C_p - \lambda$, $C_q - \lambda$ are obtained for each wind turbine. Figure 2-2(a), figure C-4(a) and figure C-5(a) show the curves for the 3-bladed high tip speed machines.

The BEM code delivered some unexpected results for the multi-bladed wind turbines. It was therefore decided to use the coefficients found with BEM at the design tip speed ratio and use that to approximate the shape of the curves. Figure C-6 gives the $C_q - \lambda$ curve and the $C_p - \lambda$ curve for the M5015 windmill. The shape is also similar to with what is expected by looking at literature as can be seen by looking at figure C-7 in which the ranges of the power and torque coefficient for different wind turbine types are illustrated. It was decided to keep the torque coefficient at $\lambda < 1$ at the same value as the torque coefficient at $\lambda = 1$. This is a somewhat conservative approximation, which was preferred above the risk of assuming a torque too high at small tip speed ratios. With the current approximation the torque at $\lambda < 1$ is already significantly higher than the torque at similar tip speed ratios for three bladed wind turbines. The power curve at design tip speed ratio (i.e. $\lambda = 1$) is in accordance with the data provided by the manufacturer as can be seen in figure C-6.

C-5 Load cases for wind turbine applications

Figure C-8 shows the power from the wind turbine as a function of rotational speed for different wind speeds. In order to extract the maximum energy from the rotor should operate close to the maximum power point for each wind speed. This desired operation mode is represented by the dotted line.

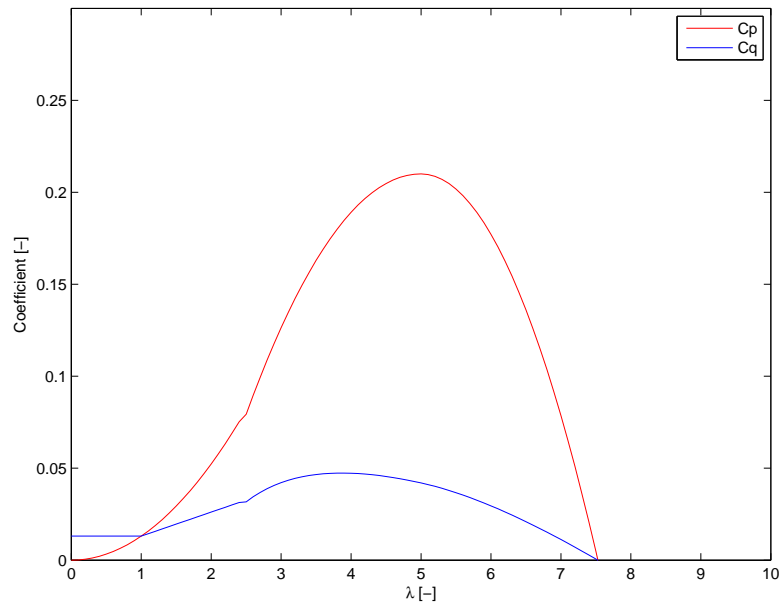
The loads applied to the wind turbine should thus preferably match the dotted line in figure C-8. A load can be described by means of torque as a function of rotational speed. The general equation to define a load is given in equation C-20, which can be simplified to equation C-21, since we are for now only interested in a rough approximation.

$$Q = a_n \cdot \omega^n + a_{n-1} \cdot \omega^{n-1} + \dots + a_1 \cdot \omega + a_0 \quad (\text{C-20})$$

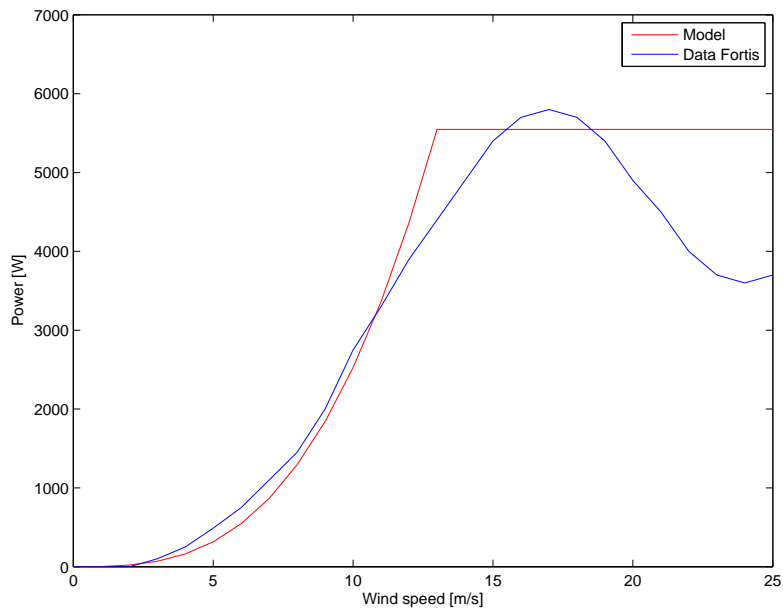
$$Q = c \cdot \omega^n \quad (\text{C-21})$$

Figure C-9 gives an overview of four common load cases:

- **n = 0**: Constant torque
Examples: drilling, sawing, weight lifting, water pumping by means of a displacement pump
- **n = 1**
Examples: viscous friction
- **n = 2**
Examples: fan, heat pump, water pumping by means of a centrifugal pump
- **n = ∞**: Constant rotational speed
Examples: synchronous generator

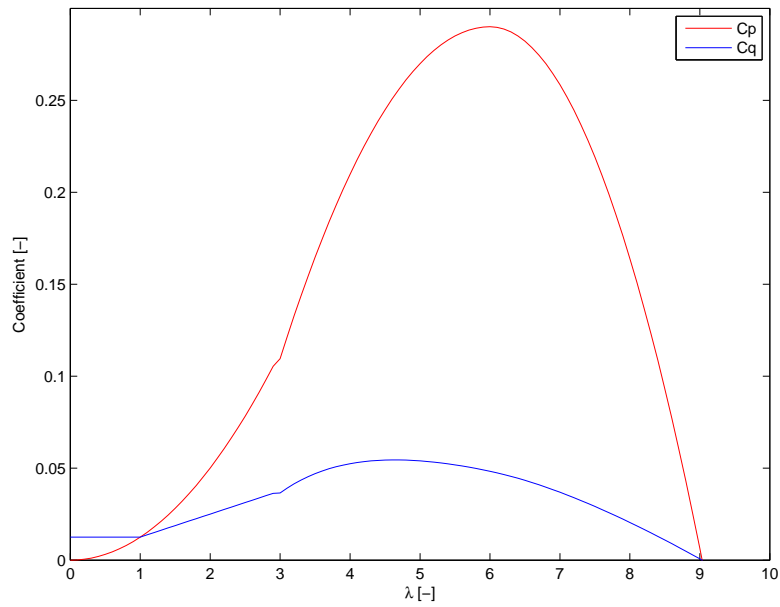


(a) Torque and power coefficient over tip speed ratio

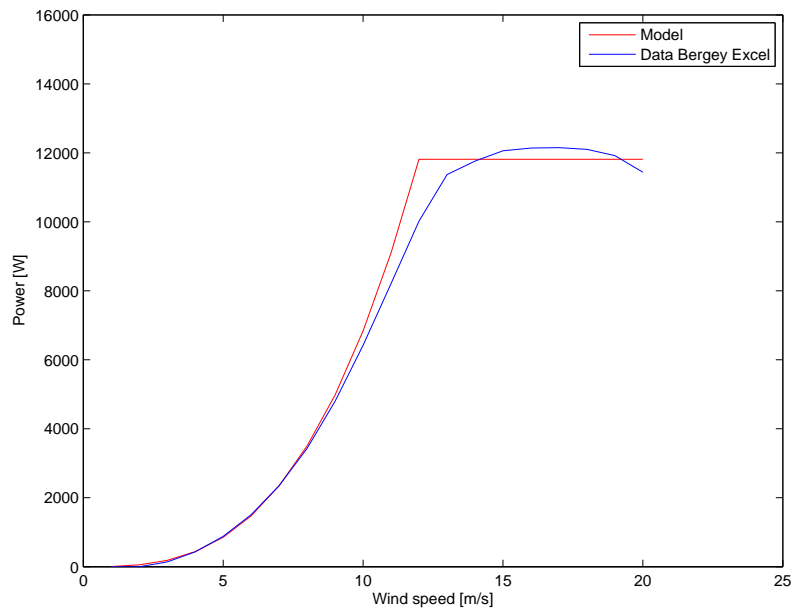


(b) Power curve from model compared to data from manufacturer

Figure C-4: Fortis Montana wind turbine performance curves

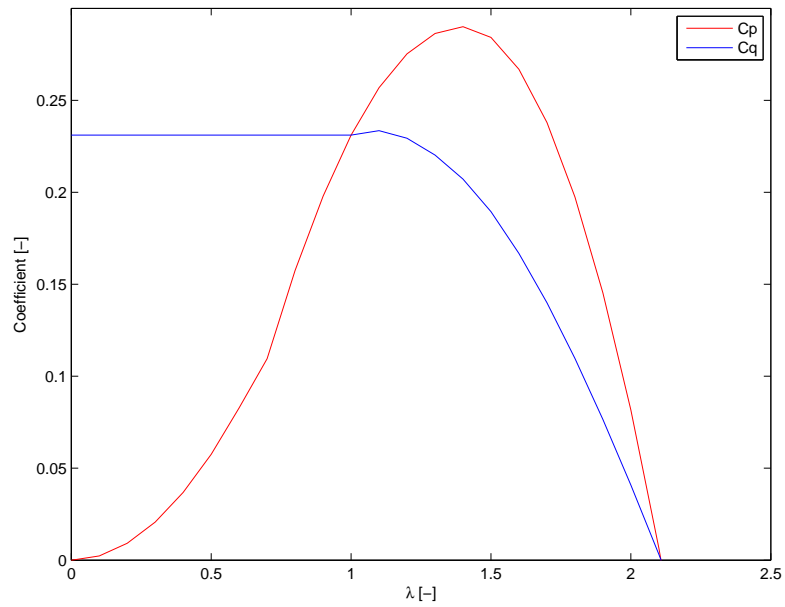


(a) Torque and power coefficient over tip speed ratio

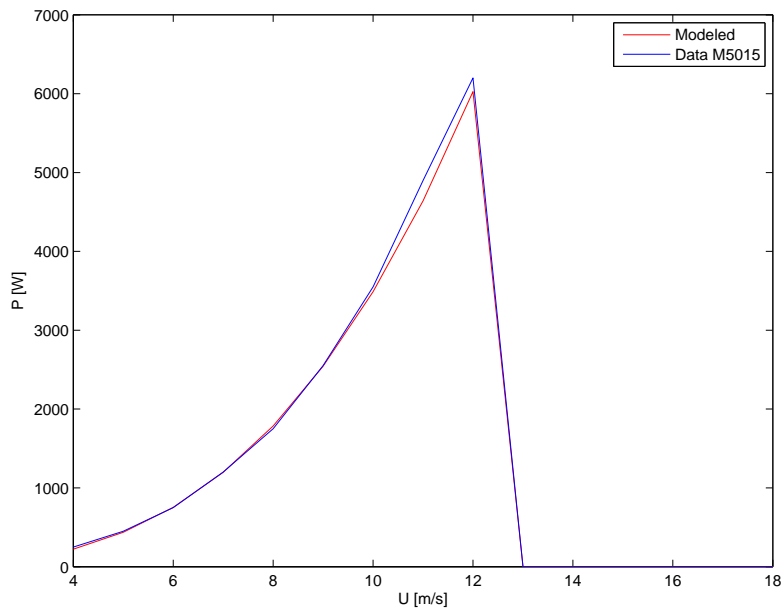


(b) Power curve from model compared to data from manufacturer

Figure C-5: Bergey Excel wind turbine performance curves



(a) Torque and power coefficient over tip speed ratio



(b) Power curve from model compared to data from manufacturer

Figure C-6: M5015 wind turbine performance curves

Load case $n = 1$ represents for example viscous friction, but no pumps or other systems that are usually driven by a wind turbine. It will thus be disregarded.

If the load case is $n = 2$, so for example when a centrifugal pump would be applied to the wind turbine, the characteristics of the turbine and the pump seem to match perfectly. It should be kept in mind however that it is an approximation and that in reality for example static friction will increase the required pump torque as shown in figure C-10.

For load case $n = 0$ and $n = \infty$ the load and wind turbine operating line do not match properly, resulting in inefficient use of the wind energy.

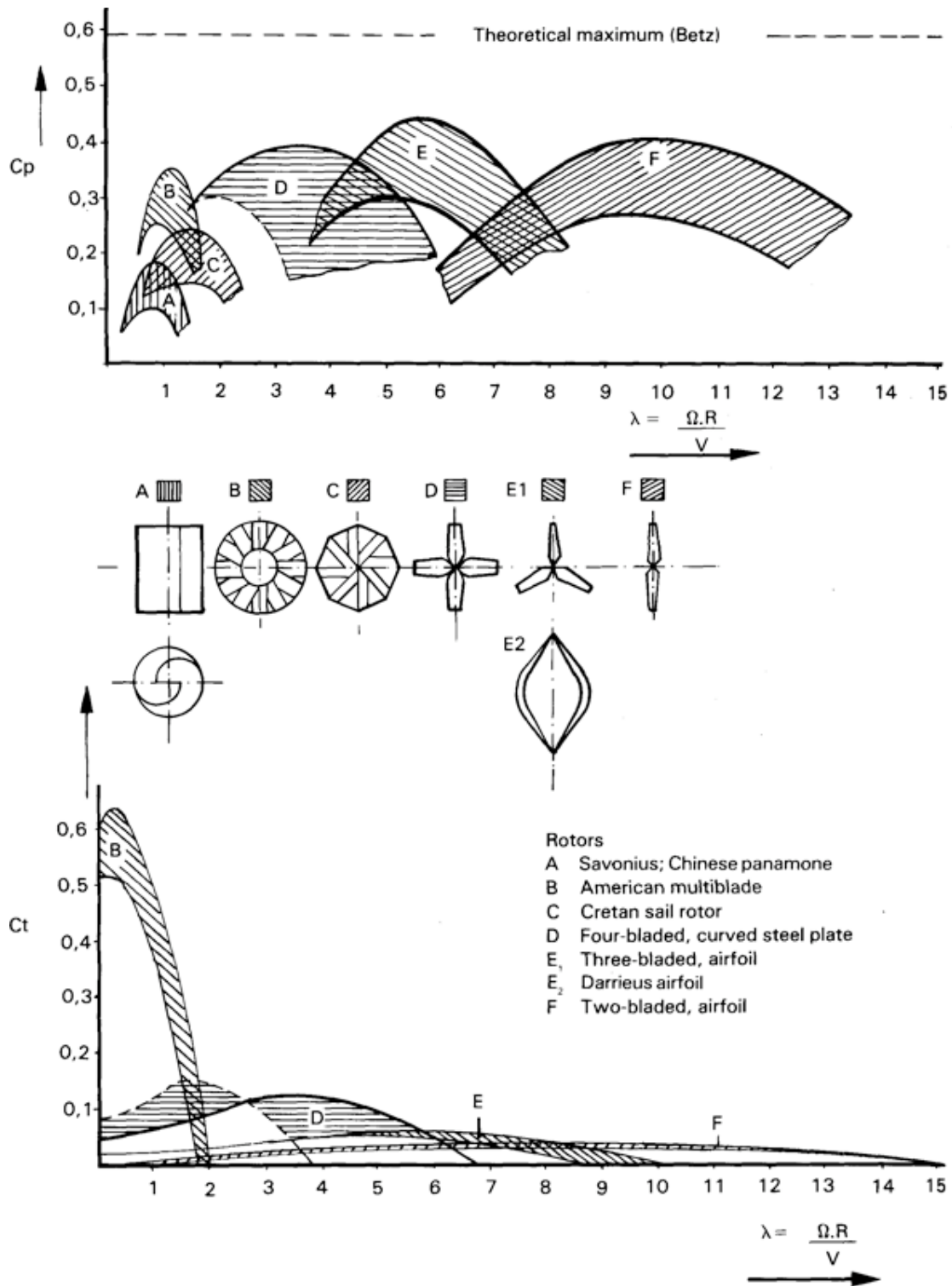


Figure C-7: Performance curves for different wind turbine types; U , velocity of undisturbed air; λ tip speed ratio, R rotor radius, C_P power coefficient, C_T , torque coefficient [Kentfield, 1996]

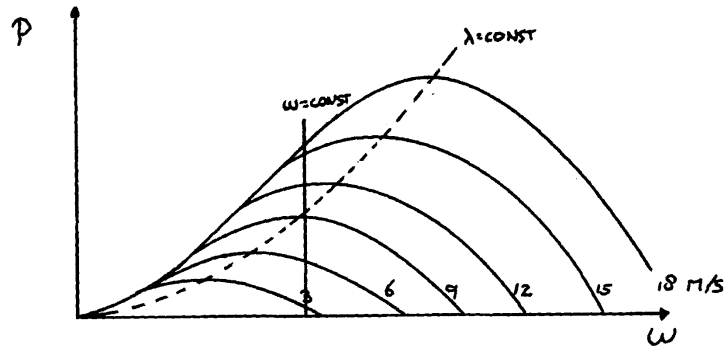


Figure C-8: Wind turbine power as a function of angular velocity for different wind speeds

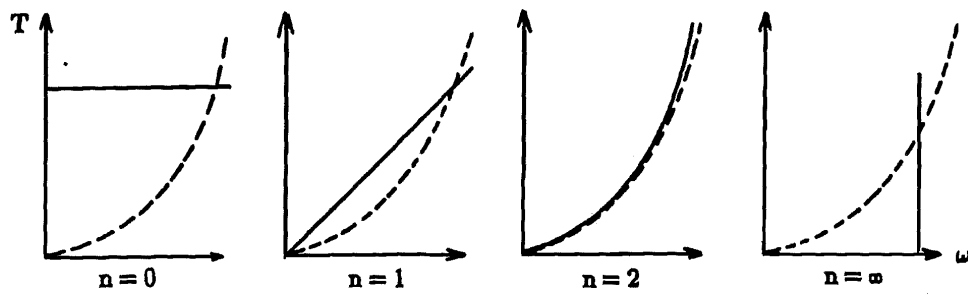


Figure C-9: The torque of the load as a function of its rotational speed for different load cases

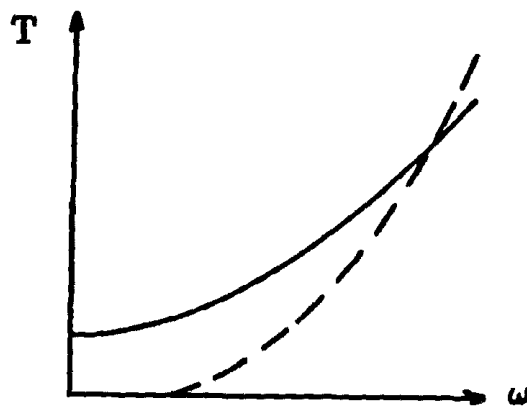


Figure C-10: Load type $n = 2$ including static friction influences

Appendix D

Additional pump information

D-1 Orbit pump equations

Franklin Electric's Orbit GW positive displacement pump is a medium pressure pump with good salt protection. Four types of Orbit pumps are implemented in the model, the GW0504, GW0704, GW0904 and the GW1304. Some general features of the Franklin Electric's Orbit pumps are:

- Helical rotor technology
- Pressure head is independent of pump speed
- Flow rate is proportional to speed
- Abrasion resistant
- Discharge head suitable for drive by electric motor, petrol or diesel engine, tractor or rotary windmill

Based on the data sheets provided by Franklin Electric relations were derived to approximate the flow rate and power required at the pump as a function of pump angular velocity and feed pressure. The datasheets are provided in section [D-1-4](#).

D-1-1 Orbit pump GW0504

Equation [D-1](#) and equation [D-2](#) approximate the performance of the GW0504 pump. The flow rate (q_f) in m^3/h is a function of the angular velocity (n) in rpm and the pressure (Pr) in bar. The start-up torque of the GW0504 is 22 Nm.

$$q_f = 4 - 0.0035 \cdot \left(\frac{Pr}{30} + 1\right)^{2.1} + \frac{1.1(n - 700)}{200} \quad (\text{D-1})$$

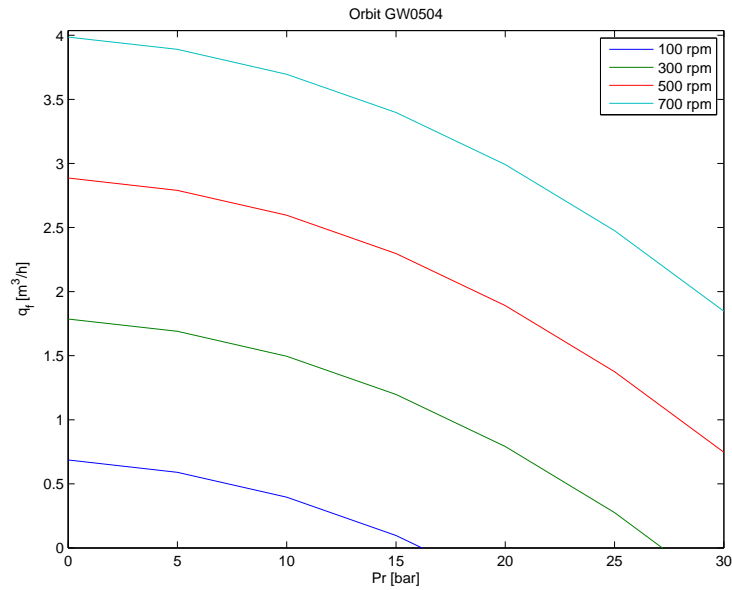
The power (P) in Watt is also a function of the angular velocity and the pressure.

$$P = 0.35 + \left(0.35 + \frac{0.1(n - 700)}{200}\right) \frac{Pr}{30} + \frac{0.15(n - 700)}{200} \quad (\text{D-2})$$

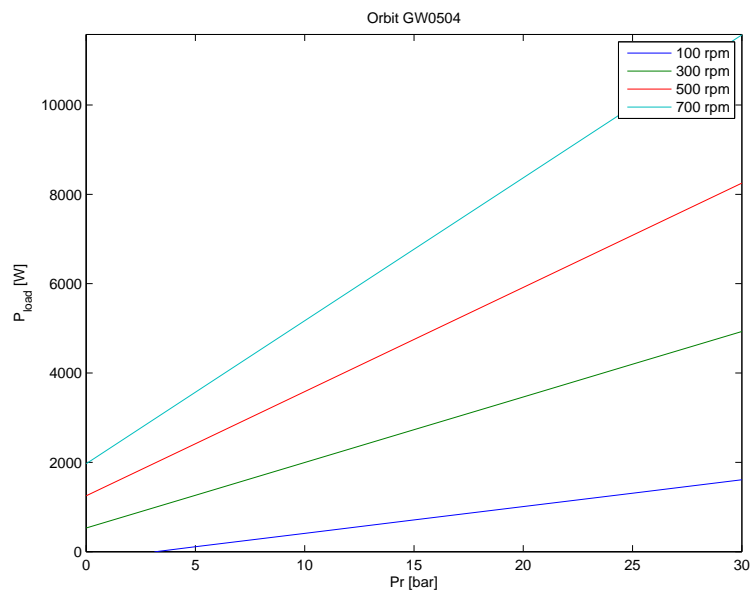
D-1-2 Orbit pump GW0704

From the graphs on the datasheet of the GW0704 equations D-3 and D-4 were formulated. The start-up torque of the GW0704 is 30 Nm.

$$q_f = 6.4 \cdot \left(1 - 0.0075 \cdot \left(\frac{Pr}{30}\right)^{1.75}\right) + 1.4 \left(\frac{n - 900}{200}\right) \quad (\text{D-3})$$



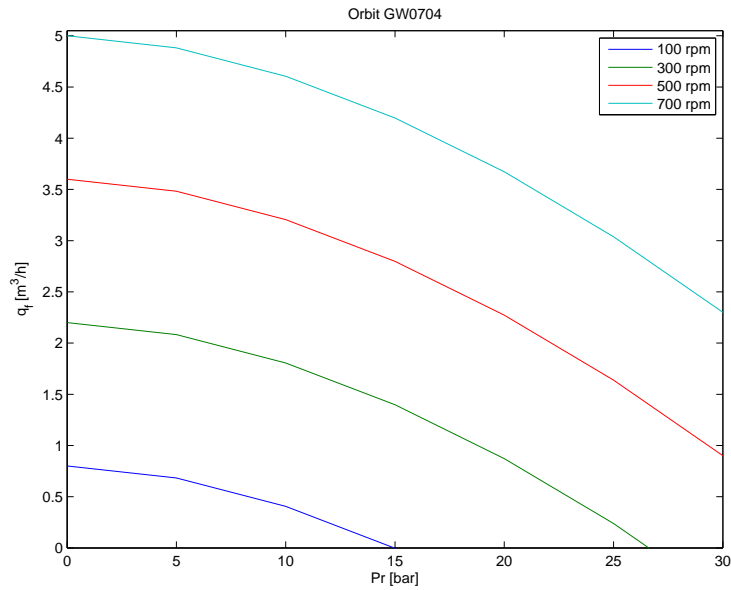
(a) Flow rate (q_f) over pressure (Pr) for different pump angular velocities (n)



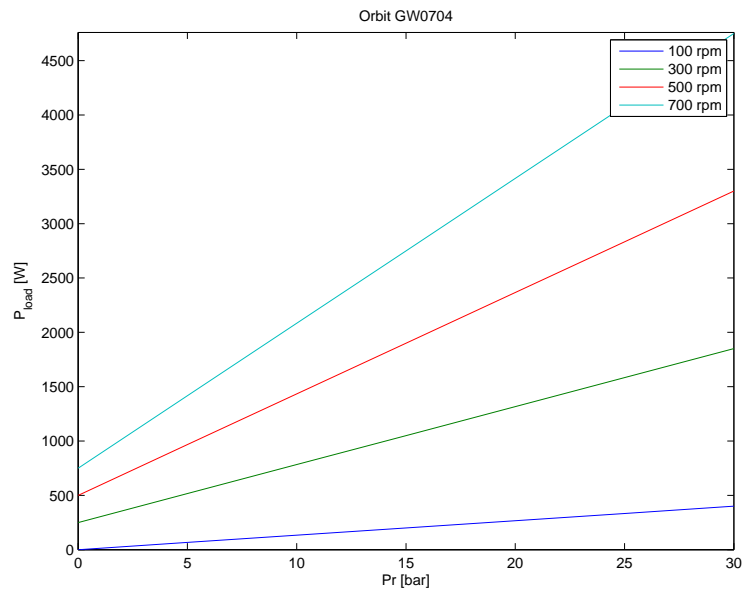
(b) Power (P_{load}) over pressure (Pr) for different pump angular velocities (n)

Figure D-1: Performance curves of the Orbit GW0504 pump

$$P = 1 + \left(\frac{(6.2 - 1) \cdot 30}{300} + 0.12 \frac{n - 900}{200} \right) \frac{Pr}{30} + 0.25 \left(\frac{n - 900}{200} \right) \quad (D-4)$$



(a) Flow rate (q_f) over pressure (Pr) for different pump angular velocities (n)



(b) Power (P_{load}) over pressure (Pr) for different pump angular velocities (n)

Figure D-2: Performance curves of the Orbit GW0704 pump

D-1-3 Orbit pump GW1304

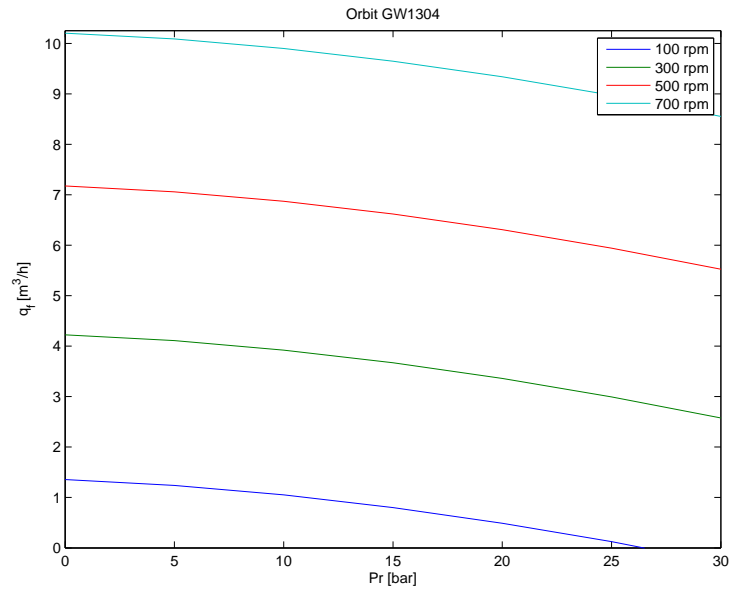
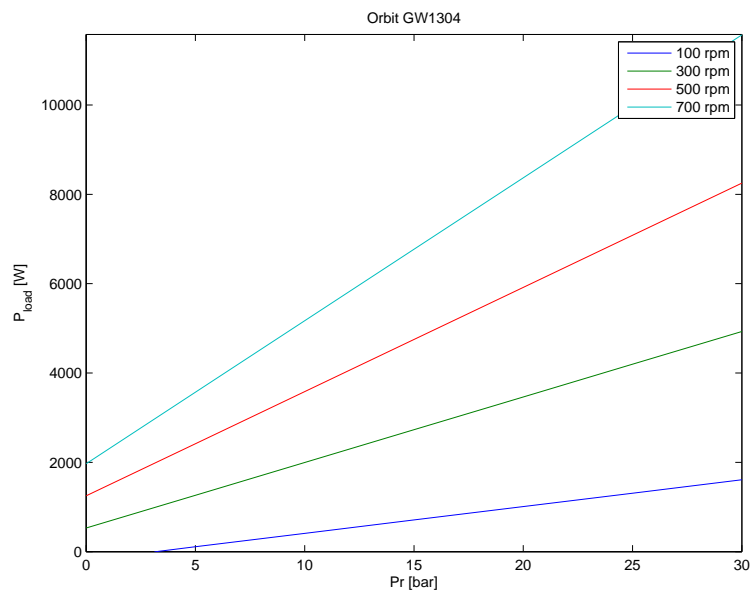
(a) Flow rate (q_f) over pressure (Pr) for different pump angular velocities (n)(b) Power (P_{load}) over pressure (Pr) for different pump angular velocities (n)

Figure D-3: Performance curves of the Orbit GW1304 pump

Equations D-5 and D-6 approximate the GW1304 pump. The start-up torque of the GW1304 is 30 Nm.

$$q_f = 7.2 \cdot (1 - 0.0035 \cdot (\frac{Pr}{30} + 1)^{1.75}) + \frac{(3.8 + 0.125(\frac{n-250}{500} - 1))}{250} (n - 500) \quad (D-5)$$

The power (P) in Watt is also a function of the angular velocity and the pressure.

$$P = 1.25 + (\frac{3.5 \cdot 30}{150} + 0.325 \frac{n - 500}{250}) \frac{Pr}{30} + \frac{0.9(n - 500)}{250} \quad (D-6)$$

D-1-4 Data sheets manufacturer

3. Technical data

APP pump / APM motor		APP1.0/APM0.8	APP1.5/APM1.2	APP1.8/APM1.2	APP2.5/APM2.0	APP2.5/APM1.8
1450 rpm						
Code number		180B8000	180B8002	180B8004	180B8006	180B8008
Feed flow	m ³ /h (gpm)	0.50 (2.2)	0.80 (3.5)	0.85 (3.7)	1.25 (5.5)	1.25 (5.5)
Recovery rate	%	29	28	32	29	32
Permeate (± 10%)	m ³ /h (gpm)	0.14 (0.6)	0.22 (1.0)	0.27 (1.2)	0.36 (1.6)	0.40 (1.8)
Electric motor (4 poles)		1.1 kW, IEC 90	1.5 kW, IEC 90	1.5 kW, IEC 90	2.2 kW, IEC 100	2.2 kW, IEC 100
2900 rpm						
Code number		180B8001	180B8003	180B8005	180B8007	180B8009
Feed flow	m ³ /h (gpm)	1.05 (4.6)	1.55 (6.8)	1.65 (7.3)	2.55 (11.2)	2.55 (11.2)
Recovery rate	%	29	28	32	29	32
Permeate (± 10%)	m ³ /h (gpm)	0.30 (1.3)	0.43 (1.9)	0.52 (2.3)	0.74 (3.3)	0.82 (3.6)
Electric motor (2 poles)		2.2 kW, IEC 90	3 kW, IEC 100	3 kW, IEC 100	*	*

If other flow or recovery rate is required, please contact Danfoss RO Solutions Sales Organization.
 * For this combination, please contact Danfoss RO Solutions Sales Organization.

Figure D-4: Technical data on the Danfoss APP/APM pumps

6. Power consumption

SWPE unit		APP1.0/APM0.8	APP1.5/APM1.2	APP1.8/APM1.2	APP2.5/APM2.0	APP2.5/APM1.8
Recovery rate (%)		29	28	32	29	32
kWh @	50 bar (725 psi) 1450 rpm	0.6	0.9	0.9	1.4	1.5
	50 bar (725 psi) 2900 rpm	1.2	1.7	1.9	2.8	3.0
	60 bar (870 psi) 1450 rpm	0.7	1.0	1.2	1.7	1.5
	60 bar (870 psi) 2900 rpm	1.5	2.1	2.3	3.4	3.5
	70 bar (1015 psi) 1450 rpm	0.8	1.2	1.3	2.0	2.1
	70 bar (1015 psi) 2900 rpm	1.7	2.4	2.7	3.8	4.0

The figures in the table above are calculated using an efficiency of the electric motor of 86% and provided that the pressure at the inlet of the APM motor is 1 bar less than the pressure from the APP pump.

1 hp hr = 0.75 kWh
 1 kWh = 1.34 hp hr

Figure D-5: Power requirement of the Danfoss APP/APM pumps

3. Technical data

Code number		180B3001	180B3002	180B3026	180B3003	180B3004	180B3000	180B3030	180B3032
APP pumps		APP0.6	APP1.0	APP1.5	APP1.8	APP2.2	APP2.5	APP3.0	APP3.5
Geometric displacement	cm ³ /rpm (in ³ /rpm)	4 (0.24)	6.3 (0.38)	9.3 (0.56)	10 (0.61)	12.5 (0.76)	15.3 (0.93)	17.7 (1.08)	20.5 (1.25)
Flow (3000 rpm) ¹⁾	m ³ /h (gpm)	0.6 (2.6)	1.0 (4.4)	1.5 (6.6)	1.7 (7.5)	2.1 (9.2)	2.6 (11.4)	3.0 (13.2)	3.5 (15.4)
Min. pressure ²⁾	bar (psi)	20 (290)	20 (290)	20 (290)	20 (290)	20 (290)	20 (290)	20 (290)	20 (290)
Max. pressure, cont. ³⁾	bar (psi)	80 (1160)	80 (1160)	80 (1160)	80 (1160)	80 (1160)	80 (1160)	80 (1160)	80 (1160)
Max. pressure, Intermittent ⁴⁾	bar (psi)	100 (1450)	100 (1450)	100 (1450)	100 (1450)	100 (1450)	100 (1450)	100 (1450)	100 (1450)
Max. speed cont. ⁵⁾	rpm	3450	3450	3450	3450	3450	3000	3000	3000
Min. speed cont.	rpm	700	700	700	700	700	700	700	700
Power requirement at 80 bar and 3000 rpm:	kW (hp)	1.9 (2.5)	2.9 (3.9)	4.5 (6)	4.8 (6.3)	6.0 (7.9)	7.2 (9.6)	8.4 (11.3)	9.8 (13.1)
Weight	kg (lb)	5.2 (9.7)	5.2 (9.7)	8.6 (17)	8.6 (17.0)	8.6 (17.0)	8.6 (17)	8.6 (17.0)	8.6 (17)
Integrated flushing valve		NO	NO	NO	NO	NO	NO	YES	YES
Flow through flushing valve at 1 bar pressure drop	m ³ /h (gpm)	-	-	-	-	-	-	0.8 (3.7)	0.8 (3.7)

- 1) Typical average flow at 80 bar.
- 2) For lower pressure, please contact Danfoss RO Sales Organization.
- 3) For higher pressure, please contact Danfoss RO Sales Organization.
- 4) Intermittent pressure is acceptable for less than 10 seconds per minute.
- 5) For speeds above 3000 rpm the pump must be boosted at a pressure of 2-5 bar (29.0 - 72.5 psi).

Figure D-6: Technical data on the Danfoss APP pumps

5. Power requirements

Pump model	Flow			Pressure			rpm	Calc. factor
	l/min	m ³ /h	gpm	60 bar	70 bar	80 bar		
				870 psi	1015 psi	1160 psi		
APP0.6	10.2	0.61	2.69	1.38 kW	1.61 kW	1.84 kW	2840	475.8
APP0.6	12.3	0.74	3.25	1.66 kW	1.94 kW	2.21 kW	3400	475.8
APP1.0	16.53	0.99	4.37	2.14 kW	2.49 kW	2.85 kW	2840	474.6
APP1.0	19.83	1.19	5.24	2.57 kW	2.99 kW	3.42 kW	3400	474.6
APP1.5	25.11	1.51	6.63	3.21 kW	3.75 kW	4.29 kW	2890	468.6
APP1.5	30.17	1.81	7.97	3.86 kW	4.51 kW	5.15 kW	3470	468.6
APP1.8	26.78	1.61	7.07	3.43 kW	4.00 kW	4.57 kW	2890	463.2
APP1.8	32.18	1.93	8.50	4.12 kW	4.81 kW	5.49 kW	3470	463.2
APP2.2	33.48	2.01	8.84	4.29 kW	5.00 kW	5.71 kW	2900	468.6
APP2.2	40.22	2.41	10.63	5.15 kW	6.01 kW	6.87 kW	3480	468.6
APP2.5	41.94	2.52	11.08	5.07 kW	5.92 kW	6.77 kW	2900	484.8
APP3.0	48.2	2.9	12.7	6.2 kW	7.2 kW	8.2 kW	2930	470.0
APP3.5	56.0	3.4	14.8	7.2 kW	8.4 kW	9.6 kW	2930	470.0

The power requirements can be determined using one of the following guiding equations:

$$\text{Required power} = \frac{\text{l/min} \times \text{bar}}{\text{Calc. factor}} \text{ [kW]} \text{ or } \frac{16.7 \times \text{m}^3/\text{h} \times \text{bar}}{\text{Calc. factor}} \text{ [kW]} \text{ or } \frac{0.26 \times \text{gpm} \times \text{psi}}{\text{Calc. factor}} \text{ [kW]}$$

1 hp	=	0.75 kW
1 kW	=	1.34 hp
1 gpm	=	3.79 l/min
1 l/min	=	0.26 gpm
1 m ³ /h	=	4.40 gpm
1 gpm	=	0.23 m ³ /h

Figure D-7: Power requirement of the Danfoss APP pumps

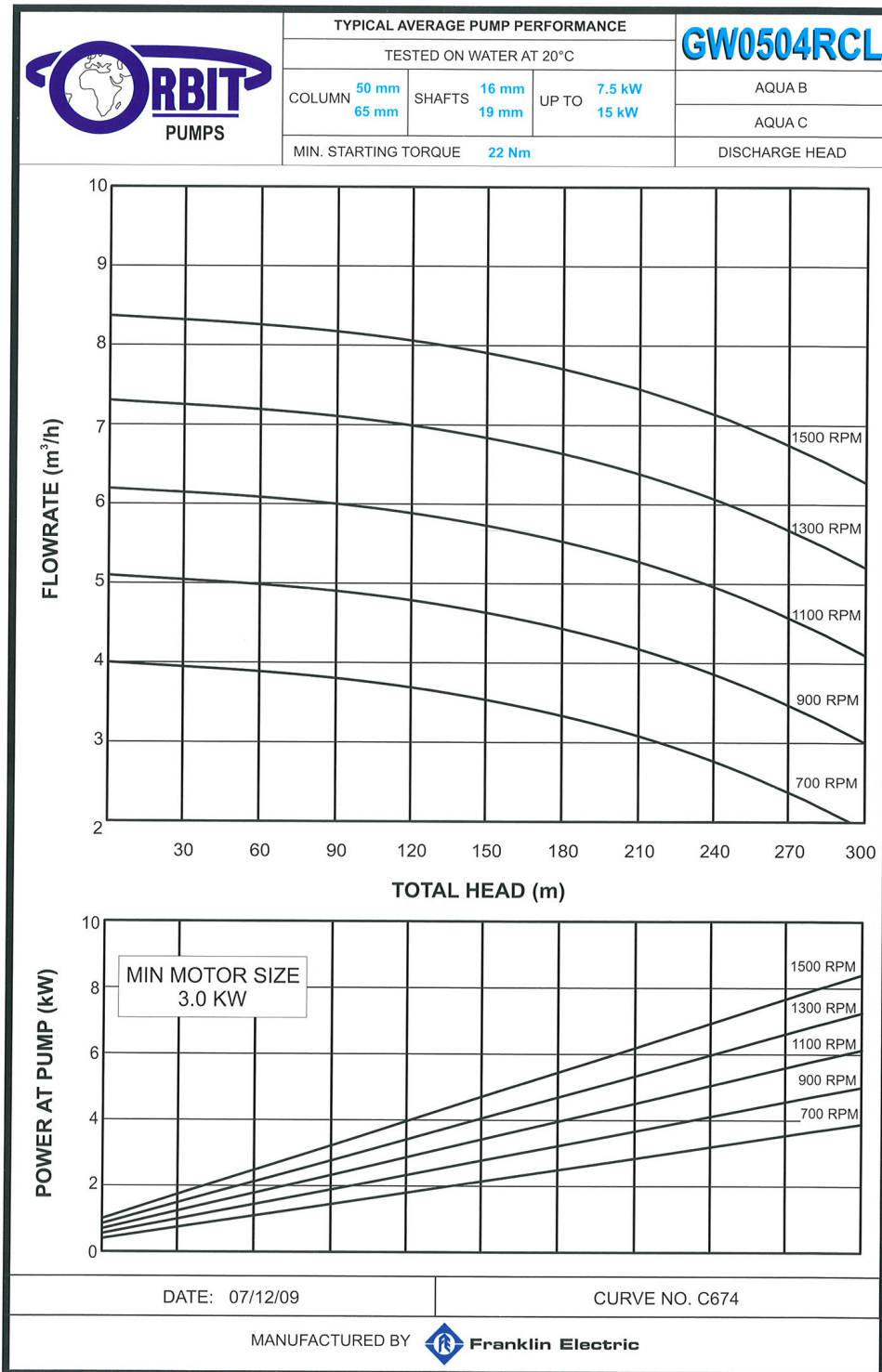


Figure D-8: Flow rate and power characteristics of the Franklin GW0504 Orbit pump

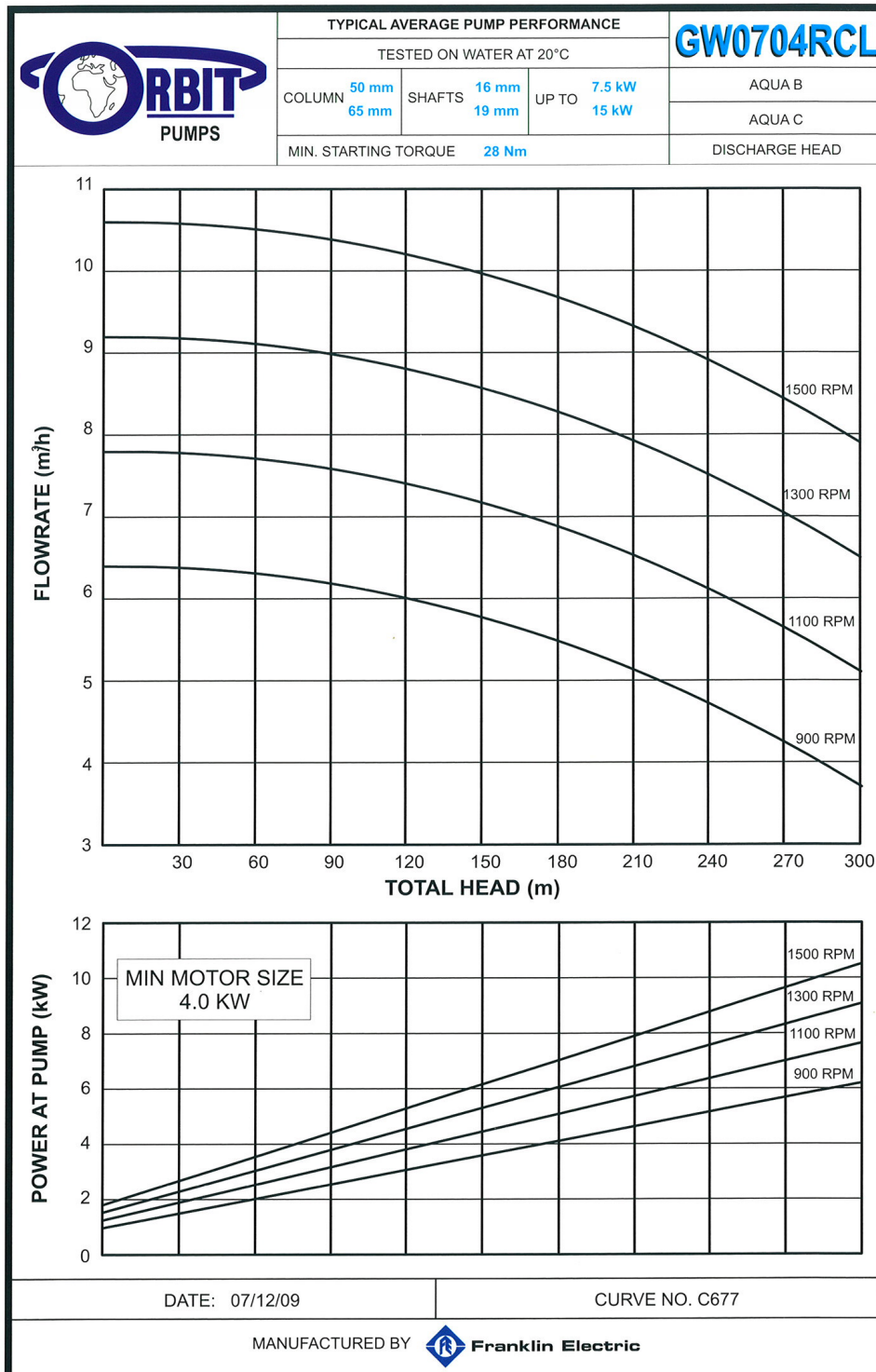


Figure D-9: Flow rate and power characteristics of the Franklin GW0704 Orbit pump

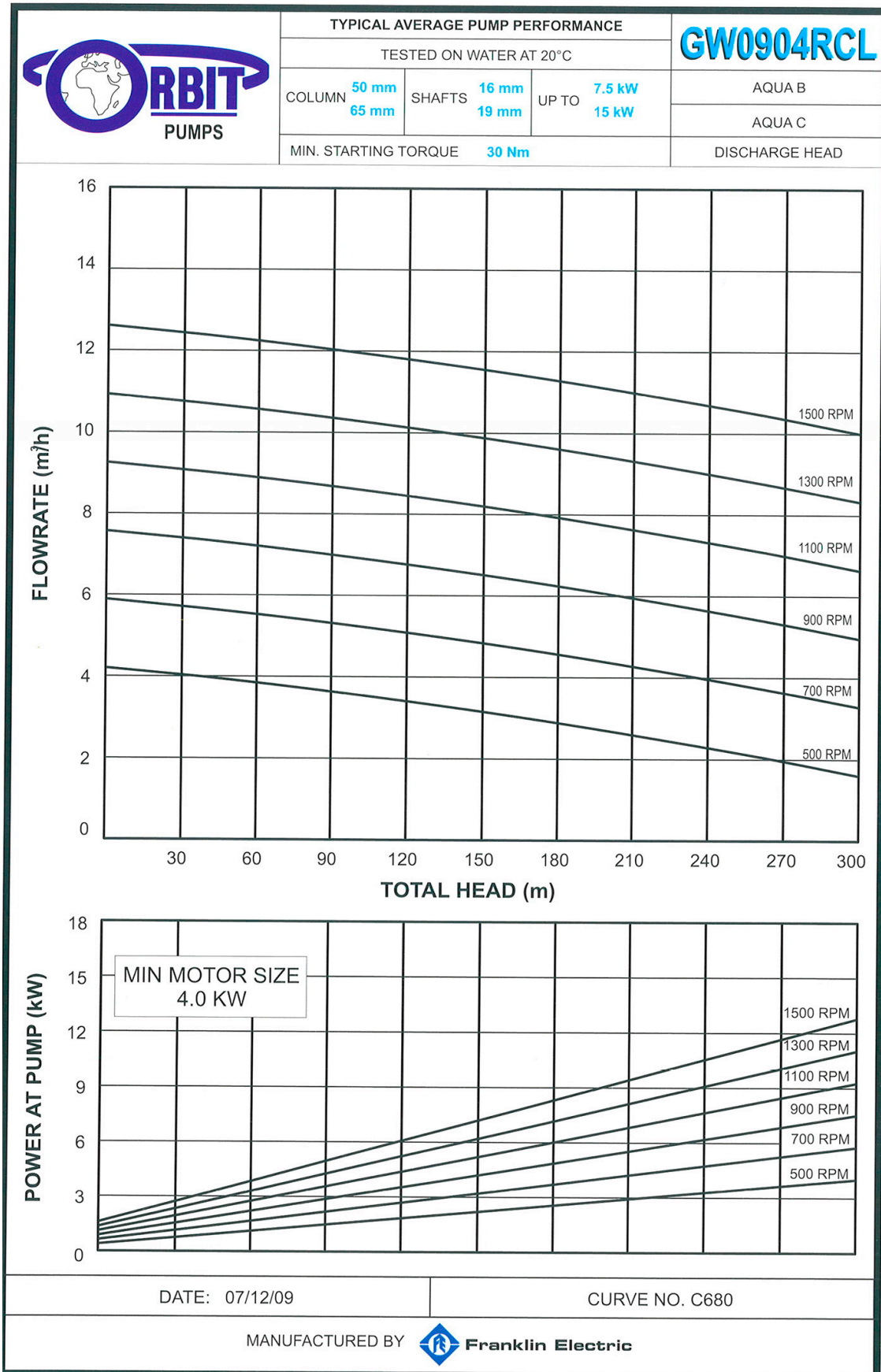


Figure D-10: Flow rate and power characteristics of the Franklin GW0904 Orbit pump

D-2 Energy recovery systems and pump combinations commonly used for RO applications

The introduction of energy recovery devices (ERD) reduced the cost of seawater desalination significantly. With ERD the pressure of the brine is reused to get the feed water to the necessary pressure. This can substantially reduce the energy demand of the RO system. The amount of reduction depends on the efficiencies of the ERD and pumps.

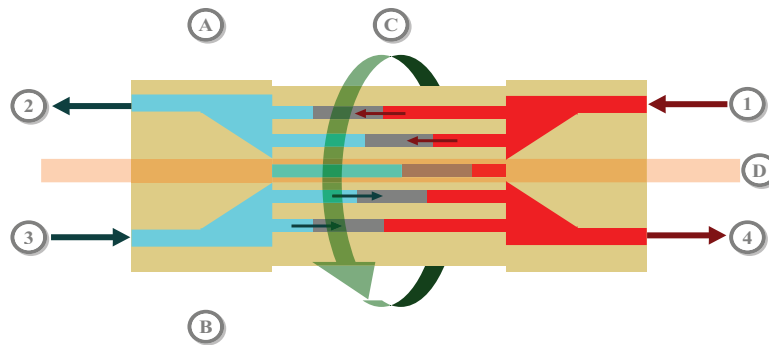


Figure D-11: Schematics of a rotary pressure exchanger. A: high pressure side, B: low pressure side, C: rotor rotation, D: sealed area

Table D-1: Energy recovery devices

	Pressure exchanger	Turbine systems
Principle	Transfer pressure directly from the brine to part of the feed water	Convert potential energy from the brine to kinetic energy supplied to the feed water directly (turbocharger) or to the feed pump (Pelton wheel)
Efficiency	96%-98%	<90%
Disadvantage	<ul style="list-style-type: none"> - Require additional equipment (high pressure circulation pump) - Increased salinity of the feed (up to 2 bar increase in osmotic pressure) 	Strong efficiency reductions when operating outside actual design point
Advantage	High efficiency maintained when changes occur due to aging, fouling etc.	Less equipment and maintenance cost, since no auxiliary equipment is needed

Two types of energy recovery systems can be distinguished, pressure exchangers and turbine systems. Figure D-11 shows the schematics of a rotary pressure exchanger. The tube in the rotor is first filled with low pressure sea-water (3), due to the rotation the tube will connect with the high pressure brine inlet (1) and the sea-water in the rotor tube will be pushed (and thus pressurized) in the feed outlet (2). The brine is now de-pressurized and will leave the rotor at the brine outlet (4) at the same time the rotor tube is filled with sea water (3). This process then repeats itself and the rotor consists of several rotor tubes working simultaneously according to this principle.

Table D-1 gives an overview of the principle, advantages and disadvantages of the different energy recovery systems. Nowadays the majority of the existing seawater desalination plants use Pelton Wheel based technology. Over the past years pressure exchangers have been installed on most of the newer (large) desalination plants, because they are typically 5-to-15 % more efficient.

The application of energy recovery systems has led to energy consumption as low as 2 - 4 kWh/m³ in seawater desalination and < 1 kWh/m³ in brackish water desalination.

D-2-1 Pump combinations commonly used for RO applications

In large systems, pelton-wheel turbines are common and fluid equipment's turbo booster and ERI's pressure exchanger are gaining acceptance, but none of these are available at small sizes [Thomson et al, 2002]. The use of Danfoss hydraulic motors for energy recovery in a small seawater RO system is a proven concept reducing the energy consumption from 13 kWh/m³ to around 5.6 kWh/m³. Tests at CREST and DUT indicated however slightly lower efficiencies and corrosion and/or wear problems. An alternative is the Clark pump, which can be described as an pressure intensifier, and is expected to have excellent efficiency (around 3.2 kWh/m³) and little to no corrosion problems [Thomson, 2003]. The pump is developed for the yachting market and therefore not designed for continuous use. Existing configurations produce around 2 to 4 m³ per day.

Spectra Clark pump

The Clark pump has been developed by Spectra Water-makers and is a small scale energy recovery device. The basic mechanism of the Clark pump is shown in figure D-13. The two pistons are connected by a rod. The medium pressure liquid and the concentrate pressure liquid act together to push the piston combination to the right and thereby pressurizing the outflow water. At the end of the stroke the ports are reversed and the piston combination moves to the left, until it again reverses. The mechanism to operate the the ports is built into the Clark pump and the overall operation is very smooth.



Figure D-12: Spectra Clark pump

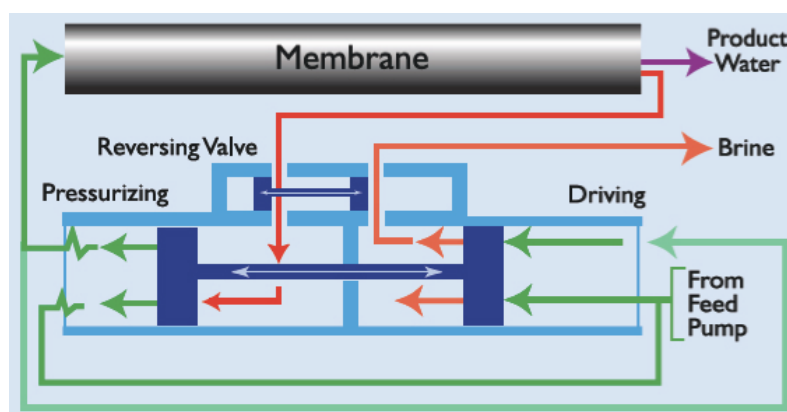


Figure D-13: Schematic overview of the Clark pump principle

Figure D-14 shows two configurations of a Clark pump in a reverse osmosis system evaluated by CREST [Thomson et al, 2002]. One being a basic configuration with only one motorized pump and no pressure regulating mechanism: the water recovery ratio (product flow to feed flow) is fixed by the ratio of the cross-sectional area of the rod to that of the piston. The performance of a Clark pump was tested by CREST in 2000. The energy efficiency turned out to be excellent and maintained over a very wide range of flow and pressure. The Clark pump is manufactured in only one size, though it is now available with different diameter rods. The standard Clark pump has a rod-to-piston area ratio of 10% and Spectra recommends that the feed should not exceed 0.22 L/s, which results in 1.9 m³ per day (with a recovery of 10%). It should be investigated if a Clark pump can be used in a configuration that results in a permeate flow of around 20 m³/day (if sufficient power is available). Changing the rod-to-piston ratio such that a recovery of 20% is achieved will increase the production to 3.8 m³. Further increasing the recovery will increase the permeate flow, but gives fouling problems. Another option is to upscale the existing Clark pump in cooperation with Spectra or place several Clark pumps in series which is a costly solution.

In order to increase product flow per Clark pump and to maintain low specific energy consumption over a wide operating range a second motorized pump can be installed as illustrated in figure D-14(b). This configuration allows the water recovery ratio to be increased to any desired value. When the available power is low, the system will operate at a low recovery ratio by only running the medium pressure pump. If the available power increases the high pressure pump is started and the recovery ratio is increased. For the application of a stand alone small scale RO system this might however not be desirable, since increasing recovery can result in fouling.

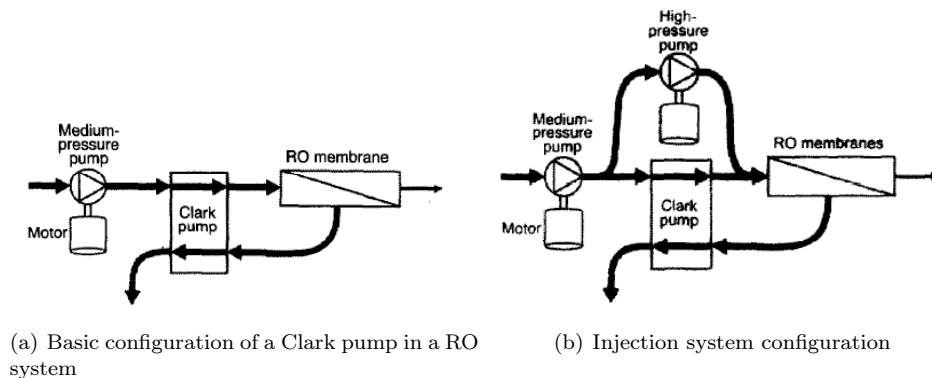


Figure D-14: Two Clark pump-RO configurations

The Clark pump needs to be fed by a medium pressure pump. Criteria for the selection of such a pump are efficiency, seawater compatibility and tolerance to occasional grain of sand. A multi-stage centrifugal pump would seem a possibility, but these offer very poor efficiency at the required flow/pressure. Also to achieve optimum efficiency the rotor speed must be matched to the flow/pressure operating point, which is a hassle in a system with variable rotor speed due to the wind. CREST finally selected a Moineau (progressing-cavity) pump, which offers reasonable efficiency at the required duty and this is generally maintained as the flow is reduced. They can handle sand, but should not run dry.

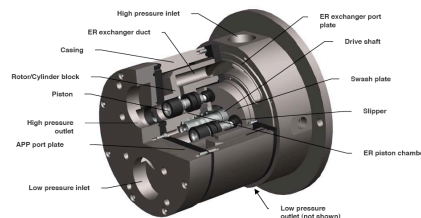
Danfoss SWPE

The sea water pump with energy recovery of Danfoss consists of an APP pump and an APM (energy recovery) motor, see figure 2-5. Since the APM has a fixed volumetric displacement the recovery rate will be fixed. The pumps and motors are based on the axial piston principle.

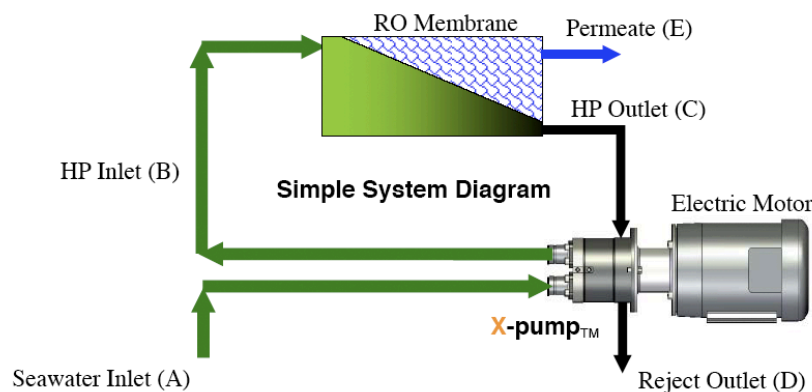
The flow is proportional to the number of revolutions of the input shaft and the pump/motor displacement. The previous version of the prototype developed by E. Rabinovitch contained a Danfoss APP1.5/APM1.2 high pressure piston pump [Rabinovitch, 2008]. Although the combination worked at a good energy efficiency (around 5 kWh/m^3), wear problems arose which need to be overcome in the future. At start up there can be no energy recovery, so the system will operate as a single APP motor. Once the system is running the system uses the energy recovery unit.

X-pump

For small scale reverse osmosis the Ocean X-pump of Ocean Pacific Technologies is not commonly used. It seems to be a fairly new technology of which the key feature is that it combines the high pressure pump and energy recovery system into a single unit. In that way the design is simple, compact and a low energy consumption is achieved [Ocean Pacific Technologies,]. The permeate flow is maximum 46 m^3 per day and the minimum required shaft velocity is 1500 rpm. The X-pump seems to be suitable for achieving the goal of increasing permeate production to around 25 m^3 , it should be calculated however if the minimum of 1500 rpm can be realized and at what cost.



(a) X-pump: an axial piston pump and pressure exchanger combined



(b) Total reverse osmosis system overview with X-pump

Figure D-15: X-pump

Appendix E

Additional reverse osmosis information

Concentration polarization Concentration polarization is a concentration build-up of the retained material in the boundary layer close to the membrane that occurs during filtration. It results in a higher osmotic pressure difference across the membrane leading to a rapid decline in flux. The decline will not continue in time as is the case with fouling. Concentration polarization can be limited by disturbance of the boundary layer. Increasing the velocity along the membrane might be a way to do that. In the Simulink model the effect of concentration polarization is not included (for now). The effect is however minimized as the recovery will only be around 20%.

E-1 Membrane cleaning

There are several different membrane cleaning methods, such as a forward flush, a backward flush and a chemical cleaning process. With a forward flush the membranes are flushed with feed or permeate water forward. It flows more rapidly than during the production phase, releasing the discharging the particles that are absorbed to the membrane. It does not release the particles absorbed in the membrane pores. A backward flush is needed for that. This is a reversed filtration process. Permeate is flushed to the feed water side of the system under pressure at twice the flux during operation. When the flux is still not restored enough after applying the backward flush, chemicals such as chlorine bleach or hydrochloric acid can be used to rinse out the contaminants.

E-1-1 Spiral wound membranes

Almost all reverse osmosis membranes are of the spiral-wound configuration, because of the high specific surface needed to obtain the necessary permeate production. The configuration of membrane sheets twisted around a permeate collecting tube is called an element. Figure E-1 illustrates how the membranes are twisted around the collecting tube to get to its fixed high specific surface but small volume configuration which is basically a long tube, the membrane element. The length of such an element is usually around 1 meter. Water is fed from one side into the element and via spacers the water is distributed over the membrane. The permeate flows into the permeate collecting tube and the retentate leaves the membrane element on the

opposite side of the feed inlet. Table E-1 summarizes the positive and negative aspects of the spiral wound modules. One of the main negative sides is that rapid fouling of the spacer channels with particulate can occur.

Table E-1: Positive and negative points of spiral wound modules

Advantages	Disadvantages
- Cheap and relatively simple production	- High feed side pressure loss
- High packing density $<1000 \text{ m}^2/\text{m}^3$	- Susceptible to fouling
- High mass transfer rates due to feed spacers	- Hard to clean

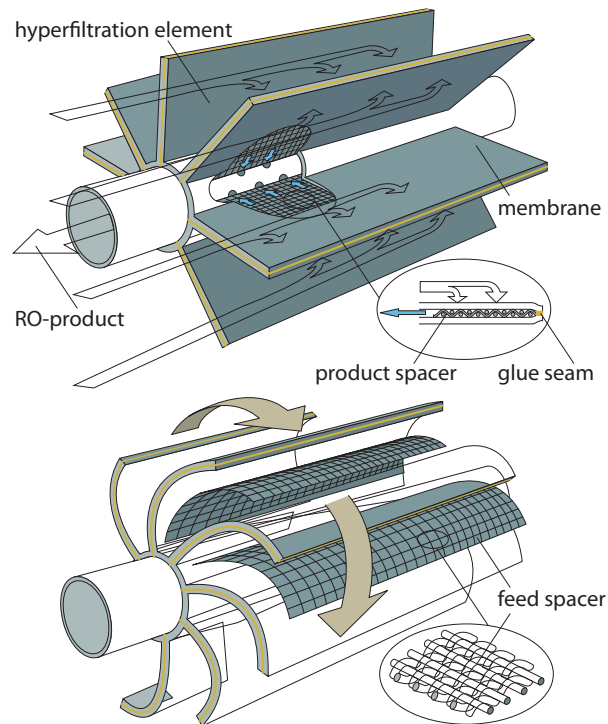


Figure E-1: Spiral-wound configuration [van Dijk, 2008]

Appendix F

Wind2Water model verification by means of EXCEL calculations

For the comparison of the model with EXCEL calculations the system configuration of the prototype on Curacao is used. The input variables that were used are given in table F-1. From this the torque delivered to the pump can be calculated with the same formulas as provided in chapter 3. Furthermore the APP1.5/APM1.2 Danfoss pump is the incorporated pump assuming that the energy recovery will take place immediately. The torque needed to get the pump running is calculated and was found to be 5.5 Nm. Subtracting the required pump torque from the delivered pump torque gives you ΔQ .

Table F-1: Input for the verification with EXCEL

Variable	Value	Description
C_f	35000 mg/L	Salt concentration in feed water
$\eta_{coupling}$	0.12	Losses in the coupling
i	40	Transmission
M_b	0.25 kg	Mass per blade
N_b	9	Number of blades
R	2.5 m	Radius of the windturbine

With equation F-1 $\Delta\omega$ can now be retrieved. Adding $\Delta\omega_{wind}$ and ω_{t-1} results in the new ω . With this new ω , the new λ followed by the new delivered torque and consequently the new ΔQ are calculated. Then the new $\Delta\omega$ can be obtained and the process repeats for this new value.

$$\Delta\omega_{t,t-1} = \int_{t-1}^t \frac{\Delta Q}{J} dt \quad (F-1)$$

If working properly the torque delivered by the windmill converges to the required pump torque. Figure F-1 shows that this is indeed the case and that the results of the model correspond with the results from the hand calculations done in EXCEL. In order to clearly show the convergence of the torque to the required value a constant wind speed was used as input for figure F-1. As expected the angular velocity of the pump calculated by the model is also similar to the velocity calculated by the hand calculations (see figure F-2).

In the case of non constant wind input the model differs slightly from the hand calculations. This small variation is probably caused by the time-lag in the integration. Changes in wind-speed input therefore result in small ΔQ differences. From figure F-3 it follows that the maximum pump torque deviation from the hand calculation is 6.6 % and for the pump angular velocity this is 18 %. Both models converge towards the same values when the wind speed is kept constant. Figure F-5 and figure F-5 show the results for a continuously increasing wind speed, with a maximum error of 8.4 % and 7.3 % for the angular velocity.

The model tested with the hand calculations is simplified. The boundary conditions of the pump are for example not taken into account. Also only running condition for the pump was assumed. But despite these simplifications, it shows that the main principle of the SIMULINK model is correct. The torque and angular velocity of the pump and wind mill are converging to its working point.

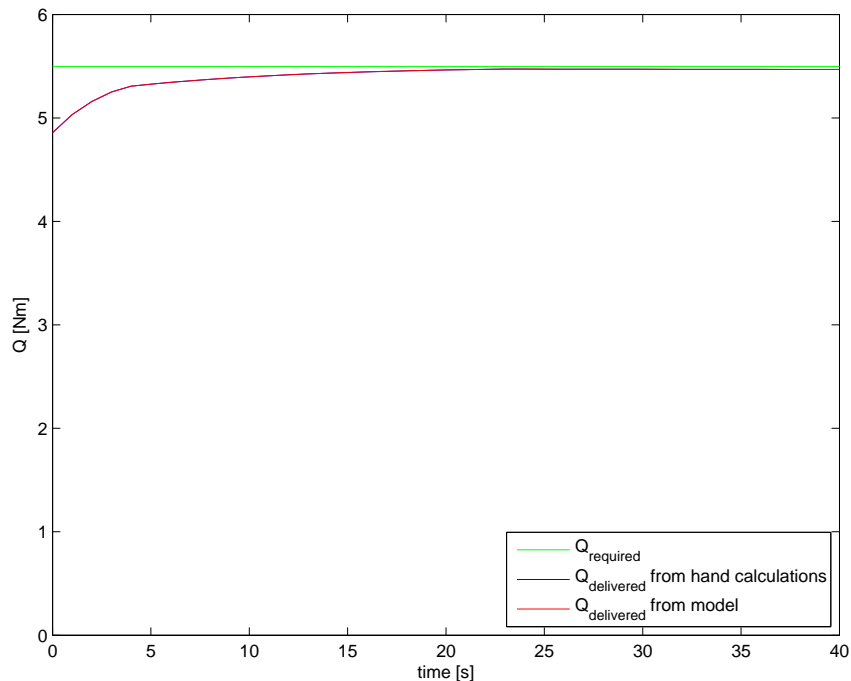


Figure F-1: Torque generated under constant wind speed

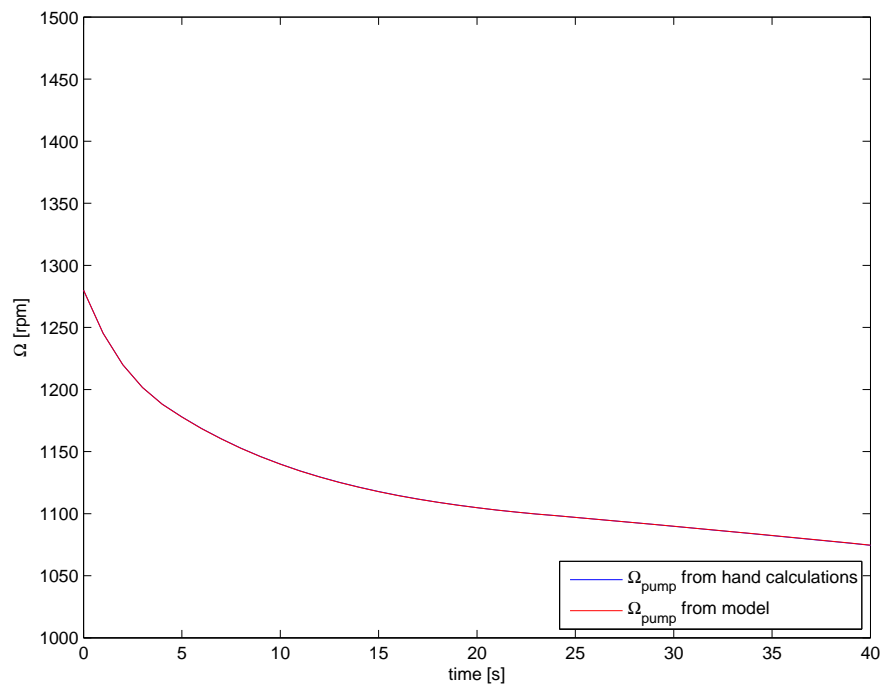


Figure F-2: Ω for constant wind speed input

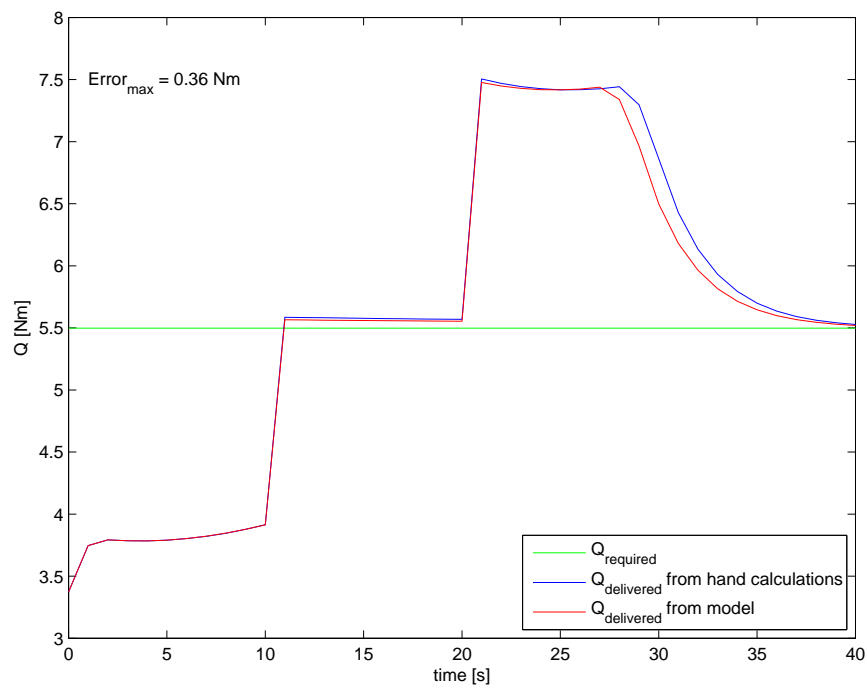


Figure F-3: Torque generated under step wise increasing wind speed input

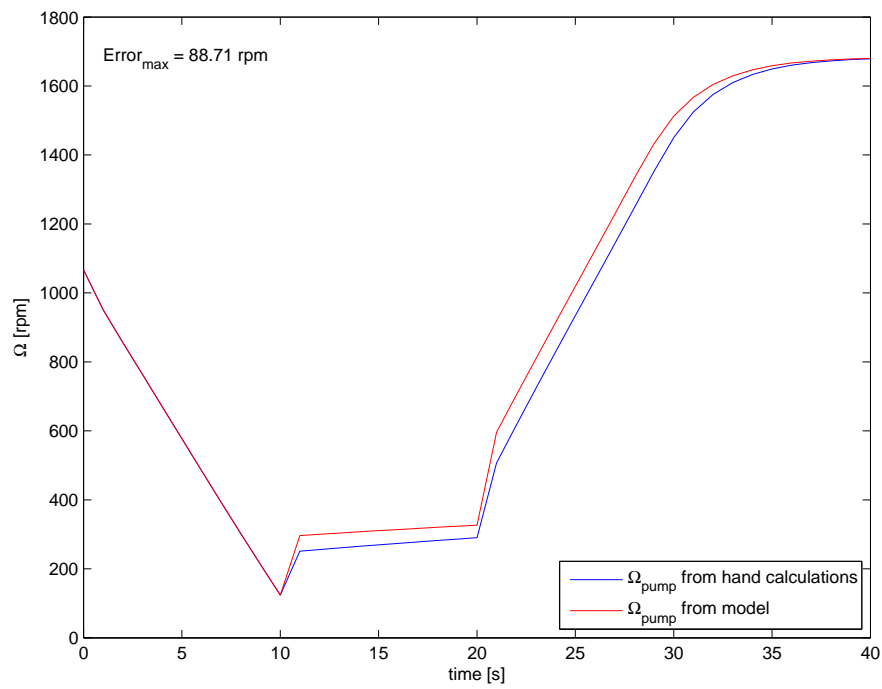


Figure F-4: Ω for step wise increasing wind speed input

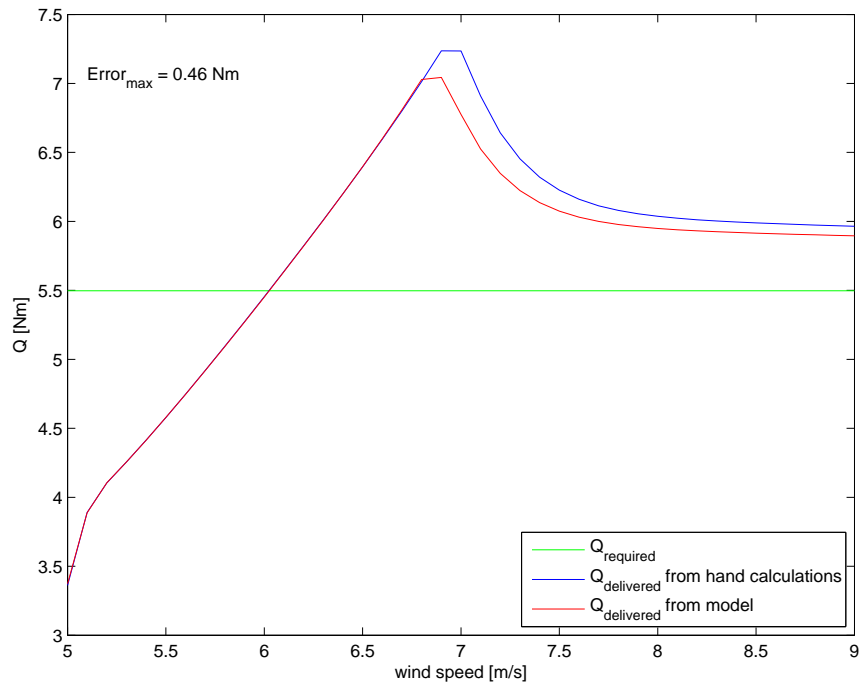


Figure F-5: Torque generated under gradually increasing wind speed input

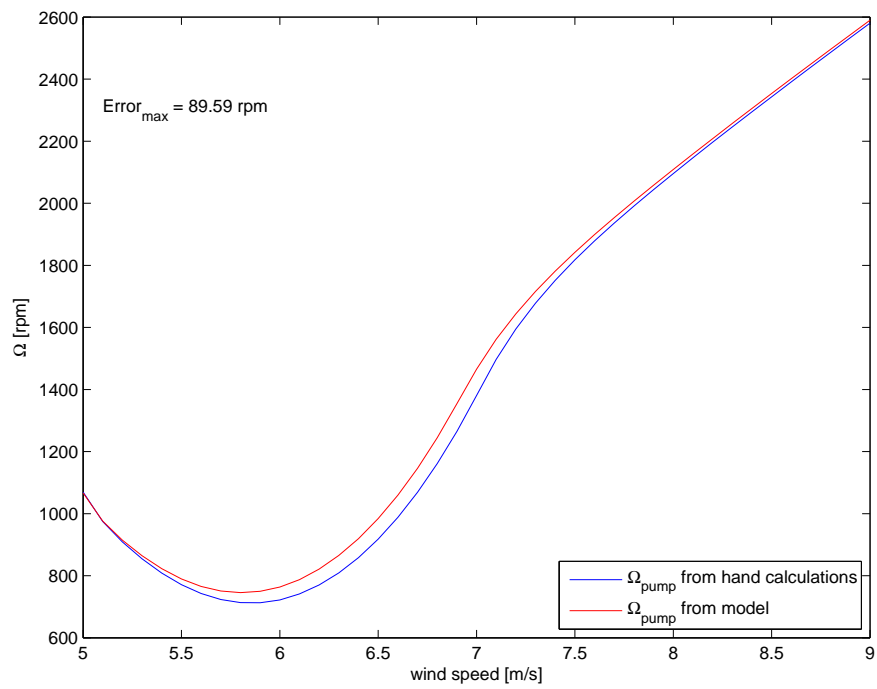


Figure F-6: Ω for gradually increasing wind speed input

Appendix G

Pearson pump model compared to experimental data

To test the of fluctuating operation on reverse osmosis membranes the TU Delft performed an experiment with a Pearson pump of Spectra as high pressure pump. Spectra's Pearson pump (type LB 1800) is a positive displacement three cylinder reciprocating high pressure pump with fixed energy recovery ratio. The result of the research was that after more than 650 hours of operation no deterioration of the membranes was observed. In this section the Spectra's Pearson pump will be added to the Simulink model. The Pearson pump is isolated from the rest of the model to see if the results match the experimental data. Also the model is made in such a way that it can be easily adapted to implement other type of positive displacement pumps.

Figure G-1 gives a schematic overview of the Pearson pump model. From the experimental data relationships between the wind speed and the power and angular velocity were found. The angular velocity serves as input for the Pearson pump model. With the angular velocity the displacement of the pump (D) is calculated (see equation G-1, with A : cross sectional area of the pump, s : length of the stroke, n : number of cylinders).

$$D = \frac{A \cdot s \cdot n \cdot \Omega}{231} \quad (\text{G-1})$$

Multiplying the displacement with the volumetric efficiency this leads to an approximation of the feed flow (q_f). The feed flow runs to the membranes and the feed pressure that is required to handle the feed flow correctly can be calculated. Since energy recovery is present in the Pearson pump only part of the power needed to pressurize the water has to be delivered from the pump, the rest comes from the high pressure concentrate flow, this behavior is included by introducing ΔPr . The required pump power is then calculated as a function of the feed flow, the needed pressure difference (ΔPr) and the mechanical efficiency of the pump.

To check the model the resulting power is compared to the power from the experiment. The model and the experimental data are showing similar results. Also the feed pressure and the feed flow are within a reasonable range of each other as can be seen in figure G-3 and G-4 respectively.

It should be noted that the experiment was done in several intervals, with only small data-sets per interval. In order to validate the model correctly only consecutive measurements are useful and therefore the evaluation is based on only a small number of data points.

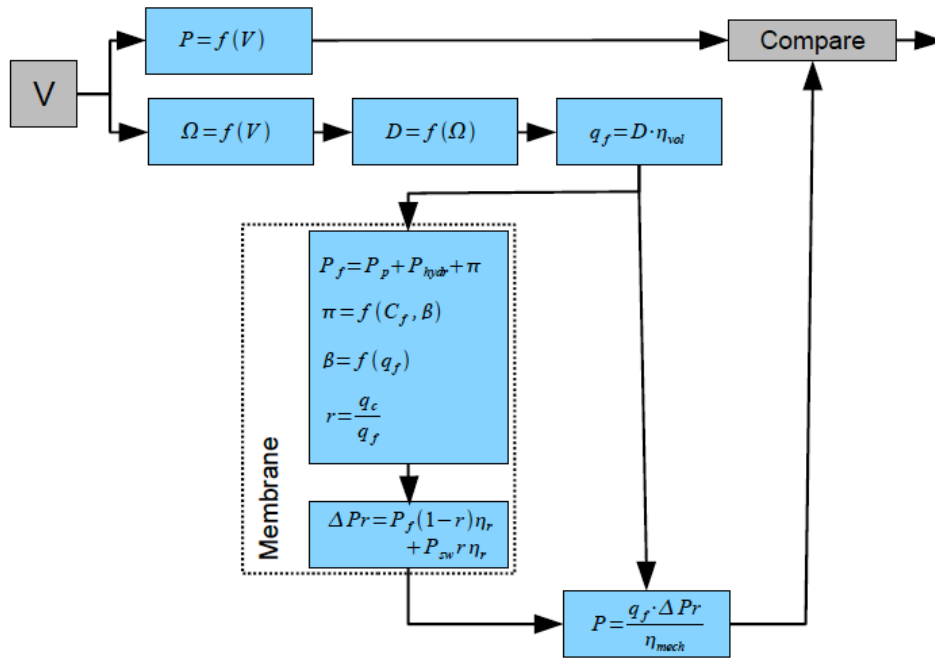


Figure G-1: Schematic overview of Pearson pump model

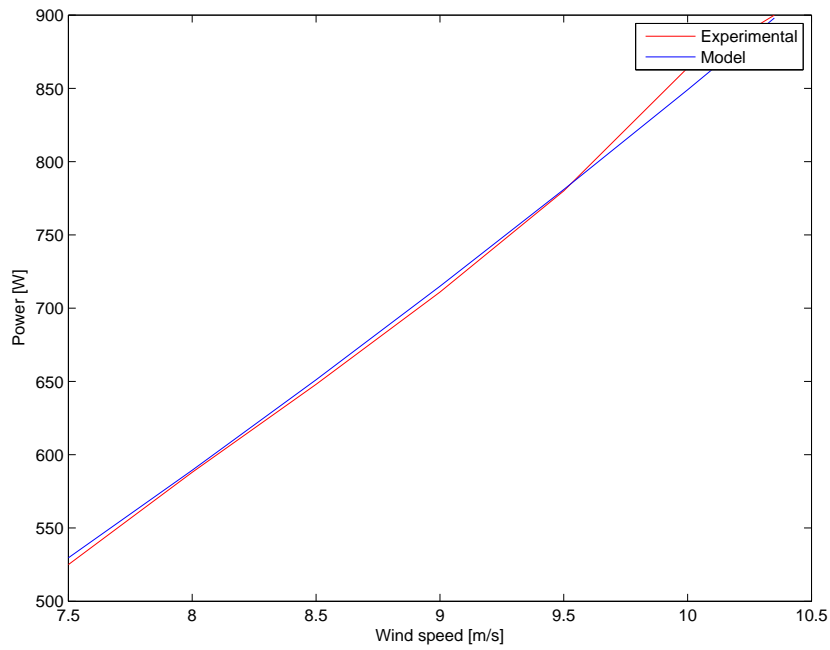


Figure G-2: Power from Pearson pump experiment compared to model

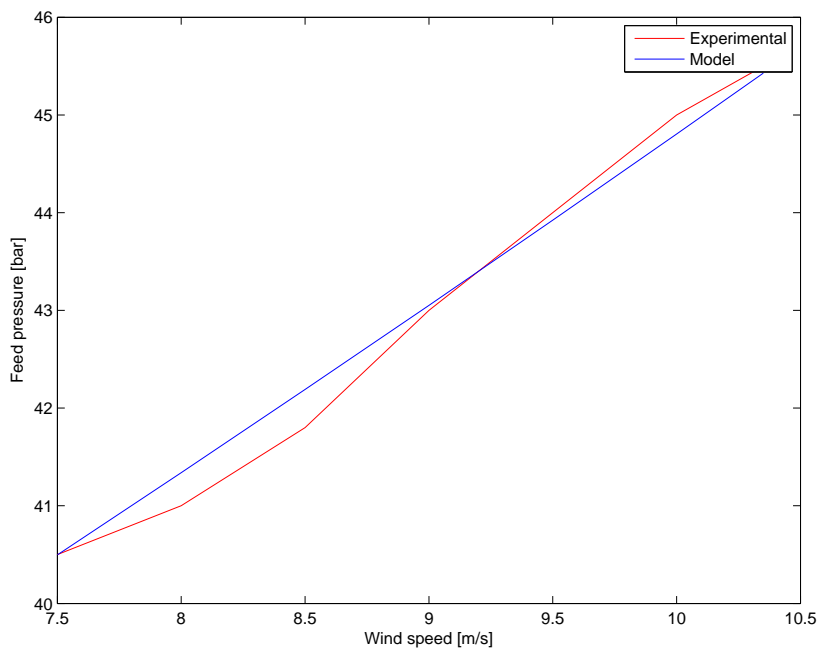


Figure G-3: Required pressure from Pearson pump experiment compared with model

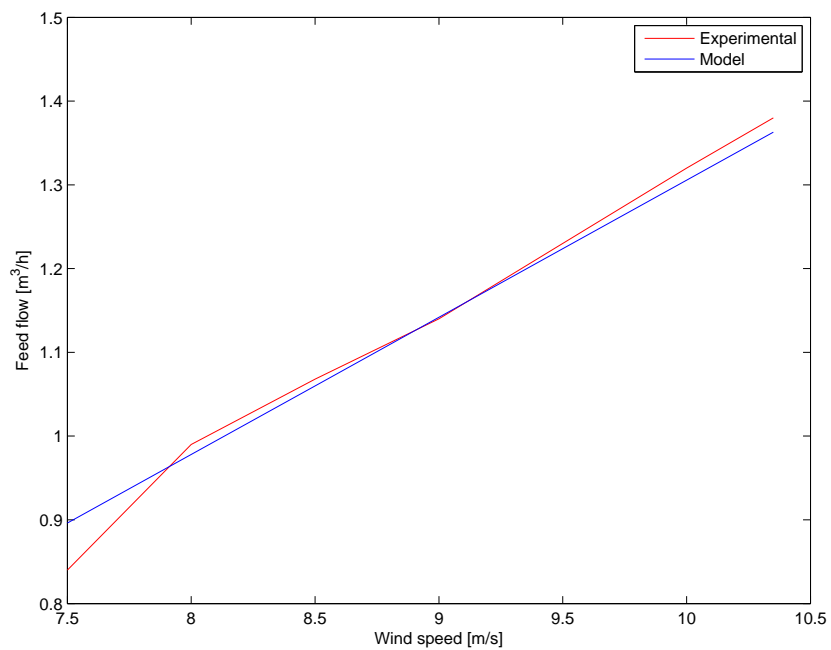


Figure G-4: Permeate flow from Pearson pump experiment compared with model

Appendix H

Batteries: system configuration and cost

The system is currently modeled as illustrated in figure H-1 at number 1. In that way the generated power always has to deal with the losses of the battery. Another way of modeling the system would be using the energy from the wind directly and adding energy from the battery when necessary. This will result in bypassing the battery losses most of the time and therefore make better use of the power. For now, the electrical system is modeled according to schematic 1, which is in accordance with the Hatendoer test set-up.

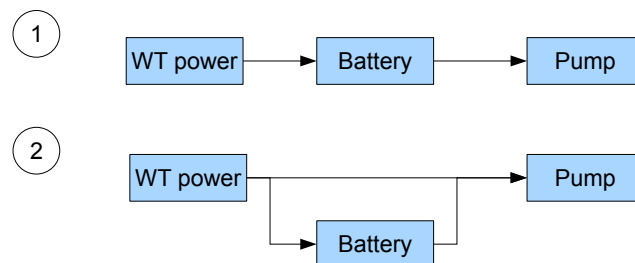


Figure H-1: Overview of two ways of including the battery in the model

As stated before, batteries are costly. Increasing the battery bank size to deal with long periods of small wind speeds should therefore be viewed from a cost per cubic m³ point of view. In figure an approximation of the cost of the system without battery, the life time of the system and of the battery are given. Playing around with these parameters can easily be done in the excel file, but for now these figures offer a good approximation. All characteristics of the configurations are given in table 4-3. The selected configurations are the configurations with either no battery (configuration 2), the battery used by Hatendoer at its full capacity (configuration 7) and at half the capacity (configuration 8) and a battery 2.5 times larger than the one used by Hatendoer (configuration 11). Configuration 7 and 8 have a 48 VDC battery of 400Ah. Configuration 11 has a battery of 48 VDC 1020 Ah. The battery costs are found on the website of GB Industrial batteries.

If the batteries operate according to the specifications and the lifetime is at least 5 years the 1020Ah battery performs slightly better from a water cost point of view as can be seen in figure

H-2. The environment for our application is however tough and the life time of the battery in those type of environments needs to be checked carefully. If the lifetime halves the cost of the water will already be better for the smaller battery (see figure H-3). Adding no battery for this design is not desirable. The current wind turbine continuously delivers less power than the required power, so without a battery the pump will not run at all. When opting for a system without batteries, better matching of wind turbine and pump is required.

System cost without battery						
Lifetime system [years]						10
Lifetime battery [years]						5

Configuration	Battery cost	Total price	qf [m3/day]	Price per m3	Relative price
2	0	\$50,000	0.34	\$40.29	100%
7	4200	\$58,400	1.62	\$9.88	25%
8	4200	\$58,400	1.55	\$10.32	26%
11	7500	\$65,000	1.89	\$9.42	23%

Figure H-2: Relative water cost for influence of battery on Hatenboer system performance

System cost without battery						
Lifetime system [years]						10
Lifetime battery [years]						2.5

Configuration	Battery cost	Total price	qf [m3/day]	Price per m3	Relative price
2	0	\$50,000	0.34	\$40.29	100%
7	4200	\$66,800	1.62	\$11.30	28%
8	4200	\$66,800	1.55	\$11.81	29%
11	7500	\$80,000	1.89	\$11.60	29%

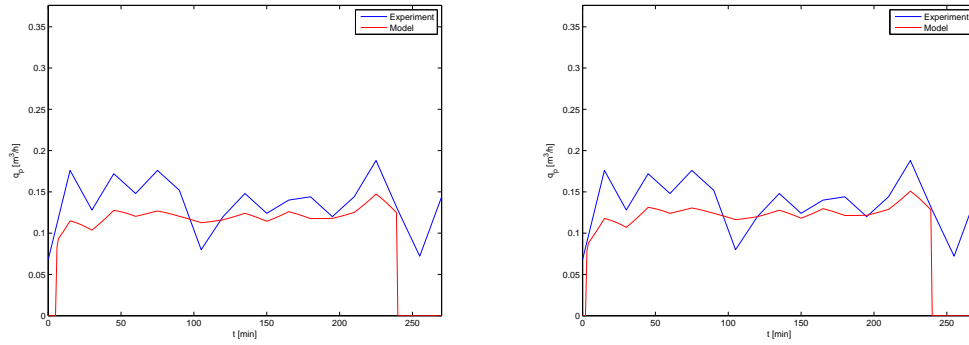
Figure H-3: Relative water cost by shorter lifetime of battery

Appendix I

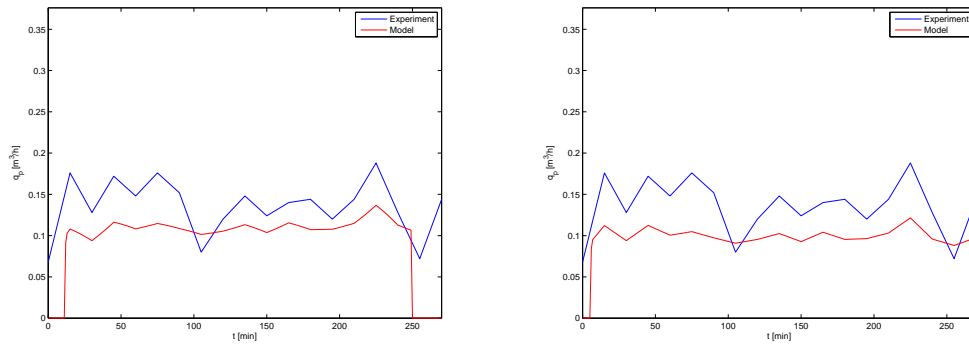
Results Curaçao model

t [min]	rpm pump	windspeed [m/s]	productie [m3/h]	druk [bar]	Torque [Nm]
0	428	4.59	0.07	30	3.40
15	1128	6.4	0.18	46	4.76
30	811	5.35	0.13	31	3.49
45	1103	6.4	0.17	30	3.40
60	875	5.71	0.15	35	3.83
75	1199	5.95	0.18	37	4.00
90	977	5.52	0.15	39	4.17
105	581	5.14	0.08	20	2.55
120	793	5.4	0.12	37	4.00
135	1080	5.8	0.15	42	4.42
150	789	5.24	0.12	41	4.34
165	969	5.88	0.14	39	4.17
180	933	5.38	0.14	40	4.25
195	845	5.43	0.12	42	4.42
210	891	5.81	0.14	35	3.83
225	1252	6.85	0.19	43	4.51
240	815	5.38	0.13	36	3.91
255	589	4.93	0.07	41	4.34
270	917	5.47	0.14	35	3.83

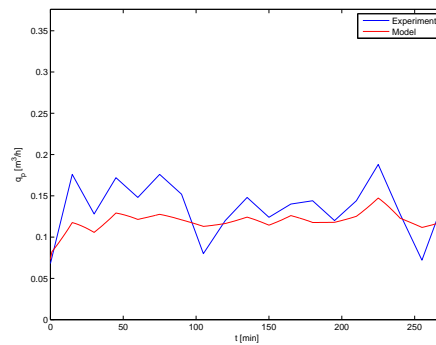
Figure I-1: Data of experiment done on Curaçao [Rabinovitch, 2008]



(a) SIMULINK configuration I: $C_f = 40000$ mg/L, (b) SIMULINK configuration II: $C_f = 35000$ mg/L, $M_b = 5$ kg, $\eta_{coupling} = 0.12$, $J_p = 0$ kg/m², $\delta_{pump} = -0.9$ Nm

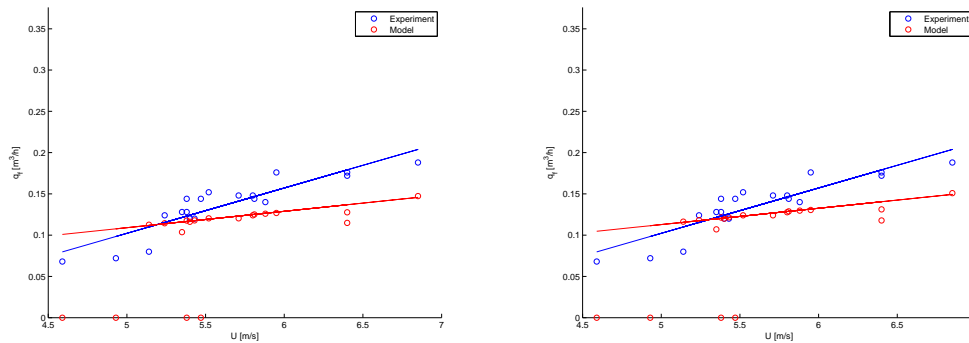


(c) SIMULINK configuration III: $C_f = 40000$ mg/L, (d) SIMULINK configuration IV: $C_f = 40000$ mg/L, $M_b = 5$ kg, $\eta_{coupling} = 0.32$, $J_p = 0$ kg/m², $\delta_{pump} = -0.9$ Nm

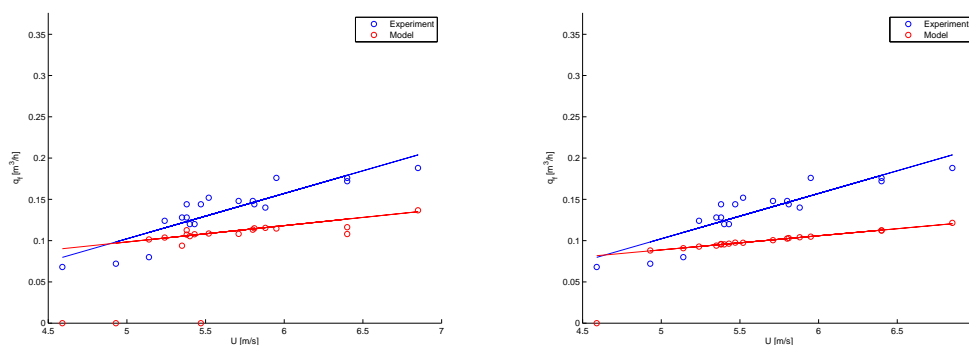


(e) SIMULINK configuration V: $C_f = 40000$ mg/L, $M_b = 5$ kg, $\eta_{coupling} = 0.12$, $J_p = 0$ kg/m², $\delta_{pump} = 3$ Nm

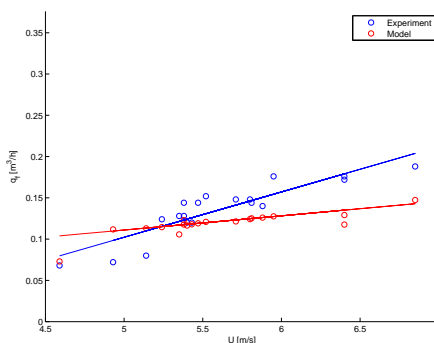
Figure I-2: Result of permeate flow (q_f) over time (t) of the SIMULINK model compared with data from Curaçao experiment.



(a) SIMULINK configuration I: $C_f = 40000$ mg/L, (b) SIMULINK configuration II: $C_f = 35000$ mg/L, $M_b = 5$ kg, $\eta_{coupling} = 0.12$, $J_p = 0$ kg/m², $\delta_{pump} = -0.9$ Nm

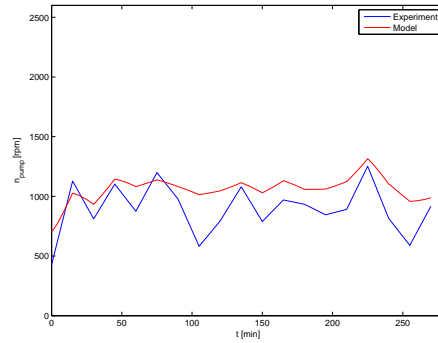
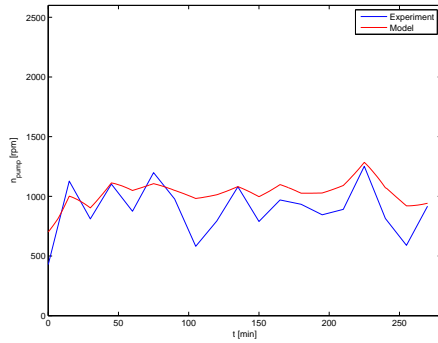


(c) SIMULINK configuration III: $C_f = 40000$ mg/L, (d) SIMULINK configuration IV: $C_f = 40000$ mg/L, $M_b = 5$ kg, $\eta_{coupling} = 0.32$, $J_p = 0$ kg/m², $\delta_{pump} = -0.9$ Nm

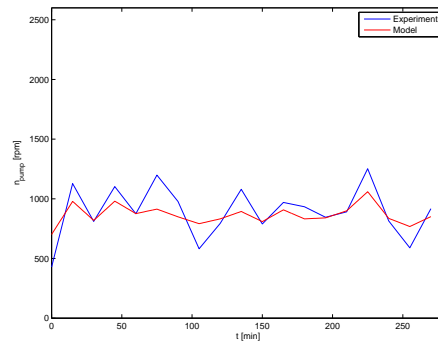
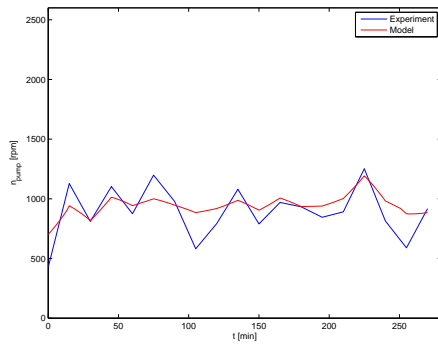


(e) SIMULINK configuration V: $C_f = 40000$ mg/L, $M_b = 5$ kg, $\eta_{coupling} = 0.12$, $J_p = 0$ kg/m², $\delta_{pump} = 3$ Nm

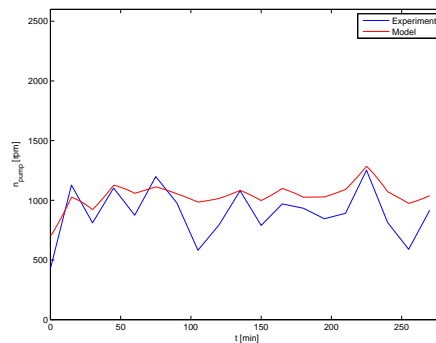
Figure I-3: Result of permeate flow (q_f) over wind speed (U) of the SIMULINK model compared with data from Curaçao experiment.



(a) SIMULINK configuration I: $C_f = 40000$ mg/L, (b) SIMULINK configuration II: $C_f = 35000$ mg/L, $M_b = 5$ kg, $\eta_{coupling} = 0.12$, $J_p = 0$ kg/m², $\delta_{pump} = -0.9$ Nm

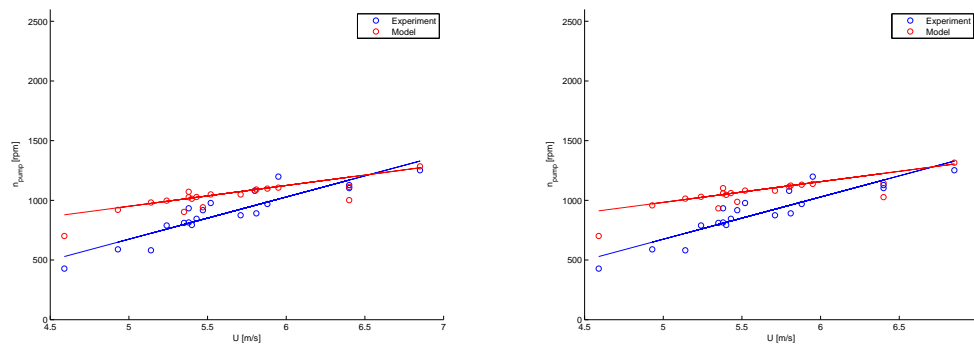


(c) SIMULINK configuration III: $C_f = 40000$ mg/L, (d) SIMULINK configuration IV: $C_f = 40000$ mg/L, $M_b = 5$ kg, $\eta_{coupling} = 0.32$, $J_p = 0$ kg/m², $\delta_{pump} = -0.9$ Nm

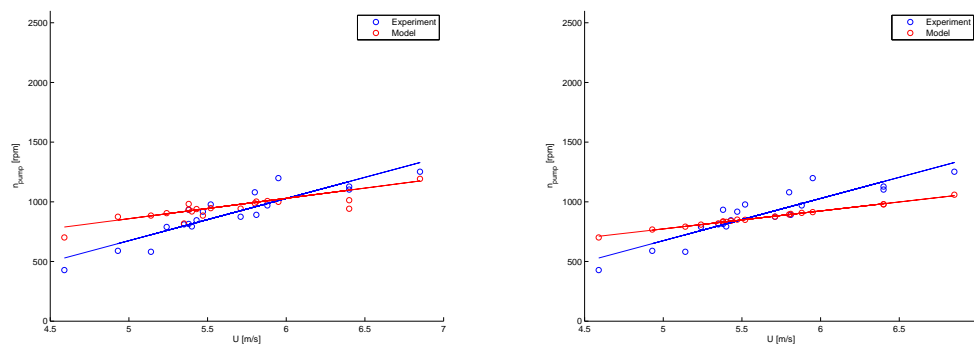


(e) SIMULINK configuration V: $C_f = 40000$ mg/L, $M_b = 5$ kg, $\eta_{coupling} = 0.12$, $J_p = 0$ kg/m², $\delta_{pump} = 3$ Nm

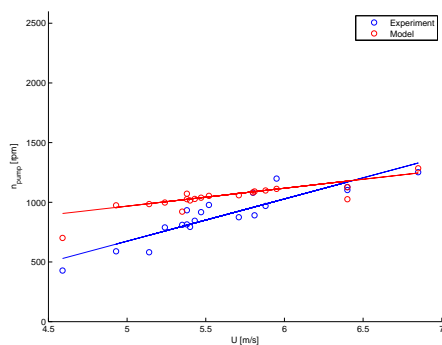
Figure I-4: Result of pump angular velocity (n_{pump}) over time (t) of the SIMULINK model compared with data from Curaçao experiment.



(a) SIMULINK configuration I: $C_f = 40000$ mg/L, (b) SIMULINK configuration II: $C_f = 35000$ mg/L, $M_b = 5$ kg, $\eta_{coupling} = 0.12$, $J_p = 0$ kg/m², $\delta_{pump} = -0.9$ Nm



(c) SIMULINK configuration III: $C_f = 40000$ mg/L, (d) SIMULINK configuration IV: $C_f = 40000$ mg/L, $M_b = 5$ kg, $\eta_{coupling} = 0.32$, $J_p = 0$ kg/m², $\delta_{pump} = -0.9$ Nm



(e) SIMULINK configuration V: $C_f = 40000$ mg/L, $M_b = 5$ kg, $\eta_{coupling} = 0.12$, $J_p = 0$ kg/m², $\delta_{pump} = 3$ Nm

Figure I-5: Result of pump angular velocity (n_{pump}) over wind speed (U) of the SIMULINK model compared with data from Curaçao experiment.